Katharina Hiebler BSc MSc

Heterogeneous palladium catalysis for the multistep synthesis of active pharmaceutical ingredients in continuous flow

DISSERTATION

to achieve the university degree of

Doktorin der technischen Wissenschaften

submitted to

Graz University of Technology

Supervisor

Assoc.Prof. Dipl.-Ing. Dr.techn. Heidrun Gruber-Wölfler

Institute of Process and Particle Engineering

Graz, September 2020

AFFIDAVIT

I declare that I have authored this thesis independently, that I have not used other than the declared sources/resources, and that I have explicitly indicated all material which has been quoted either literally or by content from the sources used. The text document uploaded to TUGRAZonline is identical to the present doctoral thesis.

Date	Signature

Go with the flow.

Danksagung

Zuallererst möchte ich mich bei all jenen Menschen bedanken, die mich während meiner PhD-Zeit begleitet haben beziehungsweise schon viele Jahre an meiner Seite sind.

Zu Beginn ein herzliches Dankeschön an meine Betreuer Prof. Johannes Khinast und Assoc.Prof. Heidrun Gruber-Wölfler für die Möglichkeit, meine Dissertation am IPPT zu schreiben. Danke Heidi, für dein Vertrauen und die vielen Freiheiten, die es mir ermöglicht haben, kreativ zu werden und selbstständig Problemlösungsstrategien zu entwickeln. Großer Dank gilt auch dem ONE-FLOW Projekt, welches diese Arbeit überhaupt erst ermöglicht hat, sowie allen Projektmitgliedern für die lehrreiche und produktive Zusammenarbeit.
Ebenfalls möchte ich mich bei den guten Seelen des Instituts, Adela, Silvi und Michi, bedanken, die mir immer gerne detaillierte Auskünfte auf meine organisatorischen Fragen gegeben haben. Danke auch an alle IPPT-KollegInnen für die unterhaltsamen Kaffeepausen sowie an die lustige Mädels-Geburtstagsrunde für die (actionreichen) Ausflüge.
Natürlich geht ein großes Dankeschön auch an die beste Arbeitsgruppe, die CoSyBro's. Bianca, Manuel, Christoph, Peter, Alessia, Sebi, Alex und Nico, es war mir eine Freude mit euch zusammenzuarbeiten. Ich werde die lockere und lustige Labor- und Büroatmosphäre sehr vermissen. Weiters möchte ich meinen fleißigen HelferInnen Mario, Daniel, Kristian, Carina, Sebi und Florian bedanken, die mich tatkräftig bei der Forschung unterstützt haben.

Meinen Freundinnen Chrisi, Tanja und Carina, danke für die vielen lieben aufbauenden Worte (wenn wieder mal ein Versuch einfach nicht funktionieren wollte) und unsere tollen Mädelsabende/-unternehmungen, die wir hoffentlich noch lange so weiterführen werden.

Ich wäre nicht an diesem Punkt angelangt ohne die fortwährende Unterstützung der besten Eltern der Welt. Danke Mama und Papa, dass ihr immer für mich da seid, ein offenes Ohr für mich habt und ich euch in allen Lebenslagen um Rat fragen kann. Ich hab euch lieb!

Last but not least, danke meinem Liebsten Max, dass du stets an meiner Seite bist, mich zum Lachen bringst und mich motivierst, an (und manchmal auch über) meine eigenen Grenzen zu gehen. Du bist mein Anker und machst meine Welt ein Stückchen bunter. Danke!

Kurz gesagt: Vielen HERZLICHEN DANK euch allen!

Abstract

In view of the outbreak of coronavirus SARS-CoV-2 in December 2019, causing a global pandemic with thousands of infected people requiring medical treatment, the efficient development and production of pharmaceuticals have received new priority. In this respect, continuous manufacturing offers great potential, as it allows quick adaption to meet current market demands. Moreover, constant product quality, enhanced energy efficiency as well as reduced waste generation belong to the numerous benefits of continuous flow technology, which promote its establishment in academia and industry. The implementation of heterogeneous catalysts further improves this powerful concept by facilitating the recycling of expensive catalytic material, in this way enabling the development of more sustainable reaction protocols. In this thesis, efforts devoted to the multistep synthesis of active pharmaceutical ingredients (APIs) in continuous flow using heterogeneous palladium catalysts are summarized, which were made possible by the ONE-FLOW research project.

In the first chapter, the implementation of heterogeneous Ce-Sn-Pd oxides into Pickering emulsions is presented. In the approach described, the solid catalyst particles are aimed to act both as emulsifiers as well as catalysts for Suzuki-Miyaura reactions. After size decrease of the metal oxide particles, they were shown to successfully stabilize various oil-in-water emulsions at low particle concentrations (<0.1 wt%) for at least 6 months. The use of the prepared Pickering emulsions for catalytic purposes in API production in continuous flow is still under evaluation.

In the second chapter, a three-step synthesis of a precursor of the antihypertensive agent valsartan in continuous flow was developed. The synthetic route comprises *N*-acylation, C-C bond formation as well as methyl ester hydrolysis. Whereas steps 1 and 3 were performed in homogeneous phase in coil reactors, the key Suzuki-Miyaura cross-coupling step was facilitated by a packed bed of heterogeneous catalyst $Ce_{0.20}Sn_{0.79}Pd_{0.01}O_{2-\delta}$. Using this modular continuous setup, the target compound was obtained in up to 96% yield (73% enantiomeric excess).

In the third chapter, the multistep continuous synthesis of a precursor of neprilysin inhibitor sacubitril is demonstrated. Once more, the critical step is Pd-catalyzed cross-coupling facilitated by the heterogeneous Pd catalyst implemented in a fixed bed reactor. The subsequent steps, Boc-deprotection as well as *N*-succinylation, have been optimized based on the statistical tool “Design of Experiments (DoE)” and were performed in coil reactor units. Performance of the three reaction steps in a consecutive fashion using an integrated continuous setup allowed the synthesis of the target molecule in 81% overall yield over 1 hour (43% enantiomeric excess).

Kurzfassung

In Anbetracht des Ausbruchs von Coronavirus SARS-CoV-2 im Dezember 2019, infolgedessen tausende Infizierte medizinische Behandlung benötigten, erlangt die effiziente Entwicklung und Produktion von pharmazeutischen Wirkstoffen einen neuen Stellenwert. In dieser Hinsicht bieten kontinuierliche Herstellungsmethoden großes Potential, da sie schnell an die aktuelle Nachfrage am Markt angepasst werden können. Zusätzlich zählen konstante Produktqualität, verbesserte Energieeffizienz als auch verminderte Abfallerzeugung zu den zahlreichen Vorteilen von kontinuierlichen Prozessen, welche deren Etablierung in Wissenschaft und Industrie vorantreiben. Die Implementierung heterogener Katalysatoren verbessert dieses Konzept überdies, da die einfachere Wiederverwendung von kostspieligem katalytischen Material ermöglicht und somit nachhaltigere Produktionswege entwickelt werden können. In dieser Arbeit sind die Bemühungen zur Verwirklichung von kontinuierlichen mehrstufigen Synthesen für die Herstellung von pharmazeutischen Wirkstoffen mithilfe von heterogenen Palladiumkatalysatoren zusammengefasst, welche durch das ONE-FLOW Forschungsprojekt ermöglicht wurden.

Im ersten Kapitel wird die Anwendung von heterogenen Ce-Sn-Pd Oxiden für die Herstellung von Pickering Emulsionen vorgestellt. Der beschriebene Ansatz strebt die Verwendung der festen Katalysatorpartikel sowohl als Emulgatoren als auch als Katalysatoren für Suzuki-Miyaura Reaktionen an. Nach einer Korngrößenreduzierung konnten die Metalloxidpartikel erfolgreich in niedrigen Konzentrationen (<0.1 Gew.%) für die Stabilisierung von verschiedenen Öl-in-Wasser Emulsionen über einen Zeitraum von zumindest 6 Monaten eingesetzt werden. Die Verwendung der hergestellten Pickering Emulsionen für katalytische Zwecke in der kontinuierlichen Wirkstoffsynthese wird derzeit noch erforscht.

Im zweiten Kapitel wurde eine kontinuierliche dreistufige Synthese für die Herstellung einer Vorstufe des blutdrucksenkenden Wirkstoffes Valsartan entwickelt. Die Syntheseroute umfasst *N*-Acylierung, C-C Bindungsknüpfung als auch Methylesterhydrolyse. Während der erste und dritte Schritt in homogener Phase in Spulenreaktoren durchgeführt werden konnten, wurde der elementare Suzuki-Miyaura Kreuzkupplungsschritt mittels eines gepackten Bettes des heterogenen Katalysators $Ce_{0.20}Sn_{0.79}Pd_{0.01}O_{2-\delta}$ bewerkstelligt. Mithilfe

dieses modularen Aufbaus konnte die Zielverbindung mit bis zu 96% Ausbeute (73% Enantiomerenreinheit) synthetisiert werden.

Im dritten Kapitel wird die mehrstufige kontinuierliche Synthese einer Vorstufe des Neprilysininhibitors Sacubitril vorgestellt. Der kritische Reaktionsschritt der Pd-katalysierten Kreuzkupplung wurde abermals mittels eines heterogenen Pd Katalysators, implementiert in einem Festbettreaktor, realisiert. Die nachfolgenden Schritte, Boc-Entschützung sowie *N*-Succinylierung, wurden basierend auf dem statistischen Instrument „Design of Experiments (DoE)“ optimiert und in Spulenreaktoreinheiten verwirklicht. Die aufeinanderfolgende Durchführung der drei Reaktionsschritte in einem ganzheitlichen Aufbau ermöglichte die Synthese der gewünschten Verbindung mit einer gleichbleibenden Ausbeute von 81% über eine Stunde (43% Enantiomerenreinheit).

Table of Contents

A Introduction

1 Suzuki-Miyaura cross-coupling

1.1 Reaction concept and mechanism

In 1979, Akira Suzuki reported the palladium (Pd)-catalyzed cross-coupling of borane species with aryl halides [1], unknowing that in doing so he would pave the way for a new era in organic chemistry. Together with Richard Heck (1972: coupling of alkenes with aryl halides) [2] and Ei-ichi Negishi (1977: coupling of organozinc reagents with aryl halides) [3], he introduced the powerful toolbox of Pd-catalyzed C-C bond formation into academic as well as industrial laboratories all over the world [4]. Since then, catalytic cross-coupling reactions have become indispensable in various chemical fields including the synthesis of natural products, active pharmaceutical ingredients (APIs) and agrochemicals [5]. In 2010, Suzuki, Heck and Negishi were deservedly awarded the Nobel Prize in Chemistry [6] for their groundbreaking work, which has revolutionized chemical synthesis.

Regarding the so-called Suzuki-Miyaura reaction, designating the Pd-catalyzed cross-coupling of organoboron reagents with haloalkanes in the presence of a base (Scheme A-1, a), the catalytic cycle involves three main steps. First, oxidative addition of the aryl halide to a Pd^0 species, which is usually produced in situ by reduction of a Pd^{II} precatalyst, leads to formation of a Pd^{II} complex. Subsequently, an exchange of the bound halide by a hydroxide molecule occurs, which renders the organopalladium complex more reactive towards nucleophiles. Second, transmetalation of the catalyst species with a base-activated borate takes place, releasing the hydroxide as borate salt. Third, the final coupled product is obtained via a reductive elimination step, that regenerates the Pd catalyst (Scheme A-1, b) [7,8].

Depending on the stability of used reagents, the catalytic system as well as the employed reaction conditions, competitive processes were observed to cause the formation of side products in Suzuki-Miyaura cross-coupling reactions. In this regard, homocoupling of the respective cross-coupling partners (R^1-R^1, R^2-R^2), protodeboronation of the boronate species (R^2-H) as well as oxidative processes (R^1-H, R^2-OH) have been observed to decrease the reaction selectivity. Strategies to minimize these events involve the rigorous exclusion of oxygen from

the reaction environment as well as the stepwise addition of the (masked) organoboron reagent [9].

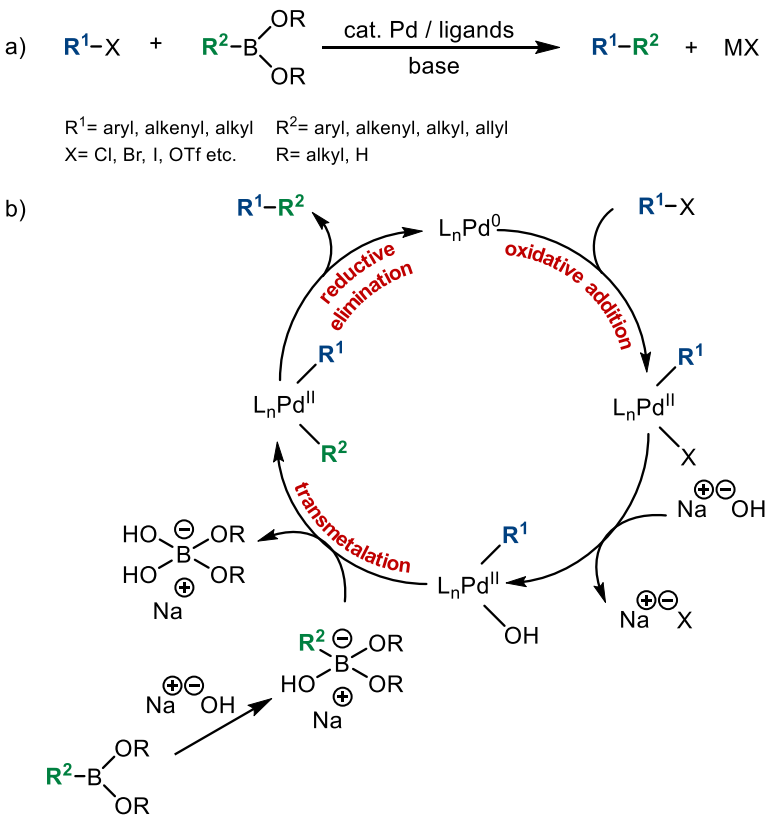

Scheme A-1: a) General reaction scheme of Suzuki-Miyaura cross-coupling [7];
b) Catalytic cycle of Suzuki-Miyaura cross-coupling [10].

Owing to its remarkable synthetic power, Suzuki-Miyaura cross-coupling has made its way into the chemical laboratories all over the world. Hence, numerous important applications and further developments have been reported, which will be discussed hereafter.

1.2 Importance of Suzuki-Miyaura cross-coupling in organic synthesis

The establishment of Pd-catalyzed Suzuki-Miyaura cross-coupling as a fundamental tool in organic synthesis did not come by chance. This strategy of C-C bond formation features persuasive advantages including 1) the use of air- and moisture-stable organoboron reagents, 2) mild reaction conditions tolerated by various functional groups as well as 3) simple removal of inorganic by-products [4,11]. These characteristics make the Suzuki-Miyaura reaction highly attractive for industrial applications. Hence, it is not surprising that it was ranked among the five most frequently occurring reactions in medicinal chemistry in 2014 [12] and is the key reaction

step in a number of well-established large-scale processes including the synthesis of the anti-hypertensive losartan [13] as well as the anti-cancer agent crizotinib [14] (Figure A-1). The interest in this class of transformation is further highlighted by the significant increase in patents and publications since the beginning of the new millennium, with Suzuki-Miyaura cross-coupling being the most prominent field of research [15].

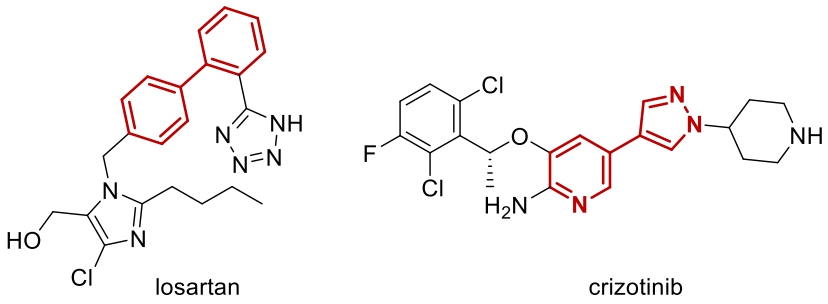

Figure A-1: Structures of the active pharmaceutical ingredients losartan and crizotinib, whose biaryl unit (highlighted in red) is formed via Suzuki-Miyaura cross-coupling on a large scale.

1.3 Developments and advances in the field of Suzuki-Miyaura cross-coupling

From the time of its first discovery, the Suzuki-Miyaura cross-coupling concept has continuously been developed further and improved by numerous research groups worldwide [7,11,16–18]. The efforts regarding optimization of the reaction can roughly be devided into three waves [4] focusing on 1) the search for suitable and selective metal catalysts, 2) the extension of the scope of the boronic acid derived cross-coupling partner as well as 3) the reaction fine tuning by choice of highly selective and reactive ligands, electrophilic coupling reagents and mild process conditions. In the following, each wave will be commented briefly to get a general overview of the progress in this field.

Regarding the ongoing pursuit for the ultimate metal catalyst for Suzuki-Miyaura cross-coupling reactions (wave 1), palladium is still the dominant choice [17]. Although also other transition metals such as nickel [19], copper [20] and iron [21] have been reported to successfully facilitate Suzuki-type cross-coupling reactions, palladium catalysis plays the lead owing to its remarkable versatility as well as compatibility [17]. As far as the originally used organoboronic acid coupling partner is concerned, the development of alternative reagents such as organotrifluoroborate salts (RBF_3K) [22,23], *N*-methyliminodiacetic acid (MIDA) boronates [24] or magnesium diorganoboronate species [25] led to an improve in reaction

selectivity and allowed the use of milder reaction conditions (wave 2). Concerning the third extensive area of Suzuki-coupling research, reaction fine tuning (wave 3), a myriad of different ligands increasing the catalytic efficiency of the homogeneous palladium precatalyst have appeared in literature [17]. In particular, phosphine-based ligands [17,26,27] are a common choice but also others such as *N*-heterocyclic carbenes (NHC) [28–30] have been employed frequently. Palladacycles and related pincer complexes (incorporating two fused palladacycles) [31,32], which belong to the class of cyclic Pd complexes comprising one or more carbon-palladium bonds, have also gained considerable attention for their use in Suzuki-Miyaura cross-coupling reactions. The optimization of ligands for homogenous Pd catalysis resulted in a significant improvement of the initial concept by A. Suzuki in terms of catalyst robustness, reaction rates as well as selectivity. Many of them facilitate C-C bond forming reactions under mild reaction conditions in an aqueous environment at very low catalyst loadings [33–35]. As a consequence, novel methodologies including the use of unactivated aryl chlorides [36–39] as coupling partners, which are cheaper and generate less waste than their bromide and iodide counterparts [40], have emerged. Also, the utilization of unconventional substrates like arenediazonium salts [41,42], aromatic amides [43], fluorinated sulfonates [44] and aromatic nitrocompounds [45] has attracted substantial interest in the last years. A graphical overview of the main developments concerning the different reaction components of Suzuki-Miyaura cross-coupling is given in Figure A-2.

Apart from above stated fairly well-established developments for Suzuki-Miyaura cross-coupling, there are also a number of less-known sophisticated approaches concentrating on alternative reagent activation, tuning of the reaction selectivity as well as novel reaction media. Besides cross-coupling reactions facilitated by CH-activation [46] or visible light [47], there has been progress on the topic of asymmetric C-C bond formation [48,49] allowing the synthesis of axially chiral biraryls. Furthermore, poor substrate solubility in aqueous solutions has been improved by the use of surfactants [34,50,51]. Regarding the search for new highly functional catalyst species, computational analysis of 25000 homogeneous catalysts has revealed effective metal-ligand combinations for different prominent cross-coupling reactions. According to the authors, obtained data could serve as a starting point for systematic catalyst optimization and the approach is believed to be especially promising for the exploration of novel chemistries [52].

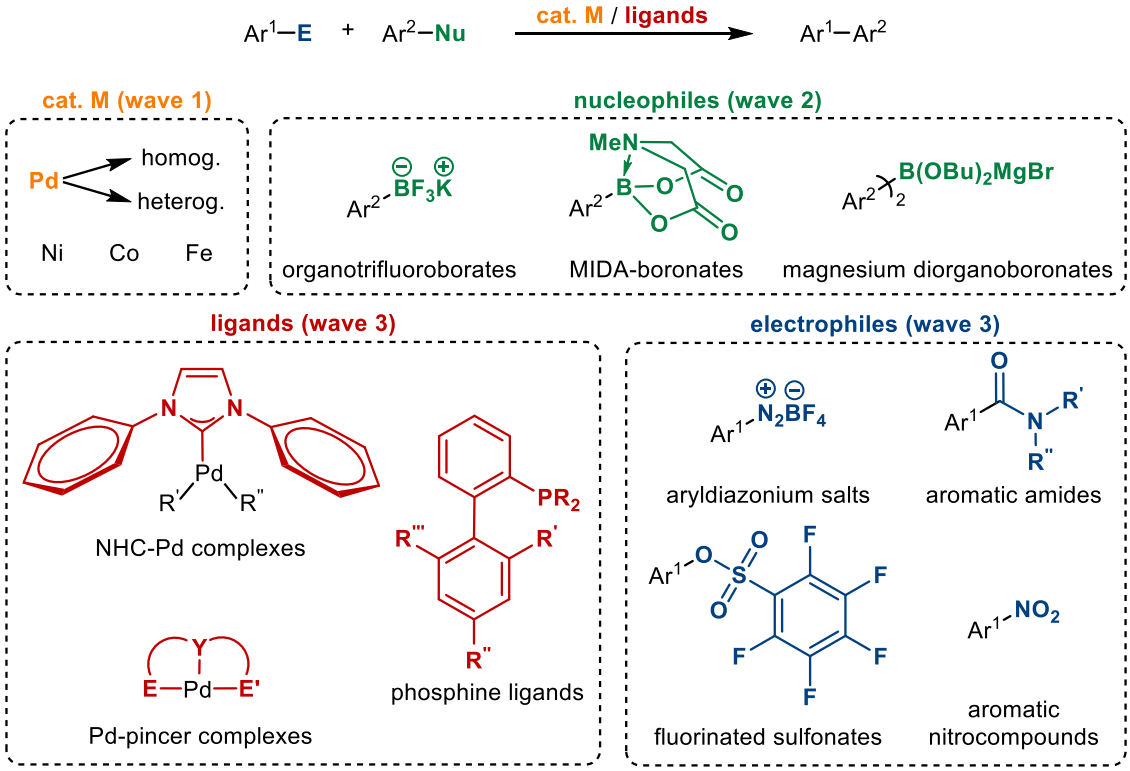

Figure A-2: Overview of selected important concepts and developments in the field of Suzuki-Miyaura reaction in terms of catalytic species, nucleophilic coupling partners, ligands (E= neutral species) and alternative electrophiles [17,19-32,41-45].

Apparently, in the past decades there has been a constant progress on Suzuki-Miyaura cross-coupling facilitated by homogeneous Pd species. Catalyst activity as well as selectivity could be significantly improved, allowing the effective synthesis of important chemical intermediates and biologically active molecules. However, homogeneous catalysis lacks the possibility for easy catalyst separability and recycling, which belong to the key aspects of "green chemistry" [53]. This concept developed in the early 1990s targets per definition the "design of chemical products and processes to reduce or eliminate the use and generation of hazardous substances" [54]. Furthermore, transition metal contamination of the final product is a common problem when using homogeneous palladium catalysts and often tedious purification steps are required to achieve an acceptable product quality [55,56]. Hence, several heterogeneous alternatives addressing these issues have been developed in the course of past years, which will be discussed in more detail in chapter 2.

In conclusion, the seminal paper by Suzuki on palladium-catalyzed cross-coupling of aryl halides with organoboron reagents [1] has permanently affected the way chemists construct molecules. Owing to its remarkable versatility as well as compatibility, the Suzuki-Miyaura

reaction has found extensive use for the formation of high-value chemical compounds and has become an indispensable tool in synthetic organic chemistry. Especially the C-C bond formation facilitated by heterogeneous palladium catalysts has received great attention lately, aiming the implementation of more sustainable reaction protocols. An outline of past and recent developments in this area of research as well as insights into the characteristics of heterogeneous palladium catalysis will be given in the following chapter.

2 Heterogeneous palladium catalysis

In search for more sustainable Suzuki-Miyaura cross-coupling protocols, the replacement of toxic organic solvents by water as well as the use of "ligandless" catalysts have marked crucial advances in this field [17]. However, applied homogeneous palladium catalysis has several intrinsic shortcomings including catalyst removal and recycling problems as well as Pd contamination in the final product [55]. Instead, the use of highly stable heterogeneous catalysts allows a fast and easy separation of the catalytic species from the reaction mixture, which facilitates the reuse of the precious transition metal catalyst. The repeated utilization of the expensive catalyst is not only favored in terms of the development of greener synthetic processes [54] but also due to economic reasons. What has to be kept in mind though is that heterogeneous catalysis often requires harsher reaction conditions in comparison to the homogeneous type and hence undesired leaching effects, reduced selectivity as well as the formation of side products might occur [57]. Consequently, substantial efforts have been devoted to the synthesis and application of efficient and nonleaching heterogeneous alternatives for catalyzing Suzuki-Miyaura cross-coupling reactions, which will be summarized in the following.

2.1 Definition of heterogeneous catalysis

Before discussing the application of heterogeneous Pd catalysis for Suzuki-Miyaura cross-coupling, it is important to define the term "heterogeneous catalyst". As commonly known, "catalysis" refers to the rate acceleration of a chemical transformation by lowering the activation energy of the reaction and without the catalytic species being consumed. "Heterogeneous catalysis" moreover designates that the catalyst is present in a different phase than the reactants and catalysis therefore occurs at the interface [58].

Over the course of the years, a variety of different concepts for immobilization of catalytically active metals have been developed involving covalent/ionic bonding, adsorption or encapuslation. In order to achieve anchoring of the metal onto the solid support, different chemical and physical techniques including decomposition, (co-)precipitation, impregnation or ion exchange are used [59].

2.2 The quasihomogeneous nature of heterogeneous Pd catalysts for Suzuki-Miyaura cross-coupling

As far as the use of heterogeneous palladium catalysts for C-C bond formation is concerned, their so-called “quasihomogeneous” mode of action is a topic of intense discussion. It originates from the fact that several Pd catalysts, originally considered as heterogeneous, have been demonstrated to act as a reservoir for homogenous Pd species that leach into the reaction solution during the catalytic cycle (Scheme A-2). After the reaction is completed, dissolved palladium then readsorbs onto the solid support to a certain extent, thus regenerating the heteogeneous catalyst. Although this dissolution-readsorption hypothesis has been widely accepted among the scientific community, it cannot be ruled out with certainty that also “truly” heterogeneous catalysis takes place at the liquid-solid interface [8,17,55,57,60–62]. What is more, the circumstance that cross-coupling was reported to be efficiently catalyzed by homeopathic doses of dissolved palladium (found as contaminant in commercially available reagents) does not make the evaluation of the true nature of the catalytically active species an easy task [63,64].

Regarding heterogeneous palladium catalysis for Suzuki-Miyaura coupling, leaching of the catalytically active species from the solid support is obviously undesirable as it results in limited catalyst recyclability (due to a loss of activity) as well as contamination of the final product. The latter is especially critical in terms of the synthesis of active pharmaceutical ingredients as the palladium concentration in the product must not exceed 5 ppm [56]. Although strategies for the efficient removal of leached palladium species from the reaction solution have been developed, such as the use of multidentate sulfur-based silica scavengers [65], the prevention of Pd leaching would undoubtably be preferred.

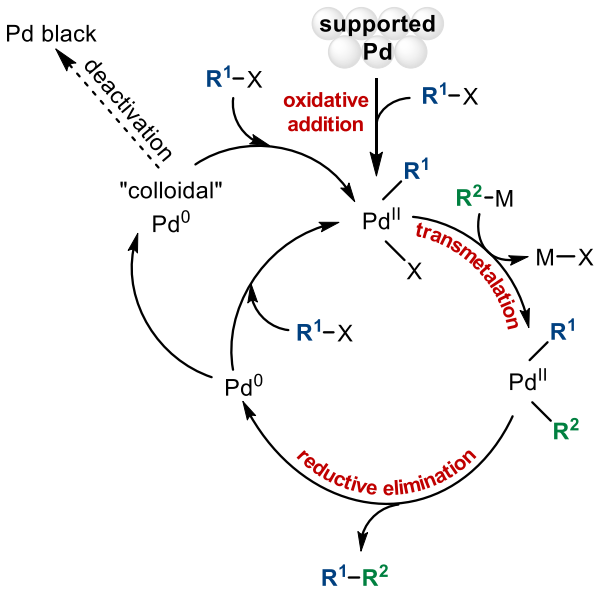

Scheme A-2: Accepted catalytic cycle for Suzuki-Miyaura cross-coupling facilitated by heterogeneous Pd catalysts operating via a "quasihomogeneous" reaction mechanism [66–68].

Nevertheless, the concept of heterogeneous Pd catalysis for C-C bond formation has fascinated researchers ever since and many efforts have been devoted to the search for the holy grail of a truly heterogenous transition metal catalyst. Consequently, a vast number of different approaches for solid-supported palladium catalysts have been developed in the course of past years.

2.3 Different classes of heterogeneous palladium catalysts for Suzuki-Miyaura cross-coupling

The large group of heterogenized palladium catalysts for C-C cross-coupling can be classified according to various aspects including the chemical nature (in/organic) of the solid matrix as well as the way the catalyst is attached to it (chemical or physical entrapment). This again depends on the character of the entrapped catalytic species [e.g. organometallic Pd complex, Pd nanoparticles (NP)] [55,68]. As the presence or absence of stabilizing ligands was shown to considerably affect the activity and selectivity of Pd catalysts [69,70], in the following we will differentiate between immobilized "ligand-free" palladium catalysts as well as palladium bound to immobilized ligands.

Prior to discussing the different strategies for Pd immobilization according to this point of view, the use of palladium nanoparticles for Suzuki-Miyaura cross-coupling [71–74] reactions

will be reviewed separately. As their utilization provides advantages of both homo- (high activity and good selectivity) as well as heterogeneous (recovery and recyclability) catalysis, they are commonly considered as “semi-heterogeneous” catalysts [60,75]. In fact, their catalytic properties were discovered unintentionally when using homogeneous Pd species for C-C bond formation. Closer examination of the catalytic processes revealed that complexes comprising weakly nonvalent bound Pd^0 tend to dissociate and release atomic palladium, which in turn can aggregate into palladium nanoparticles [17]. Concerning the application of Pd-NPs for catalysis, cross-coupling can be accomplished via unsupported as well as supported palladium nanoparticles [17]. In the first case, stabilization of the Pd-NPs is often achieved by additives (e.g. sufactants, quaternary ammonium/phosphonium salts, ligands) that adsorb onto the nanoparticles’ surface and thus prevent their aggregation by formation of a protective layer [17]. Regarding the latter, a variety of different solid supports for Pd-NPs have been developed including polymers [76] or dendrimers [77]. Likewise, carbon [39,78] and both inorganic [79] and magnetic oxides [80] have been used for supporting Pd nanoparticles to achieve Suzuki-Miyaura cross-coupling. In contrast to unsupported Pd-NPs, the use of nanoparticulate Pd on tangible solid supports allows their facile separation from the catalytic process as well as their reuse, which is one of the fundamental advantages of heterogeneous catalysis.

Coming back to the approaches for immobilized ligand-free palladium catalysis for Suzuki-Miyaura cross-coupling, silica, alumina and carbon belong to the most common solid support materials as they are cheap, thermally stable, nontoxic and easily available [59]. Especially palladium on charcoal (Pd/C) is a popular choice to heterogeneously catalyze Suzuki-Miyaura reactions [57]. Moreover, palladium has also been immobilized on and within ceria-based perovskites [81,82], which have been successfully utilized for Suzuki-Miyaura cross-coupling reactions in continuous flow [81,83–85]. In addition, Pd nanoparticles loaded onto monolithic supports or magnetic oxides belong to the group of ligand-free heterogeneous palladium catalysts for cross-coupling [68]. Another interesting method for Pd immobilization is the deposition of Pd^0 films on the internal surface of capillary coils, which can directly be used in continuous cross-coupling setups [86]. Furthermore, in 2002 Ley et al. introduced polyurea encapsulated palladium as ligand-free heterogeneous catalyst for Suzuki-Miyaura cross-coupling reactions [87]. The commercialized catalyst PdEnCat features palladium(II) acetate

entrapped in a microsized polymeric urea coating and has been employed for batch as well as continuous organic synthesis [88], even on a larger scale [89].

Apart from the development of mentioned ligand-free immobilization concepts, the fixation of palladium to ligands bound to a solid support has been extensively investigated. Besides the fact that the presence of a ligand often enhances the catalytic activity as well as selectivity of a metal catalyst, it can also increase its stability by inhibiting metal degradation processes [90–92]. Concerning the used solid support materials, both organic (e.g. organic fibers [93], polyurea capsules [94], polystyrene [95,96], polymeric monoliths [97]) and inorganic (especially silica [98] including functionalized silica [99] or fused silica capillaries [100]) matrices have been successfully applied [55]. One of the first classes of ligands examined for their ability to stabilize palladium in cross-coupling reactions were phosphine ligands including triphenylphosphine (PPh_3) or tri-*tert*-butylphosphine ($P\mathit{t}Bu_3$) [101]. A prominent example is the commercial sol-gel entrapped catalyst Silica*Cat* DPP-Pd, which comprises diphenylphosphine ligands bound to an amporphous organosilica matrix [102]. Another important group of solid-supported ligands are so-called salen ligands, which can bind palladium via their Schiff base-type moiety and have demonstrated to catalyze cross-coupling reactions [103]. Also, bidentate ligands such as phenantroline or *N*-heterocyclic carbenes have proven to be powerful ligands when immobilized onto a solid support and have been employed for the cross-coupling of *para*-tolylboronic acid with various aryl halides [97].

After synthesis of the supported metal catalyst and investigation of its catalytic activity, the experimental determination of the homo- or heterogeneous nature of the actual catalytic species is of high importance. For that purpose, a number of different approaches have been developed, which are outlined below.

2.4 Methods for assessing the heterogeneity of supported palladium catalysts

General procedures for assigning the homo- or heterogeneity of any kind of supported palladium catalyst include the hot filtration test [104], the three-phase test [105] as well as catalyst poisoning [106]. In the hot filtration test developed by Hamlin et al., the nominally heterogeneous catalst is filtered off the hot reaction mixture and rinsed with solvent. After addition of fresh reagents, the catalytic capacity of the resulting filtrate is determined. If any

catalytic product formation is observed, the test suggests the formation of a homogeneous catalyst species that must have passed through the filter and speaks against a truly heterogeneous mode of action [104]. Another method to assess the presence of a free reaction intermediate during the catalytic cycle is the performance of the three-phase test. Therefore, one of the reagents is first immobilized on a solid support and is thus not in contact with the heterogeneous catalyst. Hence, for the catalytic reaction to occur, an active soluble catalyst species must form, which would disprove the heterogeneity of the tested catalyst [105]. Moreover, selective catalyst poisoning is a common procedure for evaluation of the homo- or heterogeneous nature of a catalyst. A decrease of catalytic activity upon the addition of a resin-bound scavenger capable of removing potentially formed soluble catalyst species indicates catalyst leaching [106]. Regarding palladium-catalyzed transformations, immobilized thiols [107] as well as polyvinylpyridine [108] are known to act as poisons for dissolved Pd. In addition to mentioned tests, a variety of different analytical methods have been used as well to validate the heterogeneous properties of a catalyst. For that purpose, analysis via inductively coupled plasma (ICP) and infrared (IR) spectrometry, X-ray methods, dynamic light scattering (DLS) and microscopy has been applied frequently [106], also in combination with continuous setups [109,110].

Summarizing, in the past years a plethora of different concepts for the immobilization of palladium for Suzuki-Miyaura cross-coupling have been developed, including ligand-free as well as ligand-based strategies utilizing all different kinds of organic and inorganic support materials [17,55,68]. The intrinsic separability and recyclability of these catalysts make them predestined for the utilization in continuous flow applications, which is currently a “hot topic" among the scientific community [68] and will be discussed in subsequent chapter.

3 Continuous flow technology and industrial API production

3.1 Definition and fundamentals of continuous flow technology

Continuous flow synthesis defines the performance of one or more subsequent chemical reaction steps in a continuous stream, with the substrates and reagents being continuously charged into the reactor and the products being constantly discharged [111]. It is a modular technique comprising different unit operations, which in general can be designated to the

seven basic categories shown in Scheme A-3. As far as the key element of a continuous setup for organic synthesis is concerned, the continuous reactor, various types of flow reactors can find application such as continuous stirred tank, plug flow and packed bed reactor [112,113].

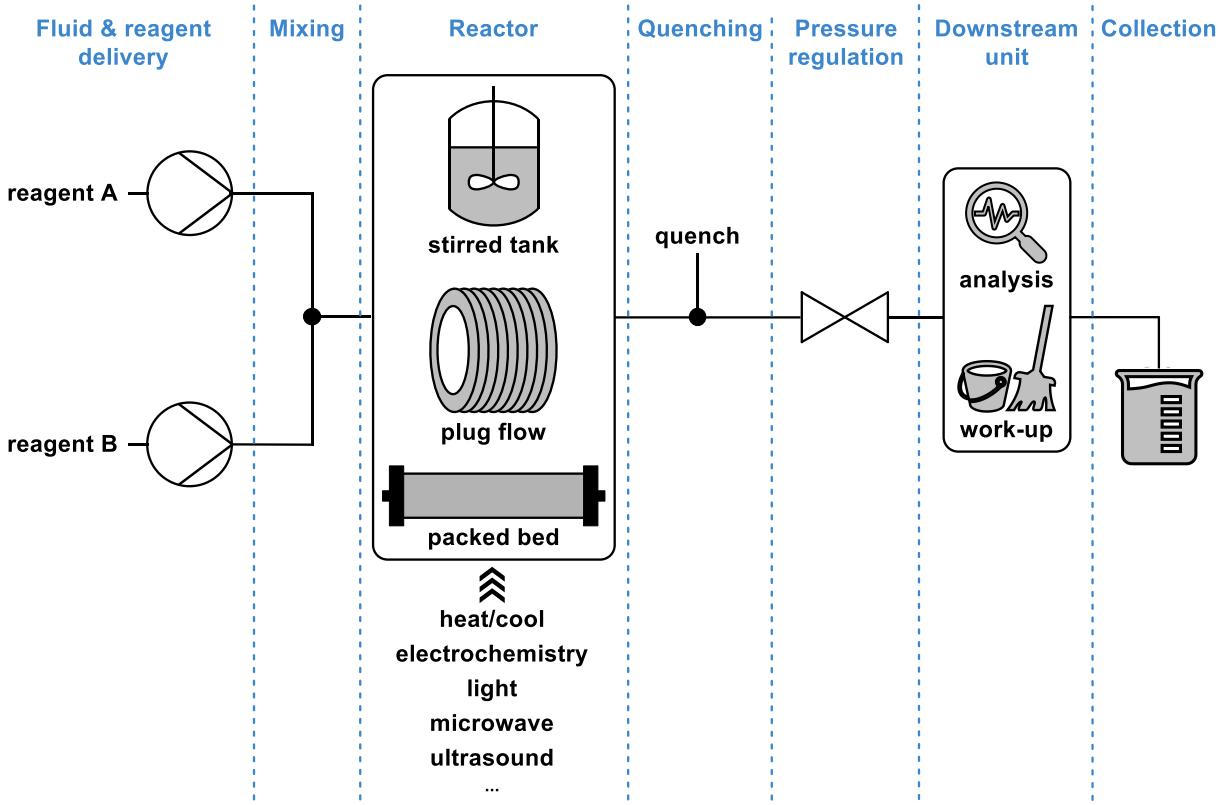

Scheme A-3: Standard zones of a continuous flow reaction setup [112,113].

Continuous flow technology has already been established for the production of commodity chemicals in the petrochemical and bulk industry, where the development of cost-effective and high-performing operations is driven by strong competition. Instead, processes in the pharmaceutical and fine chemistry have traditionally been performed in multipurpose (semi)batch reactors, which can be applied for diverse transformations and are easily adaptable to new production routes [114]. However, in the last years the picture has started to change and the pharmaceutical industry has put increasing efforts into the development of continuous processes for the production of active pharmaceutical ingredients [114–118].

3.2 Benefits of continuous flow technology

The application of continuous flow technology for API production has not been strongly pursued in the recent past without good reasons. Compared to batch chemistry, continuous flow

methodology offers a variety of advantages in terms of process optimization as well as economics. Regarding reaction tuning, the benefits of continuous synthesis mostly arise from the precise adjustment of reaction parameters. This is, among others, facilitated by the use of micro- and mesofluidic equipment, which enables enhanced mixing of reagents as well as increased interfacial contact. The resulting efficient mass transfer is especially profitable for multiphasic but also for very fast chemical reactions, as yield and selectivity are highly influenced by the presence or absence of local concentration gradients. Apart from that, the utilization of small-dimensioned tube reactors enables an effective heat transfer, in this way allowing precise temperature regulation (determining the product-to-side-product ratio), process intensification (by applying high-temperature/high-pressure, “Novel Process Windows” [119]) and the performance of highly exothermic, hazardous reactions (by preventing a thermal runaway, “Forbidden Chemistry” [120]). Also, the short path length in low-volume continuous reactors makes them increasingly being used in photo- as well as electrochemical applications [112,114,121,122] .

Besides providing the opportunity to accurately set the reaction parameters, another advantage of continuous flow manufacturing is its remarkable flexibility. On the one hand, the implementation of in- and on-line analytical techniques [such as nuclear magnetic resonance (NMR) or IR spectroscopy] into continuous operations allows real-time process monitoring [123]. On the other hand, computer-aided automation enables feedback optimization and eliminates potential sources of human error. The combination of these two technologies allows to quickly detect and immediately respond to out-of-specification processes, which can for instance be caused by lot-to-lot variation of used raw materials [124]. What is more, the scale up of existing micro- or mesofluidic continuous reaction setups can be achieved quite easily by applying the principle of “scaling out” (increase of tube size, extension of product collection time) or “numbering up” (parallelization of identical units) [125].

As far as process costs in pharmaceutical industry are concerned, switching from batch to continuous processing can save more than 30% costs [126,127], which is the main driver for manufacturers to change traditional ways of production. Primarily, automation can be hold responsible for the reduction of labor costs, resulting from fewer processing steps, machine-based quality control as well as less material handling and storage. In addition, a decrease in

energy consumption by effective temperature control and a smaller amount of generated waste requiring disposal contribute to the overall savings potential of continuous flow technology. [117,126,127]

Generally speaking, continuous flow processing broadens the scope of chemical reactions applicable for high-quality API production, saving time and money at the same time. Furthermore, it aligns with the principles of green chemistry [53] and allows the implementation of more sustainable synthetic protocols. The endeavors of the Food and Drug Administration (FDA) [128,129] to establish continuous flow methodology in API production [114–118] are bearing their first fruit, which will be exemplarily discussed in the following part.

3.3 Continuous manufacturing for the synthesis of APIs

As highlighted above, the synthesis of active pharmaceutical ingredients in continuous flow offers new chances and possibilities in terms of alternative and effective synthesis strategies as well as green process design. However, while in secondary manufacturing of pharmaceuticals continuous unit operations play an increasingly important role [130–132], production of the active pharmaceutical ingredients is still mostly performed in batch [132]. As a matter of fact, manufacturers often shy away from abandoning well-operating, long-established batch processes and hesitate to invest into innovative continuous technologies, which would require re-approval by regulatory authorities [118]. Nevertheless, there has been considerable progress in the implementation of continous flow technology for pharmaceutical synthesis.

As far as research and development within the pharmaceutical sector are concerned, fast and efficient library generation is frequently performed in a continuous manner. Targeted compounds are obtained on a milligram scale, which is sufficient to examine structure-activity relationships and to make a statement about pharmacologically relevant functional groups [133–135]. Subsequently, the synthesis and optimization of identified hit and lead molecules is also increasingly often achieved continuously [114–118,136]. Regarding the manufacturing process, numerous papers showcase the successful synthesis of active pharmaceutical ingredients in fully continuous pilot plants [137,138]. One prominent example for the successful combination of API synthesis and drug product fabrication in continuous flow on a pilot

scale is the synthesis of aliskiren, which was developed by the Novartis-MIT Center for Continuous Manufacturing. The process comprising two chemical steps, salt formation as well as crystallization was achieved in a fully integrated, continuous pilot plant giving the finished tablets as final product after some secondary manufacturing steps [139,140].

Regarding recent research in the field of continuous API production, the realization of the so-called “pharmacy on demand (PoD)” concept has been heavily pursued. This approach refers to the development of modular end-to-end continuous manufacturing platforms able to synthesize a variety of active pharmaceutical ingredients. In this respect, the Defense Advanced Research Projects Agency (DARPA) launched a “Battlefield Medicine” programme targeting the creation of a reconfigurable, miniaturized platform able to synthesize a number of drugs from the World Health Organization (WHO) list of essential medicines (diphenhydramine hydrochloride, diazepam, lidocaine hydrochloride and fluoxetine hydrochloride). Using a mini-plant in the size of a commercial refrigerator, multistep chemical synthesis in continuous flow, several in-line purification and work-up steps, crystallization of the API as well as formulation were subsequently performed and simultaneously monitored, delivering the finished liquid dosage forms (Figure A-3) [141,142]. Another case study demonstrating successful multi-disciplinary efforts for the production of pharmaceuticals according to the PoD principle is the F^3 (Flexible, Fast and Future) project supported by the European Community’s Seventh Framework Programme. Over 300 experts from both academia and industry worked together to accomplish a “plug & play” design for continuous API manufacturing on a pilot scale. Besides the validation of new reactor technologies as well as the implementation of novel intensified processes in continuous flow, the developed platform allowed the synthesis of various chemical products (drugs, polymers, surfactants) according to green chemistry principles [143].

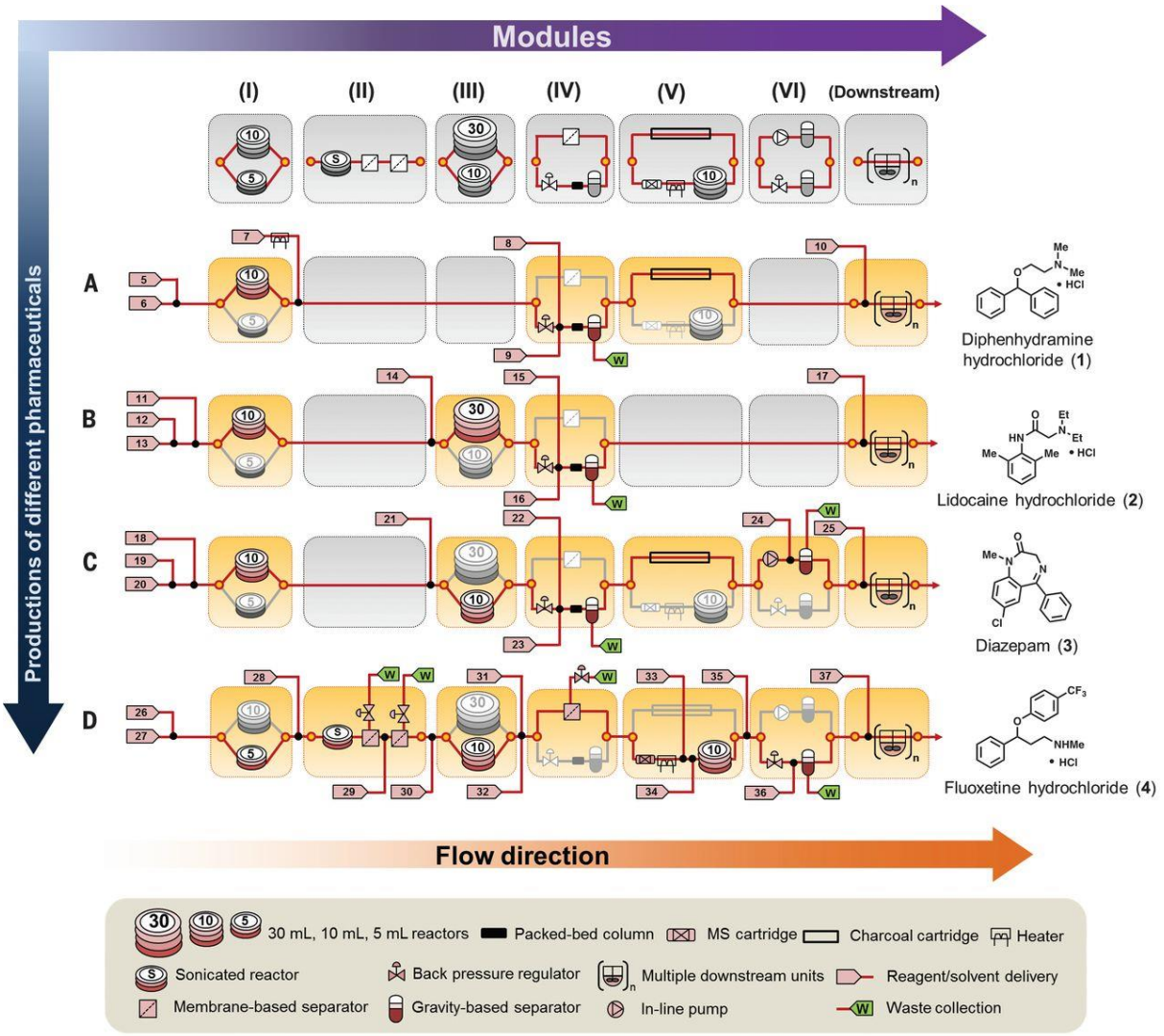

Figure A-3: Realization of the "pharmacy on demand" concept within the DARPA-funded "Battlefield Medicine" programme – Flowcharts of the continuous syntheses of liquid dosage forms of four essential medicines using a refrigerator-sized platform (reproduced from [141]).

Although in the course of last years quite a number of publications presenting the multistep continuous production of APIs have appeared in literature, only few reported processes are in compliance with "current good manufacturing practices (cGMP)" [144–146]. Hence, there are apparently still a few critical challenges regarding the continuous manufacturing of pharmaceutical compounds, which have to be overcome in order to achieve widespread implementation of continuous flow methodology [136]. However, there are already some scarce evidences of the successful realization of continuous API synthesis on an industrial scale, such as the two-ton production of an intermediate of the anti-tumorigenic drug brivanib alaninate [147].

While the envisioned fully continuous, end-to-end manufacturing of active pharmaceutical ingredients for commercial purposes still seems a bit remote, there are numerous examples showing the high potential of continuous API processing from batch to pilot plant scale. Also, major investments by market-leading pharmaceutical companies such as Eli Lilly [130] and GlaxoSmithKline (GSK) [131] into continuous manufacturing sites illustrate the eagerness of the pharmaceutical industry to implement this promising technology.

3.4 Pd-catalyzed cross-coupling on an industrial scale

Concerning the industrial realization of C-C cross-coupling, which is a common step in synthetic routes towards APIs as described in chapter 1.2, traditional batch procedures utilizing homogeneous palladium catalysis predominate. Although some commercial scale Suzuki-Miyaura reaction protocols rely on heterogeneous Pd systems, most frequently Pd/C, the well-established stirred tank reactor still continues to be the reaction system of choice for the pharmaceutical industry [148]. This can probably be contributed to the fact that in a continuous process transition metal leaching caused by the underlying quasihomogeneous catalytic mechanism would inevitably lead to a loss of palladium, as it is being “chromatographed” through the fixed bed unit [68].

Despite the ongoing developments in the field of heterogeneous catalysis and green continuous process design, a survey among pharmaceutical market leaders revealed that there is still a need for improving the sustainability of various reaction concepts, including Suzuki-Miyaura cross-coupling [149]. The ONE-FLOW project addresses these issue and even goes a step further, as discussed in the next chapter.

4 The ONE-FLOW approach

The ONE-FLOW project [150], funded by the European Commission under the Horizon 2020 programme (project launch January 2017), aims the development of catalyzed cascade reaction by applying the novel concept of so-called “horizontal hierarchy”. This means, that the single steps of a reaction sequence are not performed in a consecutive fashion in confined compartments but different chemo- and biocatalysts work simultaneously next to each other, therefore achieving multiple reactions in “one step” like the role model nature. The required

compartmentalization is envisioned to be achieved by the implementation of Pickering emulsions, chemisorbed catalysts, block copolymer-based polymersomes as well as “smart” (functional and green) solvents. Also, the integration of automated intelligence into the respective cascades is pursued in terms of process optimization and control. Using this innovative concept, the 4-year project targets the synthesis of four top-list drugs (valsartan, sacubitril, capecitabine, ursodeoxycholic acid) [150]. Within the framework of this project, we were responsible for the development of multistep cascade reactions for the synthesis of valsartan and sacubitril in continuous “ONE-FLOW” (Figure A-4). Our efforts and results in this respect have been published in peer-reviewed journals, which are collected in this thesis.

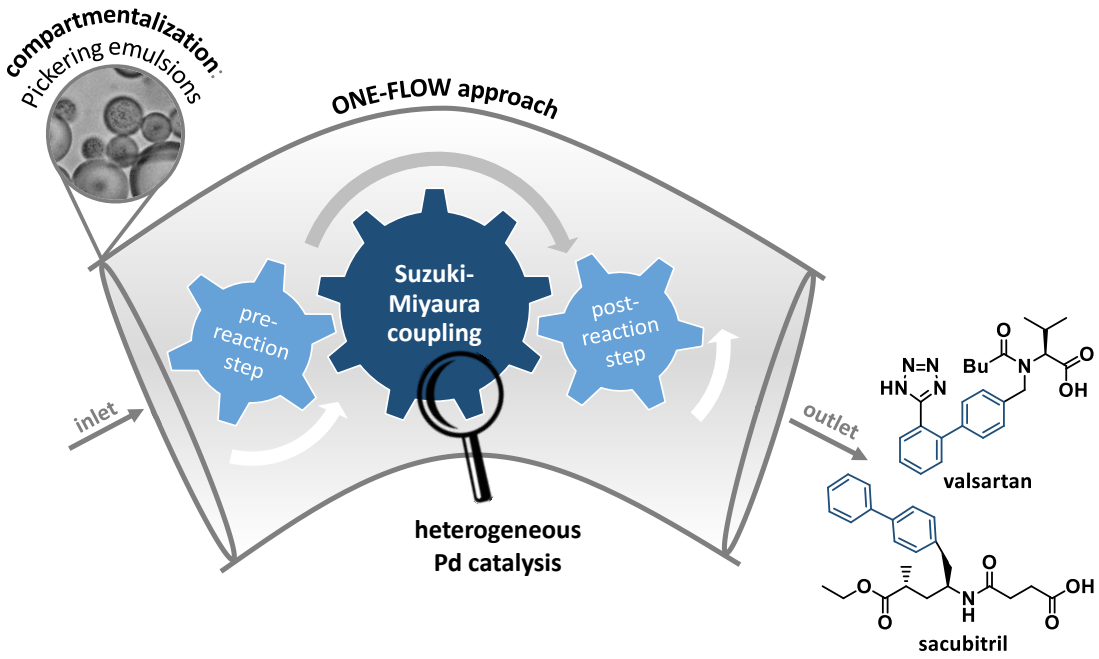

Figure A-4: Graphic representation of our ONE-FLOW approach for the multistep synthesis of valsartan and sacubitril in continuous flow.

5 References

1. Miyaura N, Suzuki A (1979) J Chem Soc Chem Commun 866–867
2. Heck KF, Nolley JP (1972) J Org Chem 37:2320–2322
3. Negishi E, King AO, Okukado N (1977) J Org Chem 42:1821–1823
4. Johansson Seechurn CCC, Kitching MO, Colacot TJ, Snieckus V (2012) Angew Chem Int Ed 51:5062–5085
5. Torborg C, Beller M (2009) Adv Synth Catal 351:3027–3043

6. Press release (2010) Nobel Media AB. https://www.nobelprize.org/prizes/chemistry/2010/summary/. Accessed 18 Mar 2020
7. Miyaura N, Suzuki A (1995) Chem Rev 95:2457–2483
8. Phan NTS, Van Der Sluys M, Jones CW (2006) Adv Synth Catal 348:609–679
9. Blakemore DC (2016) Suzuki – Miyaura Coupling. In Synthetic Methods in Drug Discovery: Volume 1, Blakemore DC, Doyle PM, Fobian YM (Eds.), Royal Society of Chemistry, London
10. Fortun S, Beauclair P, Schmitzer AR (2017) RSC Adv 7:21036–21044
11. Kotha S, Lahiri K, Kashinath D (2002) Tetrahedron 58:9633–9695
12. Brown DG, Boström J (2016) J Med Chem 59:4443–4458
13. Larsen RD, King AO, Chen CY, Corley EG, Foster BS, Roberts FE, Yang C, Lieberman DR, Reamer RA, Tschaen DM, Verhoeven TR, Reider PJ, Lo YS, Rossano LT, Brookes AS, Meloni D, Moore JR, Arnett JF (1994) J Org Chem 59:6391–6394
14. De Koning PD, McAndrew D, Moore R, Moses IB, Boyles DC, Kissick K, Stanchina CL, Cuthbertson T, Kamatani A, Rahman L, Rodriguez R, Urbina A, Sandoval A, Rose PR (2011) Org Process Res Dev 15:1018–1026
15. Colacot TJ (2011) Platin Met Rev 57:73-151
16. Hassan J, Sévignon M, Gozzi C, Schulz E, Lemaire M (2002) Chem Rev 102:1359–1469
17. Beletskaya IP, Alonso F, Tyurin V (2019) Coord Chem Rev 385:137–173
18. Campeau LC, Hazari N (2019) Organometallics 38:3–35
19. Han FS (2013) Chem Soc Rev 42:5270–5298
20. Yang CT, Zhang ZQ, Liu YC, Liu L (2011) Angew Chem Int Ed 50:3904–3907
21. Bedford RB, Hall MA, Hodges GR, Huwe M, Wilkinson MC (2009) Chem Commun 6430–6432
22. Darses S, Genet JP (2003) Eur J Org Chem 4313–4327
23. Molander GA, Ellis N (2007) Acc Chem Res 40:275–286
24. Knapp DM, Gillis EP, Burke MD (2009) J Am Chem Soc 131:6961–6963
25. Haag BA, Sämann C, Jana A, Knochel P (2011) Angew Chem Int Ed 50:7290–7294
26. Martin R, Buchwald SL (2008) Acc Chem Res 41:1461–1473
27. Fu GC (2008) Acc Chem Res 41:1555–1564
28. Valente C, Çalimsiz S, Hoi KH, Mallik D, Sayah M, Organ MG (2012) Angew Chem Int Ed 51:3314–3332

29. Froese RDJ, Lombardi C, Pompeo M, Rucker RP, Organ MG (2017) Acc Chem Res 50:2244–2253
30. Fortman GC, Nolan SP (2011) Chem Soc Rev 40:5151–5169
31. Bruneau A, Roche M, Alami M, Messaoudi S (2015) ACS Catal 5:1386–1396
32. Selander N, Szabó KJ (2011) Chem Rev 111:2048–2076
33. Hooshmand SE, Heidari B, Sedghi R, Varma RS (2019) Green Chem 21:381–405
34. Lipshutz BH, Taft BR, Abela AR, Ghorai S, Krasovskiy A, Duplais C (2012) Platin Met Rev 56:62–74
35. Chatterjee A, Ward TR (2016) Catal Lett 146:820–840
36. Gstöttmayr CWK, Böhm VPW, Herdtweck E, Grosche M, Herrmann WA (2002) Angew Chem Int Ed 41:1363–1365
37. Littke AF, Fu GC (1999) Angew Chem Int Ed 37:3387–3388
38. Botella L, Nájera C (2002) Angew Chem Int Ed 41:179–181
39. LeBlond CR, Andrews AT, Sun Y, Sowa JR (2001) Org Lett 3:1555–1557
40. Xu LY, Liu CY, Liu SY, Ren ZG, Young DJ, Lang JP (2017) Tetrahedron 73:3125–3132
41. Oger N, Felpin FX (2016) ChemCatChem 8:1998–2009
42. Mo F, Dong G, Zhang Y, Wang J (2013) Org Biomol Chem 11:1582–1593
43. Zhou T, Ji CL, Hong X, Szostak M (2019) Chem Sci 10:9865–9871
44. Joseph JT, Sajith AM, Ningegowda RC, Nagaraj A, Rangappa KS, Shashikanth S (2015) Tetrahedron Lett 56:5106–5111
45. Rocard L, Hudhomme P (2019) Catalysts 9:4–11
46. Nishikata T, Abela AR, Huang S, Lipshutz BH (2010) J Am Chem Soc 132:4978–4979
47. Xie J, Jin H, Hashmi ASK (2017) Chem Soc Rev 46:5193–5203
48. Baudoin O (2005) Eur J Org Chem 4223–4229
49. Zhang D, Wang Q (2015) Coord Chem Rev 286:1–16
50. Steven A (2019) Synthesis 51:2632–2647
51. Mattiello S, Rooney M, Sanzone A, Brazzo P, Sassi M, Beverina L (2017) Org Lett 19:654–657
52. Sawatlon B, Wodrich MD, Meyer B, Fabrizio A, Corminboeuf C (2019) ChemCatChem 11:4096–4107
53. Anastas P, Eghbali N (2010) Chem Soc Rev 39:301–312

54. Anastas PT, Williamson TC (1996) Green Chemistry: An Overview. In Green Chemistry – Designing Chemistry for the Environment, Anastas PT, Williamson TC (Eds.), American Chemical Series Books, Washington, DC

55. Pagliaro M, Pandarus V, Ciriminna R, Béland F, Demma Carà P (2012) ChemCatChem 4:432–445

56. Garrett CE, Prasad K (2004) Adv Synth Catal 346:889–900

57. Yin L, Liebscher J (2007) Chem Rev 107:133–173

58. McNaught AD, Wilkinson A (1997) IUPAC. Compendium of Chemical Terminology (the "Gold Book"). McNaught AD, Wilkinson A (Comps.), Blackwell Scientific Publications, Oxford

59. Kirschning A (Ed.) (2004) Immobilized Catalysts. Solid Phases, Immobilization and Applications. Springer, Berlin

60. Astruc D, Lu F, Aranzaes JR (2005) Angew Chem Int Ed 44:7852–7872

61. Schmidt AF, Kurokhtina AA (2012) Kinet Catal 53:714–730

62. Schlögl R (2015) Angew Chem Int Ed 54:3465–3520

63. De Vries JG (2006) Dalt Trans 421–429

64. Heidenreich RG, Köhler K, Krauter JGE, Pietsch J (2002) Synlett 7:1118–1122

65. Galaffu N, Man SP, Wilkes RD, Wilson JRH (2007) Org Process Res Dev 11:406–413

66. Ananikov VP, Beletskaya IP (2012) Organometallics 31:1595–1604

67. Kashin AS, Ananikov VP (2013) J Org Chem 78:11117–11125

68. Cantillo D, Kappe CO (2015) ChemCatChem 6:3286–3305

69. De Meijere A, Brse S, Oestreich M (Eds.) (2014) Metal Catalyzed Cross-Coupling Reactions and More. Wiley-VCH, Weinheim

70. Molander GA, Wolf JP, Larhed M (Eds.) (2013) Science of Synthesis: Cross Coupling and Heck Type Reactions. Georg Thieme Verlag, Stuttgart

71. Fihri A, Bouhrara M, Nekoueishahraki B, Basset JM, Polshettiwar V (2011) Chem Soc Rev 40:5181–5203

72. Taladriz-Blanco P, Hervés P, Pérez-Juste J (2013) Top Catal 56:1154–1170

73. Trzeciak AM, Augustyniak AW (2019) Coord Chem Rev 384:1–20

74. Balanta A, Godard C, Claver C (2011) Chem Soc Rev 40:4973–4985

75. Gallon BJ, Kojima RW, Kaner RB, Diaconescu PL (2007) Angew Chem Int Ed 46:7251–7254

76. Narayanan R, El-Sayed MA (2003) J Am Chem Soc 125:8340–8347

77. Narayanan R, El-Sayed MA (2004) J Phys Chem B 108:8572–8580

78. Huang Y, Zheng Z, Liu T, Lü J, Lin Z, Li H, Cao R (2011) Catal Commun 14:27–31

79. Bedford RB, Singh UG, Walton RI, Williams RT, Davis SA (2005) Chem Mater 17:701–707

80. Du Q, Zhang W, Ma H, Zheng J, Zhou B, Li Y (2012) Tetrahedron 68:3577–3584

81. Battilocchio C, Bhawal BN, Chorghade R, Deadman BJ, Hawkins JM, Ley S V. (2014) Isr J Chem 54:371–380

82. Lichtenegger GJ, Maier M, Hackl M, Khinast JG, Gössler W, Griesser T, Kumar VSP, Gruber-Woelfler H, Deshpande PA (2016) J Mol Catal A Chem 426:39–51

83. Lichtenegger GJ, Maier M, Khinast JG, Gruber-Wölfler H (2016) J Flow Chem 6:1–8

84. Hiebler K, Soritz S, Gavric K, Birrer S, Maier MC, Grabner B, Gruber-Woelfler H (2020) J Flow Chem 10:283–294

85. Hiebler K, Dertnig C, Soritz S, Maier MC, Hörmann TR, Grabner B, Gruber-Woelfler H (2020) J Flow Chem 10:259–270

86. Shore G, Morin S, Organ MG (2006) Angew Chem 118:2827–2832

87. Ramarao C, Ley SV, Smith SC, Shirley IM, DeAlmeida N (2002) Chem Commun 10:1132–1133

88. Lee CKY, Holmes AB, Ley SV, McConvey IF, Al-Duri B, Leeke GA, Santos RCD, Seville JPK (2005) Chem Commun 40:2175–2177

89. Leeke GA, Santos RCD, Al-Duri B, Seville JPK, Smith CJ, Lee CKY, Holmes AB, McConvey IF (2007) Org Process Res Dev 11:144–148

90. Lundgren RJ, Stradiotto M (2012) Chem Eur J 18:9758–9769

91. Berrisford DJ, Bolm C, Sharpless KB (1995) Angew Chem Int Ed 34:1059-1070

92. Engle KM, Yu JQ (2013) J Org Chem 78:8927–8955

93. Colacot TJ (2009) FibreCat (polypropylene-supported Pd-phosphine complexes). In Encyclopedia of Reagents for Organic Synthesis, Paquette LA (Ed.), Wiley, New York

94. Pd(II) EnCat™ (2006) Reaxa Limited. https://www.sigmaaldrich.com/content/dam/sigma-aldrich/docs/Aldrich/Brochure/al_pd-iiencat_techflier.pdf. Accessed 30 Mar 2020

95. Nishio R, Sugiura M, Kobayashi S (2005) Org Lett 7:4831–4834

96. Ibrahim MB, Abdullahi IM, Suleiman R, Fettouhi M, El Ali B (2018) Arab J Sci Eng 43:271–280

97. Gömann A, Deverell JA, Munting KF, Jones RC, Rodemann T, Canty AJ, Smith JA, Guijt RM (2009) Tetrahedron 65:1450–1454

98. Chen W, Li P, Wang L (2011) Tetrahedron 67:318–325

99. Gruber-Woelfler H, Radaschitz PF, Feenstra PW, Haas W, Khinast JG (2012) J Catal 286:30–40

100. Bolton KF, Canty AJ, Deverell JA, Guijt RM, Hilder EF, Rodemann T, Smith JA (2006) Tetrahedron Lett 47:9321–9324

101. Fleckenstein CA, Plenio H (2010) Chem Soc Rev 39:694–711

102. Pandarus V, Gingras G, Béland F, Ciriminna R, Pagliaro M (2012) Org Process Res Dev 16:117–122

103. Phan NTS, Brown DH, Styring P (2004) Tetrahedron Lett 45:7915–7919

104. Hamlin J, Hirai K, Millan A, Maitlis P (1980) J Mol Catal 7:543–544

105. Rebek J, Gaviña F (1974) J Am Chem Soc 96:7112–7114

106. Crabtree RH (2012) Chem Rev 112:1536–1554

107. Huang L, Ang TP, Wang Z, Tan J, Chen J, Wong PK (2011) Inorg Chem 50:2094–2111

108. Chen JS, Vasiliev AN, Panarello AP, Khinast JG (2007) Appl Catal, A 325:76–86

109. Barreiro EM, Hao Z, Adrio LA, van Ommen JR, Hellgardt K, Hii KK (Mimi) (2018) Catal Today 308:64–70

110. Bourouina A, Meille V, de Bellefon C (2018) J Flow Chem 8:117–121

111. Felder RM, Rousseau RW (2000) Elementary principles of chemical processes. Wiley, New York

112. Plutschack MB, Pieber B, Gilmore K, Seeberger PH (2017) Chem Rev 117:11796–11893

113. Darvas F, Dorman G, Hessel V (2014) Flow Chemistry Organic: Volume 1: Fundamentals. Walter de Gruyter, Berlin

114. Gutmann B, Cantillo D, Kappe CO (2015) Angew Chem Int Ed 54:6688–6728

115. Porta R, Benaglia M, Puglisi A (2016) Org Process Res Dev 20:2–25

116. Baumann M, Baxendale IR (2015) Beilstein J Org Chem 11:1194–1219

117. Roberge DM, Zimmermann B, Rainone F, Kockmann N (2008) Org Process Res Dev 12:905-910

118. Poechlauer P, Manley J, Broxterman R, Gregertsen B, Ridemark M (2012) Org Process Res Dev 16:1586–1590

119. Hessel V (2009) Chem Eng Technol 32:1655–1681

120. Gutmann B, Kappe CO (2017) J Flow Chem 7:65–71

121. Wiles C, Watts P (2014) Green Chem 16:55–62

122. Newman SG, Jensen KF (2013) Green Chem 15:1456–1472

123. Reizman BJ, Jensen KF (2016) Acc Chem Res 49:1786–1796

124. Lee SL, O'Connor TF, Yang X, Cruz CN, Chatterjee S, Madurawe RD, Moore CMV, Yu LX, Woodcock J (2015) J Pharm Innov 10:191–199

125. Wegner J, Ceylan S, Kirschning A (2011) Chem Commun 47:4583–4592

126. Benaskar F, Ben-Abdelmoumen A, Patil N, Rebrov E, Meuldijk J, Hulshof L, Hessel V, Krtschil U, Schouten J (2011) J Flow Chem 1:74–89

127. Schaber SD, Gerogiorgis DI, Ramachandran R, Evans JMB, Barton PI, Trout BL (2011) Ind Eng Chem Res 50:10083–10092

128. FDA Perspective on Continuous Manufacturing (2012) US Food and Drug Administration. https://www.fda.gov/downloads/AboutFDA/CentersOffices/OfficeofMedicalProductsandTobacco/CDER/UCM341197.pdf. Accessed 21 Jan 2019

129. Statement from FDA (2018) US Food and Drug Administration. https://www.fda.gov/NewsEvents/Newsroom/PressAnnouncements/ucm619024.htm. Accessed 30 Oct 2018

130. Eli Lilly and Company to invest 35M in Kinsale Campus (2016) Businessworld. https://www.businessworld.ie/article.php?alias=Eli-Lilly-and-Company-to-invest-35m-in-Kinsale-campus-563641. Accessed 1 April 2020

131. Pharma giant GSK opens $130m manufacturing facility in Singapore (2019) Singapore Economic Development Board. https://www.edb.gov.sg/en/news-and-events/news/pharma-giant-gsk-opens-130m-manufacturing-facility-in-singapore.html. Accessed 1 April 2020

132. Steiner R, Jornitz M (2017) Continuous Processing in the Pharmaceutical Industry: Status and Perspective. In Continuous Manufacturing of Pharmaceuticals, Kleinebudde P, Khinast J, Rantanen J (Eds.), Wiley, New York

133. Desai B, Dixon K, Farrant E, Feng Q, Gibson KR, Van Hoorn WP, Mills J, Morgan T, Parry DM, Ramjee MK, Selway CN, Tarver GJ, Whitlock G, Wright AG (2013) J Med Chem 56:3033–3047

134. Hwang YJ, Coley CW, Abolhasani M, Marzinzik AL, Koch G, Spanka C, Lehmann H, Jensen KF (2017) Chem Commun 53:6649–6652

135. Baranczak A, Tu NP, Marjanovic J, Searle PA, Vasudevan A, Djuric SW (2017) ACS Med Chem Lett 8:461–465

136. May SA (2017) J Flow Chem 7:137–145

137. Harsanyi A, Conte A, Pichon L, Rabion A, Grenier S, Sandford G (2017) Org Process Res Dev 21:273–276

138. Marsini MA, Buono FG, Lorenz JC, Yang BS, Reeves JT, Sidhu K, Sarvestani M, Tan Z, Zhang Y, Li N, Lee H, Brazzillo J, Nummy LJ, Chung JC, Luvaga IK, Narayanan BA, Wei X, Song JJ, Roschangar F, Yee NK, Senanayake CH (2017) Green Chem 19:1454–1461

139. Heider PL, Born SC, Basak S, Benyahia B, Lakerveld R, Zhang H, Hogan R, Buchbinder L, Wolfe A, Mascia S, Evans JMB, Jamison TF, Jensen KF (2014) Org Process Res Dev 18:402–409

140. Mascia S, Heider PL, Zhang H, Lakerveld R, Benyahia B, Barton PI, Braatz RD, Cooney CL, Evans JMB, Jamison TF, Jensen KF, Myerson AS, Trout BL (2013) Angew Chem Int Ed 52:12359–12363

141. Adamo A, Beingessner RL, Behnam M, Chen J, Jamison TF, Jensen KF, Monbaliu JCM, Myerson AS, Revalor EM, Snead DR, Stelzer T, Weeranoppanant N, Wong SY, Zhang P (2016) Science 352:61–67

142. Rogers L, Briggs N, Achermann R, Adamo A, Azad M, Brancazio D, Capellades G, Hammersmith G, Hart T, Imbrogno J, Kelly LP, Liang G, Neurohr C, Rapp K, Russell MG, Salz C, Thomas DA, Weimann L, Jamison TF, Myerson AS, Jensen KF (2020) Org Process Res Dev, https://doi.org/10.1021/acs.oprd.0c00208

143. F3 factory final report to European commission research and innovation (2013) European Commission. https://cordis.europa.eu/docs/results/228867/final1-f3-factory-keymessages-and-casestudy-summaries.pdf. Accessed 1 Apr 2020

144. Cole KP, Groh JMC, Johnson MD, Burcham CL, Campbell BM, Diseroad WD, Heller MR, Howell JR, Kallman NJ, Koenig TM, May SA, Miller RD, Mitchell D, Myers DP, Myers SS, Phillips JL, Polster CS, White TD, Cashman J, Hurley D, Moylan R, Sheehan P, Spencer RD, Desmond K, Desmond P, Gowran O (2017) Science 356:1144–1151

145. May SA, Johnson MD, Braden TM, Calvin JR, Haeberle BD, Jines AR, Miller RD, Plocharczyk EF, Rener GA, Richey RN, Schmid CR, Vaid RK, Yu H (2012) Org Process Res Dev 16:982–1002

146. May SA, Johnson MD, Buser JY, Campbell AN, Frank SA, Haeberle BD, Hoffman PC, Lambertus GR, McFarland AD, Moher ED, White TD, Hurley DD, Corrigan AP, Gowran O, Kerrigan NG, Kissane MG, Lynch RR, Sheehan P, Spencer RD, Pulley SR, Stout JR (2016) Org Process Res Dev 20:1870–1898

147. Laporte TL, Spangler L, Hamedi M, Lobben P, Chan SH, Muslehiddinoglu J, Wang SSY (2014) Org Process Res Dev 18:1492–1502

148. Biffis A, Centomo P, Del Zotto A, Zecca M (2018) Chem Rev 118:2249–2295

149. Constable DJC, Dunn PJ, Hayler JD, Humphrey GR, Leazer JL, Linderman RJ, Lorenz K, Manley J, Pearlman BA, Wells A, Zaks A, Zhang TY (2007) Green Chem 9:411–420

150. ONE-FLOW Research Project Home Page. https://one-flow.org. Accessed 20 Feb 2019

6 List of abbreviations

AcCl	Acid chloride
API	Active pharmaceutical ingredient
APT	Attached proton test
aq.	Aqueous
Ar	Aryl residue
BET	Brunauer-Emmet-Teller
BPR	Back pressure regulator
c	Concentration
calcd	Calculated
cat	Catalyst
Ce	Cerium
cGMP	Current good manufacturing practice
DARPA	Defense Advanced Research Projects Agency
DLS	Dynamic light scattering
DoE	Design of Experiments
dr	Diastereomeric ratio
eq.	Equivalents
ES	Electron spray ionization
FDA	U.S. Food and Drug Administration
f_o	Coalescence stability parameter
f_w	Creaming stability parameter
GSK	GlaxoSmithKline
HPLC	High performance liquid chromatography
ICP	Inductively coupled plasma
IR	Infrared
J	Coupling constant
k	Boltzmann constant
L x O.D. x I.D.	Length x outer diameter x inner diameter
m/z	Mass-to-charge ratio
MIDA	*N*-methyliminodiacetic acid
MS	Mass spectrometry
NHC	*N*-heterocyclic carbene
NMR	Nuclear magnetic resonance

NP	Nanoparticles
o/w	Oil-in-water
Pd	Palladium
Pd/C	Palladium on charcoal
PEEK	Polyether ether ketone
PoD	Pharmacy on demand
PTFE	Polytetrafluoroethylene
Q^2	Model predictive power
R	Organic residue
R^2	Coefficient of determination
R_f	Retention factor
RT	Room temperature
sat.	Saturated
SiO_2	Silica gel
Sn	Tin
T	Temperature
t	Time
TOF	Turn over frequency
TON	Turn over number
t_r	Retention time
v	Flow rate
V	Volume
v/v	Volume per volume
w/o	Water-in-oil
w/v	Weight per volume
WHO	World Health Organization
X	Leaving group
x_{90}	90^{th} percentile of the cumulative undersize distribution by volume
XPS	X-ray photoelectron spectroscopy
XRD	X-ray diffraction
δ	Chemical shift / oxygen vacancy
θ	Contact angle
λ	Wavelength
τ	Residence time

B Heterogeneous Pd catalysts as emulsifiers in Pickering emulsions for integrated multistep synthesis in flow chemistry

The following chapter is taken from the same-titled journal article published in Beilstein Journal of Organic Chemistry by Hiebler et al. [Hiebler K, Lichtenegger GJ, Maier MC, Park ES, Gonzales-Groom R, Binks BP, Gruber-Woelfler H (2018) Beilstein J Org Chem 14:648-658].

Within the "compartmentalized smart factory" approach of the ONE-FLOW project the implementation of different catalysts in "compartments" provided by Pickering emulsions and their application in continuous flow is targeted. We present here the development of heterogeneous Pd catalysts that are ready to be used in combination with biocatalysts for catalytic cascade synthesis of active pharmaceutical ingredients (APIs). In particular, we focus on the application of the catalytic systems for Suzuki-Miyaura cross-coupling reactions, which is the key step in the synthesis of the targeted APIs valsartan and sacubitril. An immobilized enzyme will accomplish the final product formation via hydrolysis. In order to create a large interfacial area for the catalytic reactions and to keep the reagents separated until required, the catalyst particles are used to stabilize Pickering emulsions of oil and water. A set of Ce-Sn-Pd oxides with the molecular formula $Ce_{0.99-x}Sn_xPd_{0.01}O_{2-\delta}$ (x= 0-0.99) has been prepared utilizing a simple single-step solution combustion method. The high applicability of the catalysts for different functional groups and their minimal leaching behavior is demonstrated with various Suzuki-Miyaura cross-coupling reactions in batch as well as in continuous flow employing the so-called "plug & play reactor". Finally, we demonstrate the use of these particles as the sole emulsifier of oil-water emulsions for a range of oils.

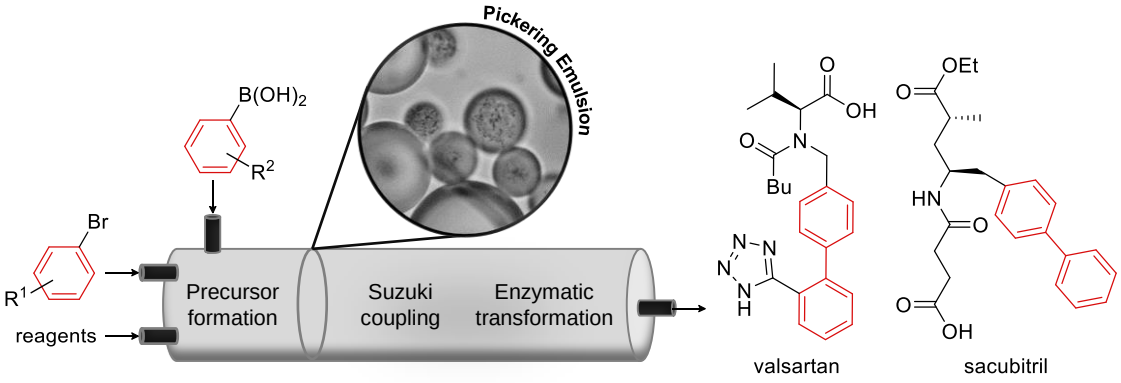

1 Introduction

Palladium (Pd) catalysis has been established as a key component in the toolbox of organic chemists. Reactions that are catalyzed by palladium benefit from the remarkable versatility and functional-group tolerance of the transition metal as well as the ability to control the reaction selectivity [1-3]. Pd catalysts have been implemented in the synthesis of various active pharmaceutical ingredients, natural products and agrochemicals amongst others [4]. In particular, Pd-catalyzed C-C cross-coupling reactions have become indispensable in many modern synthetic protocols both in the laboratory and on an industrial scale. A highly important representative of this class of transformation is the Suzuki-Miyaura reaction [5,6], involving the coupling of aryl halides with phenylboronic acids yielding the corresponding biphenyls as product [7]. The biphenyl unit is a common structural motif in various pharmaceutically active agents and plays a crucial role in the binding affinity and the oral bioavailability of diverse APIs [8], including antihypertensive [9] and antitumor agents [10]. Advantages of the Suzuki-Miyaura coupling are mild reaction conditions, commercial availability of a large number of boronic acids and simple product purification [7]. Concerning the transition metal source for C-C cross-coupling reactions, homogeneous and heterogeneous Pd catalysts are utilized.

The employment of a variety of different ligands such as phosphines, amines and carbenes allows precise tuning of the properties of homogeneous Pd catalysts, which led to significant improvements in turn over number (TON), reaction rates, enantioselectivity as well as catalyst robustness and lifetime. Apart from that, ligand-free Pd catalysts are also known in the literature [11,12]. However, homogeneous Pd catalysis often requires catalyst loadings in the order of mol% to achieve effective coupling and suffers from catalyst reuse and recycling problems [11,13]. Furthermore, concerning the synthesis of pharmaceuticals, tedious purification steps need to be performed in order to remove residual metals. Considering these drawbacks of homogeneous catalysis, easily recoverable and recyclable heterogeneous Pd catalysts are much more attractive with respect to ecological and economical aspects [13]. One possibility to prepare heterogeneous transition metal catalysts is to immobilize palladium directly on a solid support such as activated carbon [14], zeolites [15], modified silica [16-18] or molecular sieves [19] to name but a few. Another option is the complexation of palladium by ligands which are covalently bound to the support material [12]. One example of such a catalyst was

reported by our group using a bis(oxazoline) ligand bonded to 3-mercaptopropyl-functionalized silica [20]. Alternatively, the use of unsupported Pd nanoparticles or encapsulated Pd complexes are strategies to realize heterogeneous palladium catalysis [21]. Immobilization of catalytic systems on solid supports can mitigate a lot of problems of homogeneous catalysts, for example, it allows a straightforward removal of the catalyst from the reaction system. However, most heterogeneous approaches require more drastic reaction conditions in comparison to their homogeneous counterparts, which often introduce undesirable leaching effects [17,20,22,23]. Consequently, the synthesis and application of unprecedented nonleaching heterogeneous palladium catalysts for cross-coupling reactions have been investigated intensively and vigorous efforts are made to implement them in industrial synthesis [11,13,20].

The idea of the so-called “compartmentalized smart factory” within the ONE-FLOW project [24] is to go a step further and combine different kinds of chemo- and biocatalysts in one “compartment". For this approach and to keep the reagents separated until required, the catalysts are contained within Pickering emulsions of oil and water phases. Emulsions are thermodynamically unstable mixtures of two immiscible liquids, e.g. oil and water, with typical droplet sizes in the micron range. Traditionally, emulsions have been kinetically stabilized by molecular species including surfactants, polymers or proteins all of which possess water-liking groups and oil-liking groups enabling them to adsorb to freshly created oil-water interfaces preventing to some extent coalescence between neighboring droplets [25]. So-called Pickering emulsions, however, are stabilized solely by solid colloidal particles which can adsorb to droplet interfaces forming a protective layer endowing the emulsion with extremely high stability to coalescence [26]. Examples of suitable particles include silica, alumina, metals, polymers and proteins of different sizes and shapes. One of the key factors influencing the effectiveness of a particle to act as an emulsifier is its wettability normally quantified by the contact angle θ the particle makes with the oil-water interface (through water). For relatively hydrophilic particles, θ<90° and preferred emulsions are oil-in-water (o/w). For relatively hydrophobic particles, θ>90° and water-in-oil (w/o) emulsions are preferred [27]. Particles of intermediate wettability are well held at a fluid interface as the energy required to remove them can be several thousand kT (k is Boltzmann constant, T is temperature); such particles are deemed irreversibly adsorbed under quiescent conditions. As summarized recently [28], the two liq-

uids may be oil and water, two immiscible oils or even two immiscible water phases and different particles need to be designed in each case to impart stabilization of dispersed drops in a continuous phase. In 2010, Crossley et al. [29] put forward the idea that catalyst particles may both act simultaneously as an emulsifier in Pickering emulsions and serve as the catalyst in which water-soluble reactants and oil-soluble reactants react at the oil-water interface populated by catalyst particles. They deposited metallic Pd onto carbon nanotube-inorganic oxide hybrid nanoparticles and used them in emulsions for the hydrodeoxygenation of a phenolic compound and the hydrogenation and etherification of an aldehyde. The advantages of such a system include a high interfacial area for reaction, the ultrastability of emulsion drops during reaction and easy recovery of the catalyst particles and products as emulsions may be rendered unstable subsequently. A mini-review of the area of Pickering emulsion interfacial catalysis appeared in 2015 [30].

In this work an outlook on the planned realization of the integrated multistep continuous flow synthesis of valsartan and sacubitril within the frame of the ONE-FLOW project is given. The compounds are well known as APIs in a combination drug for the treatment of hypertension and chronic heart failure (Entresto®, Novartis) [31-35]. A preliminary scheme of the planned synthetic route is shown in Figure B-1. As can be seen, the key step of our processes is the formation of the biaryl unit via a Suzuki-Miyaura cross-coupling reaction. To provide solid Pd catalysts with a high potential for the planned approaches, a set of Ce-Sn-Pd oxides with the molecular formula $Ce_{0.99-x}Sn_xPd_{0.01}O_{2-\delta}$ (x= 0-0.99; δ indicates the oxygen vacancies in the crystal lattice of the oxides, the values for δ are rather small, thus the value for oxygen is ≈2, [36,37]) is tested for that approach. The tolerance of the catalysts towards different functional groups and their minimal leaching, which has already been demonstrated with various Suzuki-Miyaura cross-coupling reactions in batch as well as in continuous flow employing the so-called plug & play reactor [38], is summarized. In this work we present for the first time the use of these particles as the sole emulsifier of oil-water emulsions for a range of oils.

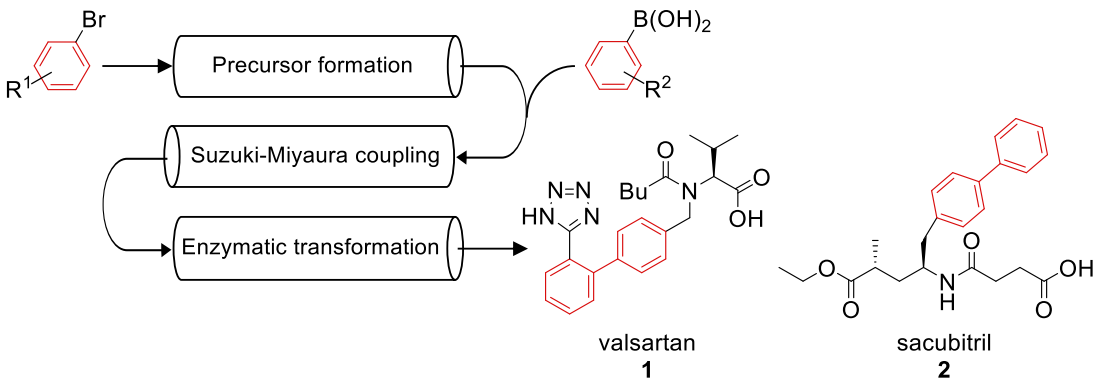

Figure B-1: Targeted integrated multistep syntheses of valsartan, **1** and sacubitril, **2**.

2 Results and discussion

2.1 Metal oxide supported ionic palladium catalysts

2.1.1 Synthesis

The heterogeneous Ce-Sn-Pd compounds were synthesized using the solution combustion technique according to Baidya et al. [39] with slight modifications [37]. The benefits of this single-step method are the simplicity of the procedure, the usage of nontoxic and inexpensive precursors and that several grams of material can be obtained within hours. To study the influence of the amounts of Ce and Sn on the catalytic behavior, five mixed oxides with the molecular formula $Ce_{0.99-x}Sn_xPd_{0.01}O_{2-\delta}$ (x= 0, 0.20, 0.495, 0.70 and 0.99) were synthesized and attained in quantitative amounts (>99%). The obtained solids can be used directly for characterization as well as for the activity tests.

2.1.2 Characterization

The Ce-Sn-Pd catalysts were analyzed using different state-of-the-art methods. Details of the characterization were published recently [37]. Here, only the most important characteristics are summarized. The obtained X-ray diffraction (XRD) profiles proved the nanocrystallinity of the catalyst particles, which either show single phase cubic, tetragonal or a more amorphous cubic/tetragonal mixed phase structure depending on the content of Sn. As far as palladium substitution in the lattice is concerned, XRD and X-ray photoelectron spectroscopy (XPS) analysis approved the predominant cationic nature of incorporated palladium (Pd^{2+}) and revealed only minor amounts of metallic Pd. Brunauer-Emmett-Teller (BET) measurements showed

that the specific surface areas of the five catalysts range from 27-98 m^2/g. Particle sizes of ≈10-100 µm were measured with a monomodal size distribution for the cerium-rich catalysts and a polymodal distribution for catalysts rich in tin.

2.2 Suzuki-Miyaura coupling reactions

2.2.1 Batch reactions

The catalytic activity of the synthesized catalysts in the Suzuki-Miyaura reaction was investigated using phenylboronic acid **3** in combination with various bromoarenes **4a-e**, featuring *ortho*- and *para*-substitution of electron-donating as well as electron-withdrawing functional groups, as coupling partners (Scheme B-1). Concerning the targeted synthesis of **1**, aryl halide **4e** was of special interest as the cyano group is known to be convertible to the *ortho*-tetrazole moiety [9] present in the API. Based on prior optimization studies [37], reactions were performed in EtOH/H2O=7:3 (v/v) at 75 °C using K_2CO_3 as inorganic base. Phenylboronic acid as well as K_2CO_3 were added in 50% molar excess relative to the corresponding aryl bromide, whereas a catalyst amount corresponding to 0.05 mol% of Pd was used. The reaction progress was monitored by high performance liquid chromatography (HPLC).

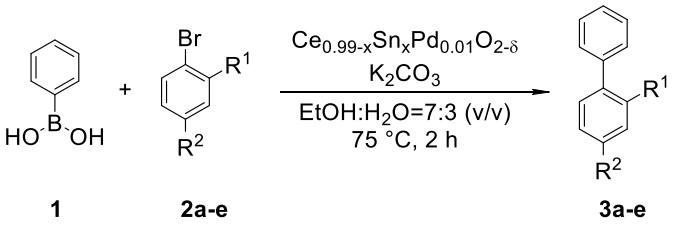

1 **2a-e** **3a-e**

Scheme B-1: Suzuki-Miyaura coupling of phenylboronic acid **3** with various bromoarenes **4a-e** (**a**: R^1= H, R^2= CH_3; **b**: R^1= H, R^2= OH; **c**: R^1= H, R^2= $COOCH_3$; **d**: R^1= H, R^2= CF_3; **e**: R^1= CN, R^2= H).

In general, the catalysts with tin proportions of 0.20, 0.79 and 0.99 proved to be most effective in the desired transformations with exceptional high activities (turn over frequency, TOF >12,000 h^{-1}) in all tested Suzuki-Miyaura cross-coupling reactions. While *para*-substituted bromoarenes were converted quantitatively within a reaction time of 2 h with an order of 4-bromoacetophenone (**4c**) ≥ 4-bromobenzotrifluoride (**4d**) > 4-bromotoluene (**4a**) > 4-bromophenol (**4b**), the coupling of 2-bromobenzonitrile (**4e**) required the 4-fold amount of catalyst to reach full conversion. *Para*-bromobenzenes containing electron-withdrawing substituents showed higher reactivity than bromobenzenes containing electron-donating groups. When

$Ce_{0.495}Sn_{0.495}Pd_{0.01}O_{2-\delta}$ was employed as catalyst, however, the catalytic activity was found to be significantly lower and the binary oxide $Ce_{0.99}Pd_{0.01}O_{2-\delta}$ showed to be least efficient for the explored Suzuki-Miyaura couplings. Regarding the selectivity of the catalysts in the selected cross-coupling reactions, no bromoarene-deriving side products (dehalogenation product Ar' and bromoarene homocoupling product Ar'Ar') could be detected. However, both boronic acid homocoupling (ArAr) and boronic acid oxidation (ArOH) occurred to a small extent as indicated by HPLC. As the side product formation mainly occurs when the bromoarene coupling partner gets depleted, highest reaction selectivity (up to 99.5% [37]) can be achieved by termination of the transformation just at the moment of full conversion.

In conclusion, $Ce_{0.99-x}Sn_xPd_{0.01}O_{2-\delta}$ (x= 0-0.99) proved to be very active catalysts for Suzuki-Miyaura reactions. Based on the experimental results, the tin and cerium content of the catalysts, respectively, do not seem to be directly connected to their catalytic activity. Nevertheless, there are indications that the surface area and the particle size distribution play a role in the catalytic performance of the palladium substituted metal oxides. In view of the aimed application of the Pd metal oxides for targeted API synthesis, the obtained results are very promising although the relevant transformation needed higher catalyst amounts.

2.2.2 Recyclability and metal leaching

In the context of heterogeneous catalysis, it is essential to investigate the actual nature of the catalysts during the reaction as well as the reusability and stability of the catalytic active compounds. To assess the reusability of the heterogeneous catalysts, the Pd-substituted metal oxides were subjected to Suzuki-Miyaura couplings of 4-bromotoluene with phenylboronic acid in five subsequent reactions, i.e. after one reaction was finished, the particles were separated from the solution via filtration, washed, dried and reused for a new reaction with new substrates. Although during the filtration and drying steps catalyst loss could not be prevented, a high degree of recyclability was established and only a minor decrease of mass specific catalyst activity was observed [37].

As far as palladium leaching is concerned, ICP-MS measurements revealed 0.06-0.14 mg/L Pd in the reaction solution after the third reaction run [37]. This finding is in accordance with the theory that the actual catalyst of the coupling reaction is leached palladium and supports a

reaction mechanism via homogeneous catalysis. For the purpose of elucidating the homo- or heterogeneous nature of synthesized catalysts in more detail, further studies including a hot filtration test and catalyst poisoning [40,41] were performed [37]. In summary, the obtained results confirm a palladium release and capture mechanism. The synthesized heterogeneous metal oxides act as precatalysts, which slowly release minimal amounts of active palladium into solution. However, as levels of leached Pd are below the regulatory limits for orally administered pharmaceuticals [41], the mixed metal oxides have high potential as heterogeneous catalysts for the synthesis of APIs, such as **1** and **2**.

2.2.3 Suzuki-Miyaura reactions in continuous flow

After the applicability and versatility of the palladium substituted cerium tin oxides was confirmed in batch, the aim was to implement the catalysts in a continuous flow setup, which is also suitable for the multistep synthesis of **1** and **2**. Therefore, the so-called plug & play reactor, a versatile device featuring both exchangeable reaction segments and modules for heating/cooling and mixing [38], was employed to test the activity and stability of the catalysts in continuous flow. In the plug & play reactor the reaction media flow through 1 mm tubes embedded in channels filled with heating/cooling media, ensuring both enhanced mixing and rapid heat transfer. Commercially available HPLC columns filled with catalyst particles serve as fixed bed reactors and contribute to the high versatility of the device. With this approach, gas-solid, liquid-solid as well as gas-liquid-solid reactions can be realized within the upper performance limits of 200 °C and 40 bar [38].

The performance of the plug & play reactor in terms of continuous Suzuki-Miyaura cross-coupling was investigated using phenylboronic acid (**3**) in combination with different *ortho*- and *para*-substituted bromoarenes in aqueous ethanolic mixtures employing K_2CO_3 as base [38]. Monitoring of the reaction progress via inline UV-vis spectroscopy as well as offline HPLC analysis [38] led to the result that after an initial induction phase (≈30 min) a stable process was achieved, forming the respective products in high yields (up to 99%) for more than 30 h with excellent selectivity without catalyst deactivation [42]. As expected, increasing the catalyst amount and residence time by use of three sequential fixed bed reactors enhanced product formation and conversions >90% were obtained. Furthermore, analysis of the crystalline prod-

uct by means of ICP-MS confirmed only trace amounts of leached cerium (≈1 mg/kg final product), tin (≈0.2 mg/kg product) and palladium (≈1 mg/kg product). In addition to that, direct product isolation via integrated crystallization was successfully implemented as a continuous downstream protocol [42].

Concluding, the plug & play reactor is a highly versatile device, which is applicable for different kinds of heterogeneously catalyzed reactions. The results obtained strongly indicate the high potential for realizing other reactions of interest to produce pharmaceutical and fine chemical intermediates in continuous flow, including the multistep synthesis of valsartan (**1**) and sacubitril (**2**). In addition to the approach with the compartmentalized catalysts in Pickering emulsions and thus the usage of one HPLC column filled with catalytic active compounds, the setup is optimal to employ multiple columns filled with different types of catalysts. Furthermore, the implementation of other functionalized materials, e.g. solid-supported scavengers for leached metals, is straightforward.

2.3 Size reduction of catalyst particles

As mentioned before, the as-synthesized catalyst particles have particle diameters in the range of 10-100 µm. Since the stabilization of micron-sized Pickering emulsion droplets requires particle sizes <1 µm, a decrease of particle size was necessary. For that purpose, a Retsch PM10 planet ball mill equipped with metal balls (d = 8 mm, 500 rpm, 10 min milling time) was used for dry milling of powdered $Ce_{0.495}Sn_{0.495}Pd_{0.01}O_{2-\delta}$ and wet milling (suspension in water) of $Ce_{0.20}Sn_{0.79}Pd_{0.01}O_{2-\delta}$, respectively. These two catalysts were chosen since they showed the highest activities for Suzuki-Miyaura couplings in batch [37] and continuous flow [38]. After milling, the coarse and fine fractions of the particles were separated via sedimentation. For this purpose, 2 g of catalyst were suspended in 1 L water, the particles were deaggregated by ultrasonic treatment and left to sediment. After a sedimentation time of 35 min, the upper half of the suspension was removed with a pipette and fractions were dried in a muffle furnace (120 °C until dryness, then at 350 °C overnight). Table B-1 and Figure B-2 indicate that for both catalysts 90% of the particles in the separated fines fractions are <5 µm (= x_{90}) in diameter. The overall yield for this particle fraction was 20%, but future work will concentrate on the optimization of this step. Microscopic pictures indicate spherical particle shape. The density of the particles, also important for the usage of the particles as stabilizers

in Pickering emulsions, was determined to be 5.97 g/cm^3 for $Ce_{0.495}Sn_{0.495}Pd_{0.01}O_{2-\delta}$ and 5.38 g/cm^3 for $Ce_{0.20}Sn_{0.79}Pd_{0.01}O_{2-\delta}$.

Table B-1: x_{90} and specific surface area of the catalysts after milling and separation via sedimentation.

Catalyst	x_{90} [µm]	BET surface area [m^2/g]
$Ce_{0.495}Sn_{0.495}Pd_{0.01}O_{2-\delta}$	2.84	28
$Ce_{0.20}Sn_{0.79}Pd_{0.01}O_{2-\delta}$	4.20	58

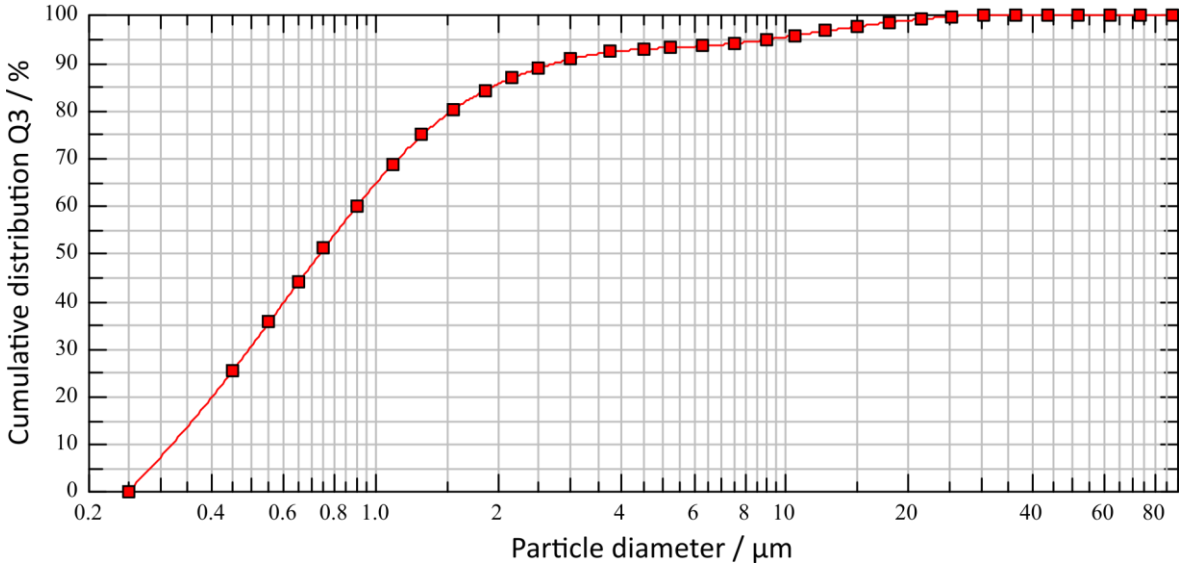

Figure B-2: Particle size distribution of $Ce_{0.495}Sn_{0.495}Pd_{0.01}O_{2-\delta}$ after size reduction via milling and separation via sedimentation in water.

2.4 Implementation of the catalyst particles in Pickering emulsions

For simplicity, we have investigated emulsions containing equal volumes of water (Milli-Q) and oil with catalyst particles first dispersed in water using an ultrasonic probe (Jencons Vi-braCell, 5 min, 130 W). The oils chosen are the aliphatic alkane octane (Sigma, >99%, density 0.699 g/cm^3), the cyclic alkane cyclohexane (Fisher Scientific, >99%, density 0.774 g/cm^3) and the aromatic oil toluene (VWR Chemicals, >99%, density 0.865 g/cm^3). Emulsions were pre-pared using a rotor-stator homogenizer (IKA T25 digital Ultra-Turrax) with a stator diameter of 8 mm for 1 min at 10,000 rpm at room temperature. Emulsion type was established using the drop test (addition of a drop of emulsion to either water or oil). The stability of emulsions to gravity-induced creaming or coalescence was assessed by monitoring the position of the water-emulsion or oil-emulsion interfaces, respectively. Microscopy images of the emulsions

were recorded using an Olympus BX53 microscope with GXCAM-U318 camera attached and GXCapture-T software.

2.4.1 Catalyst $Ce_{0.495}Sn_{0.495}Pd_{0.01}O_{2-\delta}$

Being relatively hydrophilic mixed oxides, both types of catalysts formed in water suspensions with discrete particles, at least at low concentration (0.05 wt%) (see Figure B-3).

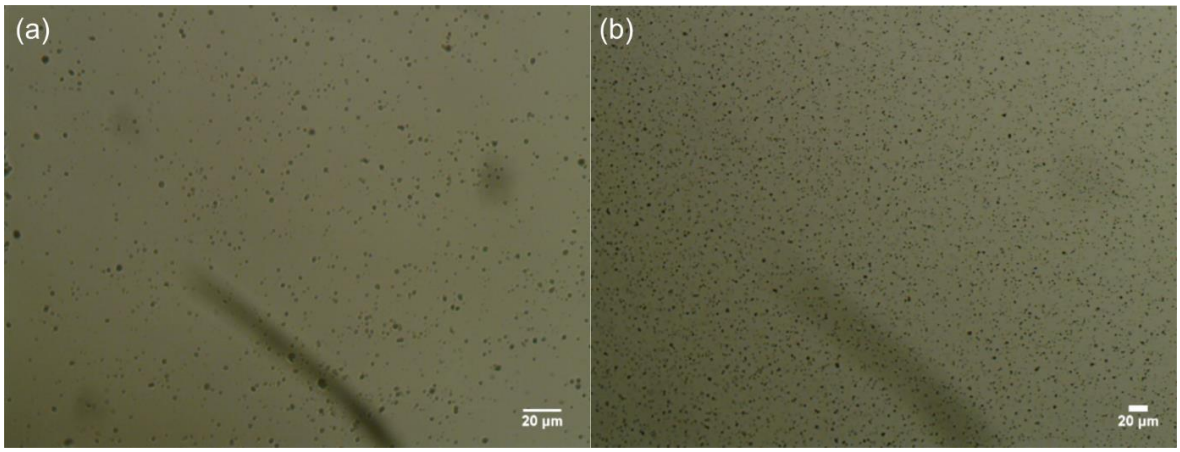

Figure B-3: Optical microscope images of fresh aqueous dispersions, 0.05 wt%, of (a) $Ce_{0.495}Sn_{0.495}Pd_{0.01}O_{2-\delta}$ and (b) $Ce_{0.20}Sn_{0.79}Pd_{0.01}O_{2-\delta}$ particles.

Emulsions of all the oils are o/w in which their stability to both creaming and coalescence as well as their average droplet size depend markedly on particle concentration. As an example, the appearance of cyclohexane-in-water emulsions with time for three selected particle concentrations can be seen in Figure B-4. This pattern of behavior is followed with the other two oils also. For particle concentrations in water between 0.01 and 0.10 wt% (upper in Figure B-4), emulsions reasonably stable to coalescence are formed although they exhibit creaming with the separation of a lower serum from which nonadsorbed particles sediment. Although the initial oil volume fraction in emulsions is 0.5 (t = 0), that in creamed emulsions after 1 day reaches as high as 0.7-0.8. Such excellent stability to coalescence in high internal phase emulsions is due to the particle layer on droplet interfaces acting as a barrier to drop fusion. Between 0.20 and 0.50 wt% (middle), although an emulsion forms initially, it rapidly coalesces until complete phase separation in some cases. At and above 1.0 wt% (lower), emulsions can be re-stabilized to some extent although visible oil drops (mm-sized) develop within the cream.

Figure B-4: Photos of vessels containing cyclohexane-in-water emulsions stabilized by particles of $Ce_{0.495}Sn_{0.495}Pd_{0.01}O_{2-\delta}$ at concentrations in water of 0.03 wt% (upper), 0.30 wt% (middle) and 1.0 wt% (lower) at different times since preparation. A is the aqueous dispersion of particles, B is after addition of oil but before emulsification.

For the stable emulsions at low particle concentrations, optical microscopy reveals the presence of catalyst particles around oil droplets in water, Figure B-5. Roughly, an increase in particle concentration results in increased coverage of droplets by particles. Since around 50% of the particles are sub-micron in size, however, a fraction of droplet interfaces may be coated in these particles which are of a size smaller than the resolution limit of the microscope. By contrast, the larger sized particles appear aggregated at droplet interfaces. The variation in the average oil droplet diameter with particle concentration is given in Figure B-6 (top). Relatively small drops (between 70 and 150 µm) exist below 0.1 wt%, drops as large as 5 mm exist at 0.3 wt% after which the drop size decreases progressively to around 1 mm at 2 wt%. For emulsion stability with respect to coalescence, we define a parameter f_o = (vol. free oil at time *t*/vol. oil initially). Likewise, the stability to creaming is given by f_w = (vol. free water at time *t*/vol. water initially). Values of both parameters can vary from 0 (completely stable) to 1 (complete phase separation). After one month, the variation of f_o and f_w with particle concentration

is given in Figure B-6 (bottom). Up to 0.1 wt%, creaming is extensive and although some coalescence ensues, the residual emulsions remain stable for at least six months. Coalescence is then very extensive at 0.2, 0.3 and 0.5 wt% and mm-sized drops are formed in the early stages. Our first hypothesis was that the sudden increase in emulsion instability at higher particle concentrations may be due to particle aggregation in water prior to emulsification. Such large particle aggregates of high density would be weakly retained at the oil-water interfaces offering little protection to the coalescence between drops. However, a more detailed look at the particle size in water at different particle concentrations (Figure B-7) as well as the unexpected results of the zeta potential and the pH value at different particle concentrations (Figure B-8) are an indication that other effects, such as possible reactions of the particles with water, are the reason for the instability of the emulsions at higher concentrations.

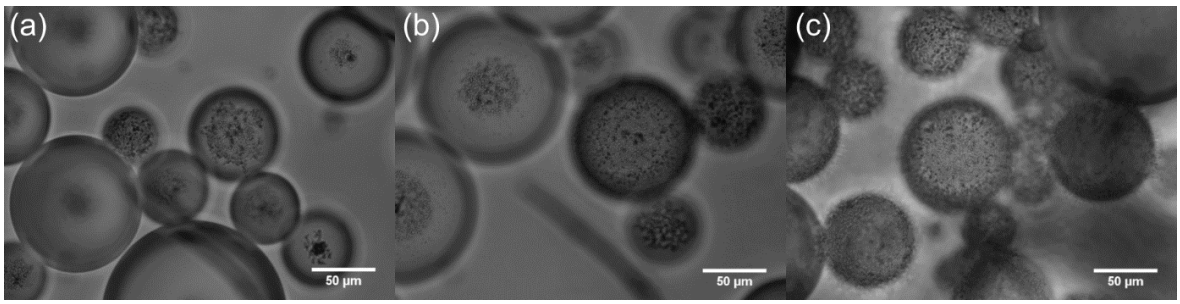

Figure B-5: Optical microscopy images of cyclohexane-in-water emulsions of Figure B-4 after 1 month for particle concentrations of (a) 0.02 wt%, (b) 0.05 wt% and (c) 0.10 wt%.

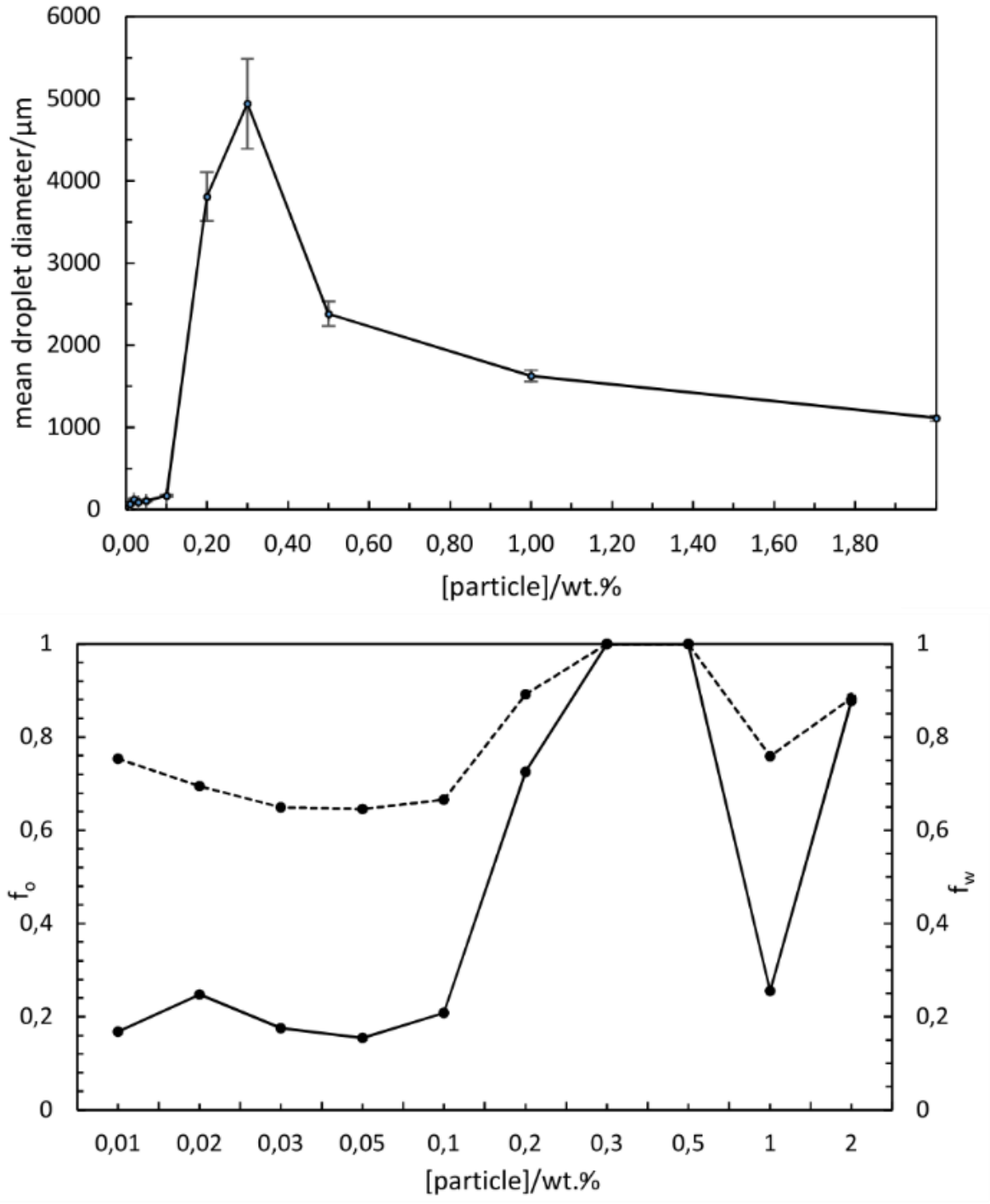

Figure B-6: (upper) Mean emulsion droplet diameter after 30 min as a function of particle concentration for system in Figure B-4; (lower) variation of f_o (solid line) and f_w (dashed line) after 1 month with particle concentration for emulsions in Figure B-4 (note nonlinear scale).

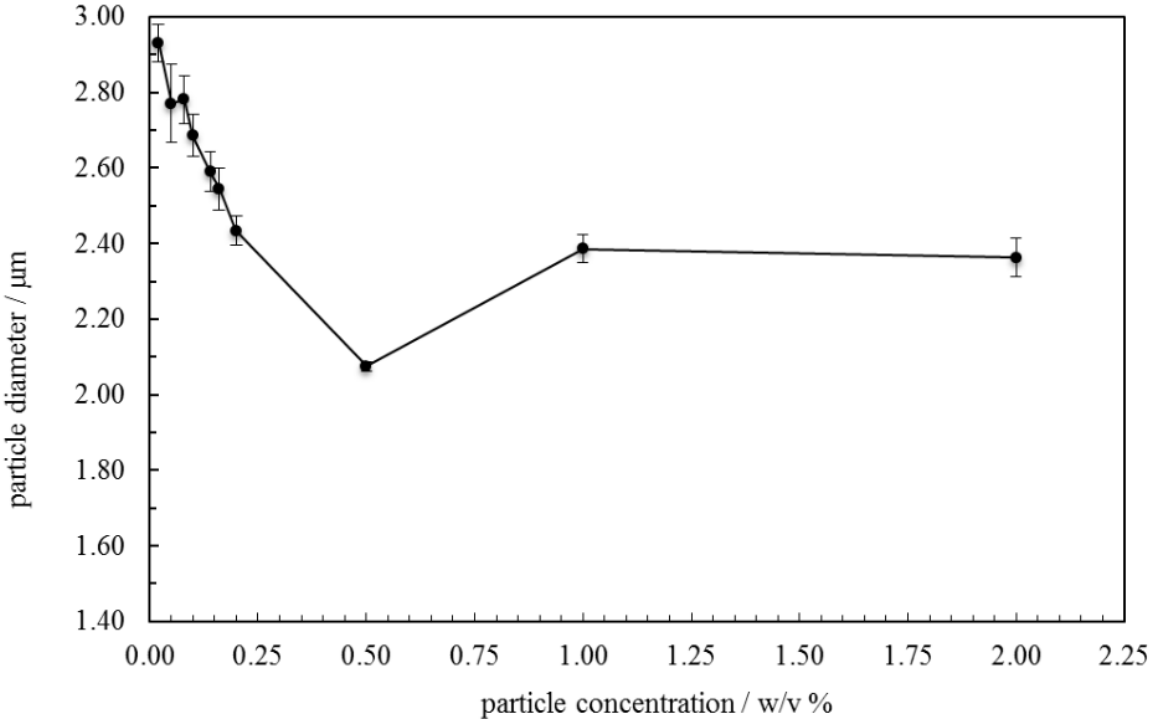

Figure B-7: Mean particle diameter in aqueous dispersions as a function of $Ce_{0.495}Sn_{0.495}Pd_{0.01}O_{2-\delta}$ concentration. Particle size measurements were carried out with a Mastersizer 2000 laser diffraction granulometer with the dispersion unit Hydro2000SM(A).

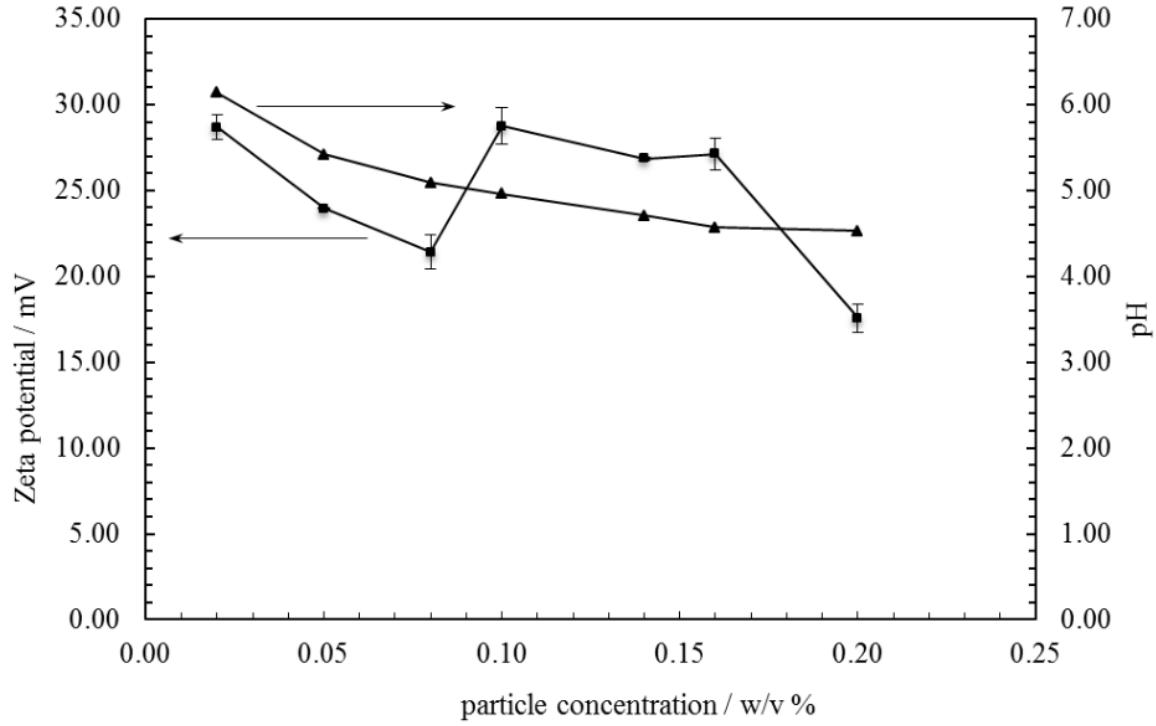

Figure B-8: Variation of the zeta potential and pH value of aqueous dispersions of $Ce_{0.495}Sn_{0.495}Pd_{0.01}O_{2-\delta}$ particles versus particle concentration. Zeta potentials were measured using the Malvern Zetasizer Nanoseries. pH values were determined at room temperature using a Jenway 3510 pH meter.

Similar trends were found with octane and toluene as the oil phase with the most stable emulsions to coalescence and creaming appearing around ≤0.05 wt% particles (Figure B-9).

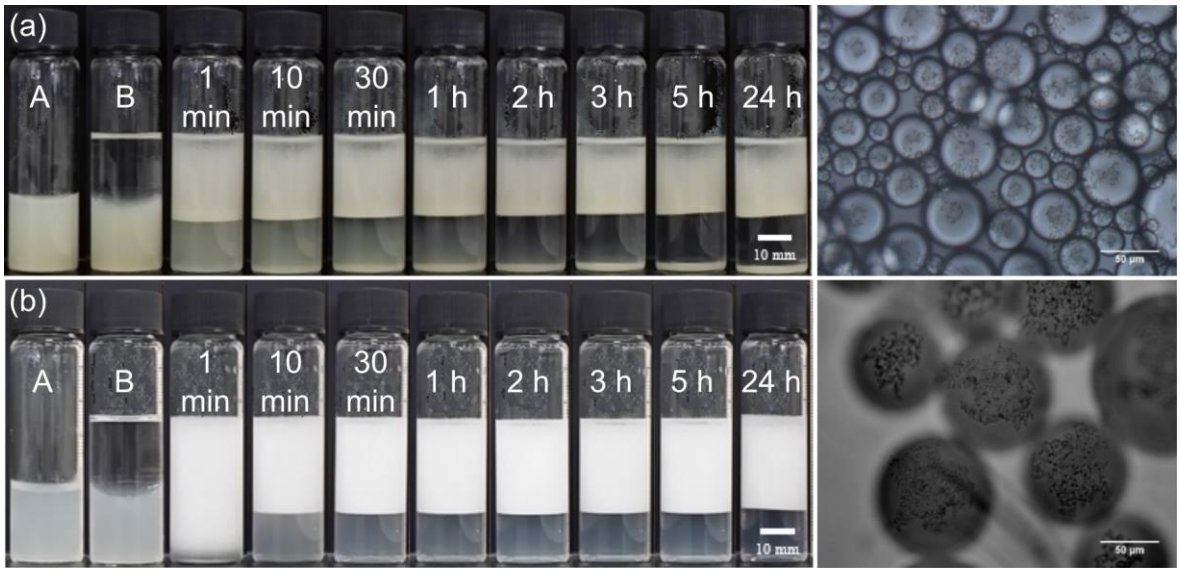

Figure B-9: (a) Appearance of octane-in-water emulsions with time at 0.05 wt% of $Ce_{0.495}Sn_{0.495}Pd_{0.01}O_{2-\delta}$ (left) and optical microscope image after 1 week (right); (b) Appearance of toluene-in-water emulsions with time at 0.01 wt% $Ce_{0.495}Sn_{0.495}Pd_{0.01}O_{2-\delta}$ (left) and optical microscope image after 1 week (right).

2.4.2 Catalyst $Ce_{0.20}Sn_{0.79}Pd_{0.01}O_{2-\delta}$

For these particles of larger mean size and with a higher Sn content, surprisingly no stable emulsion was possible using cyclohexane as oil for particle concentrations in water between 0.01 and 2.0 wt% with complete phase separation occurring within 2 h. For octane, emulsion stability to coalescence increased progressively with particle concentration up to 0.2 wt%. The average droplet size however increased from around 60 µm to 150 µm in this range (Figure B-10). It is worth noting that relatively stable emulsions (f_o = 0.2 after one month) also exist at 0.3 and 0.5 wt% particles where very large oil drops form (4-6 mm), a feature not possible using surfactants as emulsifier. Densely packed catalyst particles around oil drops can be seen in Figure B-10 enabling high stability. Similar trends in behavior are also found in toluene-in-water emulsions, Figure B-11.

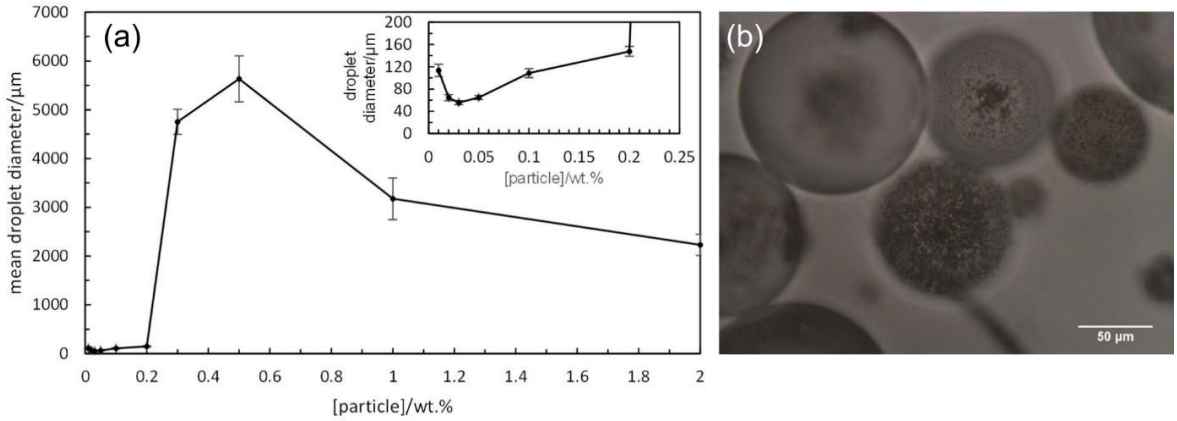

Figure B-10: (a) Variation of droplet diameter with particle concentration for octane-in-water emulsions stabilized by $Ce_{0.20}Sn_{0.79}Pd_{0.01}O_{2-\delta}$ particles after 1 month, (b) optical microscope image of the emulsion at 0.2 wt% particles.

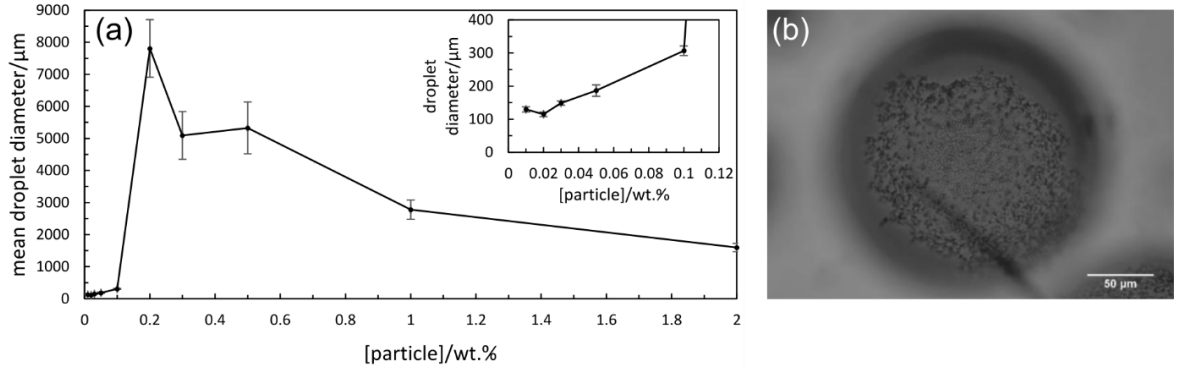

Figure B-11: (a) Variation of droplet diameter with particle concentration for toluene-in-water emulsions stabilized by $Ce_{0.20}Sn_{0.79}Pd_{0.01}O_{2-\delta}$ particles after 1 month, (b) optical microscope image of the emulsion at 0.1 wt% particles.

3 Conclusions

In this work we present a set of heterogeneous Ce-Sn-Pd oxide catalysts that can be used as stabilizers of Pickering emulsions. The catalysts were demonstrated to be very efficient and versatile for Suzuki-Miyaura reactions. The presence of low amounts of dissolved Pd indicates a release/capture mechanism with the synthesized metal oxides acting as pre-catalysts, which slowly release trace amounts of catalytically active Pd into solution. Considering the application of the palladium catalysts in a continuous flow setup, recyclability as well as stability of the catalysts was substantiated and levels of leached Pd in the reaction mixture were determined to be below the critical limit for oral pharmaceuticals. Furthermore, the palladium catalysts proved to be stable for more than 30 h in continuous flow using the so-called plug &

play reactor. Since this device can feature multiple HPLC columns, it can also be used for multistep synthesis as planned for the APIs valsartan and sacubitril. In addition, successful implementation of heterogeneous Pd catalysts in Pickering emulsions is a first promising step towards the aimed combination of chemo- and biocatalysis for the continuous formation of valsartan and sacubitril via multistep catalytic cascade reactions.

Finally, it could be shown that the two sets of Pd-containing particles act as sole emulsifiers of various oils in stabilizing oil-in-water emulsions. Emulsions stable to coalescence for at least six months can be prepared at low particle concentrations (<0.1 wt%).

Future approaches will concentrate on the applicability of the Pickering emulsions for multistep reactions as well as on the proposed procedure for the synthesis of valsartan and sacubitril.

4 References

1. Selander N, Szabo KJ (2011) Chem Rev 111:2048-2076
2. Beletskaya IP, Cheprakov AV (2009) Chem Rev 100:3009-3066
3. Wu XF, Anbarasan P, Neumann H, Beller M (2010) Angew Chem Int Ed Engl 49:9047-9050
4. Torborg C, Beller M (2009) Adv Synth Catal 351:3027-3043
5. Suzuki A (2002) J Organomet Chem 653:83-90
6. Miyaura N, Suzuki A (1995) Chem Rev 95:2457-2483
7. Kotha S, Lahiri K, Kashinath D (2002) Tetrahedron 58:9633-9695
8. Magano J, Dunetz JR (2011) Chem Rev 111:2177-2250
9. Goossen LJ, Melzer B (2007) J Org Chem 72:7473-7476
10. Hung HY, Ohkoshi E, Goto M, Bastow KF, Nakagawa-Goto K, Lee KH (2012) J Med Chem 55:5413-5424
11. Nicolaou KC, Bulger PG, Sarlah D (2005) Angew Chem Int Ed 44:4442-4489
12. Lichtenegger GJ, Gruber-Wölfler H (2015) Chim Oggi 33:12-18
13. Farina V (2004) Adv Synth Catal 346:1553-1582
14. Hagiwara H, Shimizu Y, Ohkuboc K, Hoshi T, Suzuki T, Yokoyamac C (2001) Tetrahedron Lett 42:4349-4351

15. Djakovitch L, Koehler K (2001) J Am Chem Soc 123:5990-5999
16. Crudden CM, McEleney K, MacQuarrie S, Sateesh M, Webb JD (2007) Pure Appl Chem 79:247-260
17. MacQuarrie S, Nohair B, Horton JH, Kaliaguine S, Crudden CM (2010) J Phys Chem C 114: 57-64
18. Webb JD, MacQuarrie S, McEleney K, Crudden CM (2007) J Catal 252:97-109
19. Mehnert CP, Weaver DW, Ying JY (1998) J Am Chem Soc 120:12289-12296
20. Gruber-Woelfler H, Radaschitz PF, Feenstra PW, Haas W, Khinast JG (2012) J Catal 286:30-40
21. Lee DH, Choi M, Yu BW, Ryoo R, Taher A, Hossain S, Jin MJ (2009) Adv Synth Catal 351:2912-2920
22. Glasnov TN, Findenig S, Kappe CO (2009) Chem Europ J 15:1001-1010
23. Cantillo D, Kappe CO (2014) ChemCatChem 6:3286-3305
24. ONE-FLOW Research Project: Catalyst Cascade Reactions in 'One-Flow' within a Compartmentalized, Green-Solvent 'Digital Synthesis Machinery' – End-to-End Green Process Design for Pharmaceuticals. Work programme: EU proposal 737266 - ONE-FLOW. https://one-flow.org/
25. Binks BP (Ed.) (1998) Modern Aspects of Emulsion Science. The Royal Society of Chemistry, Cambridge
26. Pickering SU (1907) J Chem Soc Transactions 91:2001-2021
27. Binks BP (2002) Curr Opin Colloid Interface Sci 7:21-41
28. Binks BP (2017) Langmuir 33:6947-6963
29. Crossley S, Faria J, Shen M, Resasco DE (2010) Science 327:68-72
30. Pera-Titus M, Leclercq L, Clacens JM, De Campo F, Nardello-Rataj V (2015) Angew Chem Int Ed 54:2006-2021
31. Vilela-Martin JF (2016) Drug Des, Dev Ther 10:1627-1639
32. Lau SH, Bourne SL, Martin B, Schenkel B, Penn G, Ley SV (2015) Org Lett 17:5436-5439
33. Aalla S, Gilla G, Bojja Y, Anumula RR, Vummenthala PR, Padi PR (2012) Org Proc Res Dev 16:682-686
34. Pandarus V, Desplantier-Giscard D, Gingras G, Beland F, Ciriminna R, Pagliaro M (2013) Org Proc Res Dev 17:1492-1497
35. Wang Gx, Sun Bp, Peng Ch (2011) Org Proc Res Dev 15:986-988
36. Guo M, Lu J, Wu Y, Wang Y, Luo M (2011) Langmuir 27:3872-3877

37. Lichtenegger GJ, Maier M, Hackl M, Khinast JG, Goessler W, Griesser T, Kumar VSP, Gruber-Woelfler H, Deshpande PA (2017) J Mol Catal A: Chem 426 Part A:39-51

38. Lichtenegger GJ, Tursic V, Kitzler H, Obermaier K, Khinast JG, Gruber-Wölfler H (2016) Chem Ing Tech 88:1518-1523

39. Baidya T, Gupta A, Deshpandey PA, Madras G, Hegde MS (2009) J Phys Chem C 113:4059-4068

40. Richardson JM, Jones CW (2009) Assessing Catalyst Homogeneity/Heterogeneity via Application of Insoluble Metal Scavengers: Application to Heck and Suzuki Reactions. In Catalysis of Organic Reactions, Prunier ML (Ed.), CRC Press, Boca Raton

41. Richardson JM, Jones CW (2007) J Catal 251:80-93

42. Lichtenegger GJ, Maier M, Khinast JG, Gruber-Wölfler H (2016) J Flow Chem 6:244-251

C Multistep synthesis of a valsartan precursor in continuous flow

The following chapter is taken from the same-titled journal article published in Journal of Flow Chemistry by Hiebler et al. [Hiebler K, Soritz S, Gavric K, Birrer S, Maier MC, Grabner B, Gruber-Woelfler H (2020) J Flow Chem 10:283-294].

Valsartan is a potent, orally active angiotensin II receptor blocker and is widely used in the treatment of hypertension and chronic heart failure. Herein, we present an approach for the continuous synthesis of a late-stage precursor of valsartan in three steps. The applied synthetic route involves N-acylation, Suzuki-Miyaura cross-coupling and methyl ester hydrolysis. After optimization of the individual steps in batch, they were successfully transferred to continuous flow processes employing different reactor designs. The first step of the synthetic route (N-acylation) as well as the third step (methyl ester hydrolysis) are performed in coil reactor set-ups. The key step of the reaction cascade (Suzuki-Miyaura cross-coupling) is catalyzed by a heterogeneous palladium-substituted cerium-tin-oxide with the molecular formula $Ce_{0.20}Sn_{0.79}Pd_{0.01}O_{2-\delta}$*. The catalyst particles are implemented in an in-house developed packed bed reactor, which features an HPLC column as fixed bed. The combination of the individual reaction modules facilitates the consecutive performance of the three reaction steps. Using the developed multistep continuous setup, the targeted valsartan precursor was obtained with up to 96% overall yield.*

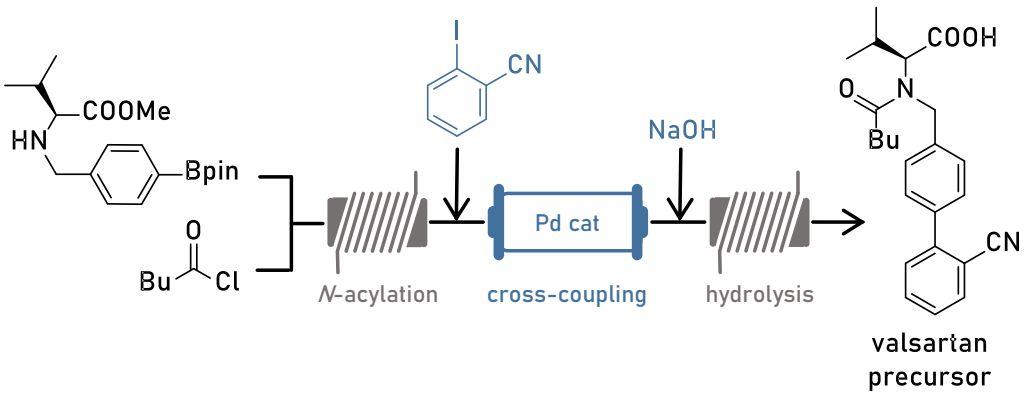

1 Introduction

According to the World Health Organization (WHO), in 2015 about 31% of deaths were ascribable to cardiovascular diseases, thus being the leading cause of death globally. Especially people suffering from high blood pressure belong to the risk group to develop cardiovascular complaints. Therefore, a number of different medications for the treatment of hypertension are available on the market [1,2]. One popular therapy for lowering the patients' blood pressure is the administration of the nonpeptide angiotensin II receptor blocker valsartan **1**. The active pharmaceutical ingredient (API) belongs to the class of sartans, which feature a biphenyl moiety as common structural unit. The biaryl scaffold plays a crucial role in the oral bioavailability as well as the binding of the API to the biological target [3,4]. Valsartan **1** was first introduced onto the market as Diovan® by Novartis in 1997 [5,6]. In the course of ensuing years, several other combination preparations followed, such as Diovan HCT®(+hydrochlorothiazide, 1998), Exforge® (+amlodipine, 2007), Exforge HCT® (+amlodipine+hydrochlorothiazide, 2009), Valtura® (+aliskiren, 2009) and Entresto® (+sacubitril, 2015) [7,8]. Regarding the synthesis of the antihypertensive **1**, it was first patented by Ciba-Geigy in 1991. The route involves the coupling of L-valine methyl ester **2** with biphenyl aldehyde **3a** via reductive amination (Scheme C-1). Subsequent acylation of the resulting intermediate **4** with valeryl chloride, triazole formation with an organotin reagent as well as saponification yielded the target molecule valsartan **1** [9].

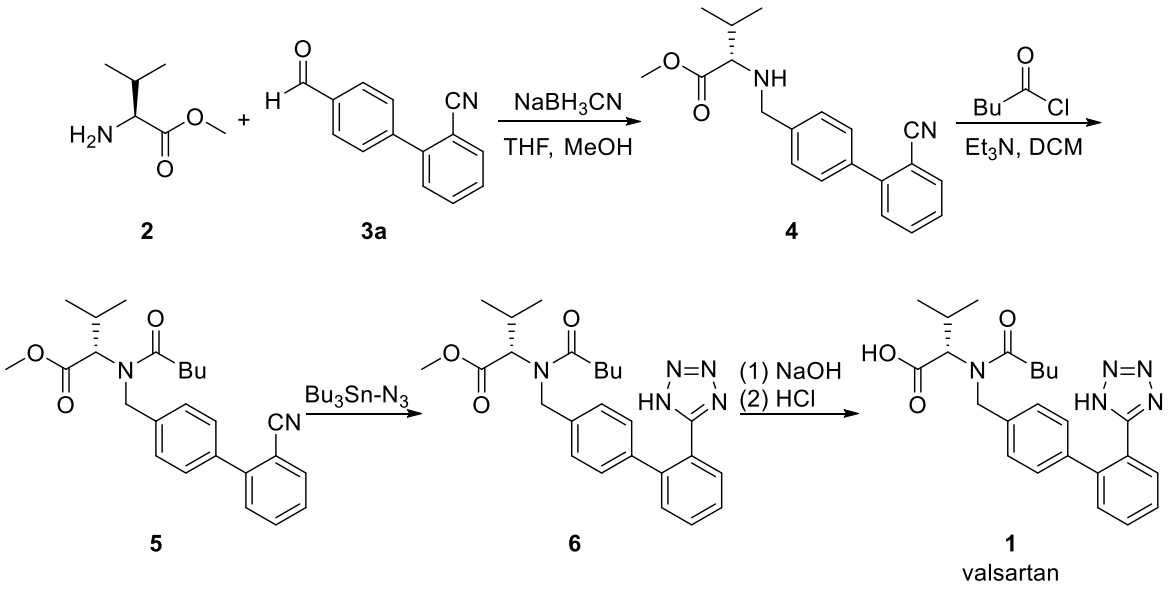

Scheme C-1: Patented Ciba-Geigy synthesis of valsartan [9].

However, the Ciba-Geigy route to **1** offered plenty of room for improvement. The use of a highly toxic tin reagent led to contamination of the final API and the process suffered from a poor overall yield of less than 10% [10]. Consequently, a substantial number of papers and patents focusing on novel synthesis strategies and optimization of the overall reaction process have been published [exemplarily 3,11-20]. Alternative approaches for the formation of valsartan **1** include Ru-catalyzed C-H activation [17], Pd-catalyzed decarboxylative biaryl coupling [3], Zn-catalyzed Negishi reaction [18] and the use of trityl-protected tetrazole intermediates in the Pd-catalyzed Suzuki-Miyaura cross-coupling [14,15]. Although differing considerably in terms of employed reagents, most strategies for the synthesis of valsartan **1** rely exclusively on traditional batch operations. Only very few papers deal with the synthesis of valsartan precursor compounds in continuous flow. Pandarus et al. reported the continuous Suzuki coupling of 2-chlorobenzonitrile **7a** with 4-methyl-phenylboronic acid **8** using a heterogeneous sol-gel entrapped Silia*Cat* DPP-Pd catalyst. Its implementation in a packed bed microreactor facilitated formation of valsartan building block **3b** (Scheme C-2, a). Nevertheless, Pandarus et al. observed rapid catalyst deactivation due to the instability of the active Pd species towards dissolved oxygen in the presence of the aryl chloride substrate **7a** [21]. Likewise, Nagaki and his group performed the continuous synthesis of valsartan intermediate **3a**. First, organoboron species **9** is generated using a two-step tubular flow microreactor system. Then, Suzuki cross-coupling of the obtained intermediate with **10** is performed in a Pd-substituted monolithic microreactor (Scheme C-2, b). Parallelization of five of these microreactor setups using a flow distributor allowed them to synthesize valsartan intermediate **3a** on a larger scale with a productivity of 184 mg/h [22]. However, to the best of our knowledge, there are no approaches for the continuous multistep synthesis of an advanced valsartan precursor reported in literature. Therefore, the development of a multistep continuous setup for the synthesis of a late-stage valsartan precursor was the objective of our work.

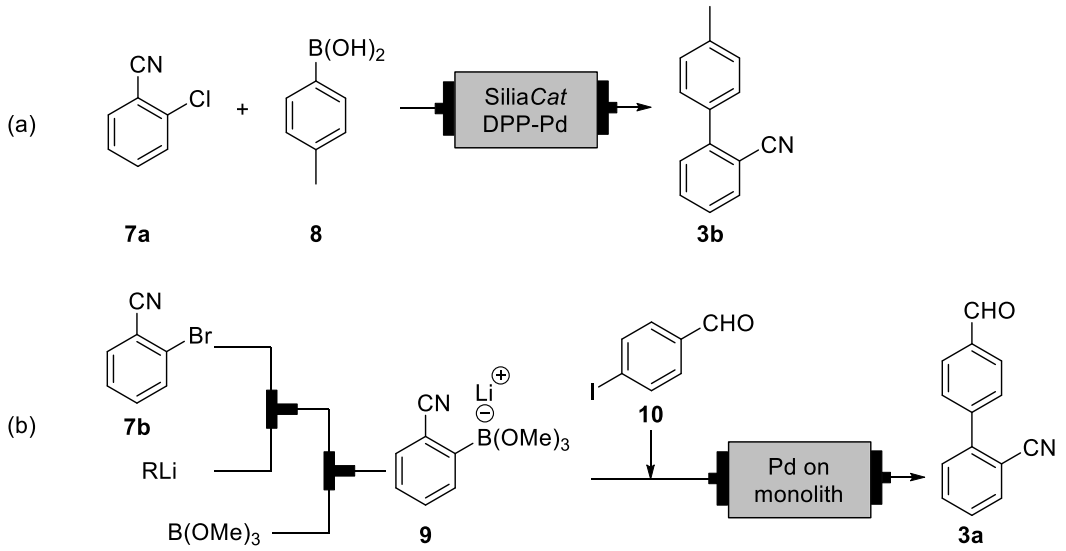

Scheme C-2: Examples of continuous syntheses of valsartan building blocks [21,22].

In contrast to traditionally employed batch operations, flow reactors have a lot of benefits including improved energy efficiency, reduced waste generation and increased safety. Therefore, the Food and Drug Administration (FDA) aims for application of continuous synthesis in pharmaceutical manufacturing [23,24]. Also, recent recalls of valsartan **1** generics, contaminated with carcinogenic *N*-nitrosodimethylamine, highlight the need for alternative synthesis methods to obtain safe and pure APIs [25]. Therefore, within the framework of the ONE-FLOW research project [26], we targeted the integrated synthesis of valsartan precursor **13** in a continuous manner over three steps (Scheme C-3). Firstly, *N*-acylation of boronic acid pinacol ester **11** with valeryl chloride yields the functionalized intermediate **12**. Secondly, Suzuki-Miyaura cross-coupling of **12** with 2-halobenzonitrile **7b-c** gives biphenyl compound **5**. The key step of the reaction cascade is catalyzed by heterogeneous Ce-Sn-Pd oxides with the molecular formula $Ce_{0.99-x}Sn_xPd_{0.01}O_{2-\delta}$ [27]. Thirdly, hydrolysis of the methyl ester group is achieved by aqueous base and yields the target compound **13**. The valsartan precursor **13** can then be transformed to the targeted API **1** by the use of azides [28], but this transformation was not included in this work. However, it will be addressed in future approaches.

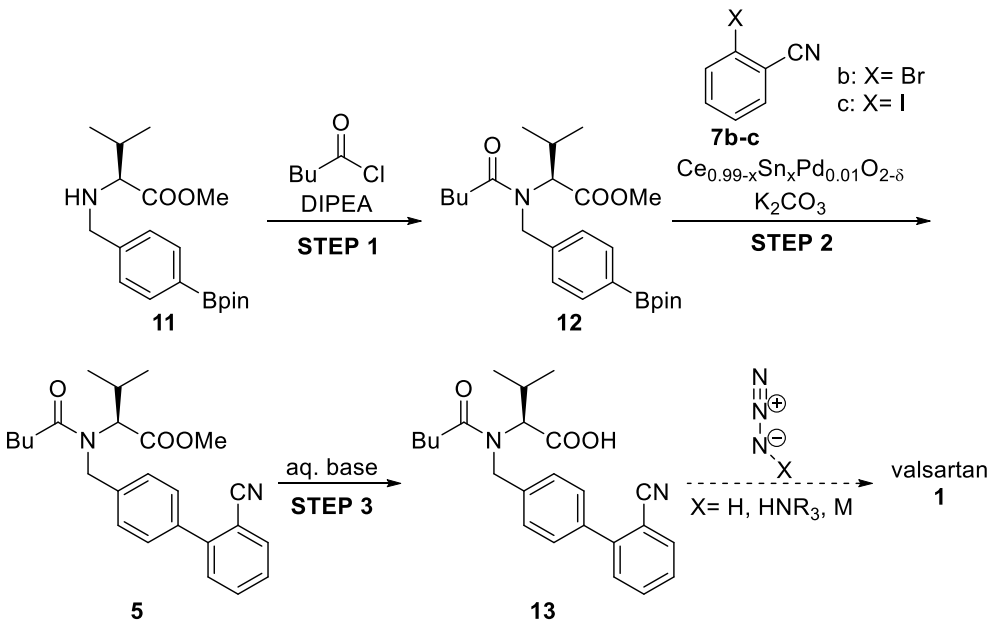

Scheme C-3: Targeted three-step synthesis of valsartan precursor **13** in continuous flow (synthesis of **1** via tetrazole formation with organic azides is not included in this paper).

For the Suzuki-Miyaura cross-coupling, the use of in-house developed Pd catalysts with the formula $Ce_{0.99-x}Sn_xPd_{0.01}O_{2-\delta}$ is envisaged. Their applicability for cross-couplings of various *ortho*- and *para*-substituted bromoarenes with phenylboronic acid has already been reported by our group [27,29]. The heterogeneous catalysts also proved to exhibit high functional group tolerance as well as minimal leaching behavior [27,29]. Apart from that, the performance of continuous Suzuki cross-coupling reactions was successfully achieved by implementation of the catalysts in an in-house developed packed bed reactor [30], referred to as plug & play reactor. The customized reactor features exchangeable HPLC columns filled with catalyst particles as well as modules for heating, cooling and mixing. Obtained results [27,29,30] clearly indicate the high potential of the Ce-Sn-Pd oxides for the synthesis of pharmaceutical and fine chemical intermediates in continuous flow and are promising in terms of the targeted synthesis of valsartan intermediate **13**.

2 Results and discussion

2.1 Optimization of the individual steps in batch

In order to be able to design a continuous setup for the multistep synthesis of valsartan precursor **13**, we first examined the three individual steps in batch. Since we wanted to keep the consumption of our intermediates **5**, **11** and **12** to a minimum and the optimization in flow

would have required a higher amount of reagents (due to the equilibration times of our targeted continuous setups), we decided to identify a first set of suitable reaction parameters in batch. However, in view of the future improvement of the process, optimization will be performed in a continuous fashion in order to take the intrinsic dynamics and all other advantages of continuous systems into account. As the pivotal step of the reaction cascade is a Suzuki-Miyaura cross-coupling, we focused on step 2 in the beginning. For this transformation we had a number of heterogeneous Pd catalysts in hand [27], which can readily be implemented in a fixed bed reactor for continuous flow applications [30]. Based on earlier studies, we chose to test three of them ($Ce_{0.99-x}Sn_xPd_{0.01}O_{2-\delta}$, x= 0.20, 0.79, 0.99) as they gave the best results in the Suzuki coupling of 2-bromobenzonitrile **7b** with phenylboronic acid (standard reaction conditions: 1 mol eq. aryl halide, 1.5 mol eq. phenylboronic acid, 1.5 mol eq. K_2CO_3, EtOH:H_2O=7:3, 75 °C) [27]. Our initial approaches for the synthesis of valsartan **1** involved the Suzuki coupling of boronic acid derivatives carrying a (trityl-protected) tetrazole or a nitrile group in *ortho*-position. These attempts failed due to deactivation of the employed Pd catalyst and substrate degradation by rapid protolytic deboronation. However, we observed that boronic acid ester **12** couples smoothly with 2-halobenzonitrile **7b-c** in EtOH:H_2O=7:3 at 75 °C (Scheme C-3, step 2). In the employed aqueous reaction environment **12** is hydrolyzed to the free boronic acid, which is more reactive in Suzuki-Miyaura cross-couplings than its ester analogue [31]. Therefore, we chose to pursue a synthetic route involving the Suzuki coupling of **12** with **7b-c** leading to formation of valsartan precursor **13** as final product (Scheme C-3). After having identified suitable cross-coupling partners, we wanted to determine the most active Pd catalyst for our targeted transformation. Regarding the Suzuki coupling of 2-bromobenzonitrile **7b** with boronic acid ester **12** using 1 mol% of catalyst, the activity follows the order $Ce_{0.20}Sn_{0.79}Pd_{0.01}O_{2-\delta} > Sn_{0.99}Pd_{0.01}O_{2-\delta} > Ce_{0.79}Sn_{0.20}Pd_{0.01}O_{2-\delta}$ (C-1, Entries 1-3). Hence, we decided to use $Ce_{0.20}Sn_{0.79}Pd_{0.01}O_{2-\delta}$ for all further experiments. Moreover, it is commonly known that the reactivity of aryl halides in Suzuki coupling increases along the halogen group (Cl<<Br<I). As expected, a higher conversion was obtained when using 2-iodobenzonitrile **7c** instead of **7b** (Table C-1, Entry 4). Consequently, **7c** was the coupling partner of choice and the catalyst loading was decreased from 1 mol% to 0.25 mol% for further studies.

Table C-1: Optimization of reaction conditions of step 2 in batch.

Entry	Solvent	T [°C]	Pd cat.[a]	Cat. loading [mol%]	Aryl halide	Excess of 12 [mol eq.]	Conversion [%]
1	EtOH:H_2O=7:3	75	1	1.00	**7b**	1.10	10.0[b]
2	EtOH:H_2O=7:3	75	2	1.00	**7b**	1.10	60.1[b]
3	EtOH:H_2O=7:3	75	3	1.00	**7b**	1.10	47.3[b]
4	EtOH:H_2O=7:3	75	2	1.00	**7c**	1.10	95.3[b]
5	Dioxane:H_2O=65:35	80	2	0.25	**7c**	1.10	58.9[c]
6	Dioxane:H_2O=3:2	80	2	0.25	**7c**	1.10	83.6[c]
7	Dioxane:H_2O=1:1	80	2	0.25	**7c**	1.10	88.6[c]
8	Dioxane:H_2O=1:1	80	2	0.25	**7c**	1.25	92.2[c]
9	Dioxane:H_2O=1:1	80	2	0.25	**7c**	1.50	95.0[c]

[a] Pd catalyst 1: $Ce_{0.79}Sn_{0.20}Pd_{0.01}O_{2-\delta}$, Pd catalyst 2: $Ce_{0.20}Sn_{0.79}Pd_{0.01}O_{2-\delta}$, Pd catalyst 3: $Sn_{0.99}Pd_{0.01}O_{2-\delta}$

[b] Conversion of aryl halide **7b-c** after 15 min (determined by HPLC)

[c] Conversion of aryl halide **7b-c** after 10 min (determined by HPLC)

In view of the performance of a multistep reaction cascade and the realization of *N*-acylation prior to the Suzuki coupling, we next needed to identify a suitable solvent system for achieving both steps in a sequential fashion. As reported in literature [32] and experienced in our lab, water is crucial for the success of the Suzuki coupling using our class of catalysts. However, step 1 needs to be performed in an aprotic organic solvent to avoid hydrolysis of the valeryl chloride reagent. Since our chosen catalyst showed no or very low activity in two-phasic solvent systems (water + dicholoromethane/toluene/ethyl acetate), we needed a single liquid phase for the Suzuki coupling step. Highly polar water-miscible organic solvents (acetonitrile; *N*,*N*-dimethyl sulfoxide; *N*,*N*-dimethylformamide) did not prove to be compatible with our catalyst. However, considerable catalyst activity was detected in aqueous ethereal solvents (tetrahydrofuran (THF); 1,4-dioxane). As THF and water are not miscible in a 1:1 ratio at elevated temperatures [33], in this case the addition of an alcoholic solvent was further necessary to obtain one liquid phase. The choice of organic solvent also has a substantial influence on the leaching behavior of palladium, tin and cerium into the reaction solution. Our investigations in this respect showed that palladium leaching increases along with the polarity of the reaction

solvent (Table C-2). Highest levels of palladium were determined in ethanol-water (3.12 mg/kg), whereas they were found to be lowest in dioxane-water (0.37 mg/kg). Cerium leaching shows the exact opposite trend (0.89 mg/kg in ethanol-water, 2.53 mg/kg in dioxane-water, Table C-2). In contrast, leaching of tin was found to be insignificant in all tested solvents (0.06-0.08 mg/kg, Table C-2). Due to the fact that minimal leaching of the active catalytic species palladium was targeted, we chose dioxane-water as the solvent for the Suzuki coupling step.

Table C-2: Leaching of metals (Pd, Sn, Ce) into the reaction solution during step 2 using $Ce_{0.20}Sn_{0.79}Pd_{0.01}O_{2-\delta}$ (0.25 mol%) as catalyst and 2-iodobenzonitrile **7c** as aryl halide.

Entry	Solvent	T [°C]	Conversion[a] [%]	Metal content[b] [mg/kg]		
				Pd	Sn	Ce
1	Dioxane:H_2O=1:1	85	97.9	0.37	0.08	2.53
2	Dioxane:MeOH:H_2O=1:1:1	65	41.3	2.23	0.06	1.56
3	THF:MeOH:H_2O=1:1:1	65	33.5	1.90	0.06	1.29
4	EtOH:H_2O=7:3	75	78.7	3.12	0.08	0.89

[a] Conversion of 2-iodobenzonitrile **7c** after 120 min (determined by HPLC)

[b] Metal content determined by ICP-MS after acid-mediated digestion of the samples

Regarding the optimal dioxane-to-water ratio for the Suzuki coupling step, solubility issues leave a narrow margin. If the reaction mixture is rich in water (≥55 v%), employed organic compounds are not entirely soluble. If, on the other hand, dioxane is present in ≥70 v%, the inorganic base potassium carbonate (K_2CO_3) does not dissolve completely. An equivolume mixture of dioxane and water provided the best results for our reaction (Table C-1, Entries 5-7). Apart from that, as expected the use of a larger excess of boronic acid ester **12** leads to an increased reaction rate (Table C-1, Entries 8-9). Nevertheless, we decided to use 1.10 mol equivalents of **12** for the continuous reaction setup considering atom economy as well as by-product formation. Particularly, homocoupling and oxidation of the organoboron reagent were reported to occur upon depletion of the aryl halide coupling partner [27], causing a more complex reaction mixture.

After having identified optimum conditions in batch for the Suzuki coupling step, we concentrated our attention on step 1 of the reaction cascade (Scheme C-3, step 1). *N*-acylation of **11**, which was synthesized using a literature procedure [20], with valeryl chloride was performed in dioxane in presence of an organic base. We aimed for quantitative conversion of boronic acid ester **11** as previous experiments showed literature-known [34] deactivation of our Pd catalyst, which is employed in the subsequent Suzuki coupling step, by N-H functional groups. We investigated the effect of temperature as well as molar equivalents of reagents (valeryl chloride, organic base) on the conversion (Table C-3). *N*,*N*-diisopropylethylamine (DIPEA) was chosen as organic base because the formed hydrochloride salt proved to be soluble in dioxane at elevated temperatures. The rate of *N*-acylation of **11** increases with higher temperature (Table C-3, Entries 1-3) as well as a larger excess of valeryl chloride (Table C-3, Entries 4-5). Using equimolar amounts of valeryl chloride and DIPEA further accelerates the reaction (Table C-3, Entry 6), achieving almost full conversion after 5 min (98.8%).

Table C-3: Optimization of reaction conditions of step 1 in batch.

Entry	T [°C]	Mol eq. valeryl chloride	Mol eq. DIPEA	Conversion[a] t= 1 min [%]	Conversion[a] t= 5 min [%]
1	40	1.05	1.05	20.0	59.0
2	60	1.05	1.05	26.4	70.9
3	80	1.05	1.05	36.7	84.7
4	80	1.50	1.05	45.7	96.7
5	80	2.00	1.05	55.9	99.4
6	80	2.00	2.00	65.0	98.8

[a] Conversion of **11** after 1 min and 5 min, respectively (determined by HPLC as free boronic acid)

The final step of our targeted reaction cascade is the saponification of **5** to yield valsartan precursor **13** (Scheme C-3, step 3). As a dioxane-water mixture was found to be optimal for the preceding Suzuki coupling step, ester hydrolysis of **5** was performed in the same solvents. At a temperature of 80 °C, the rate of methyl ester hydrolysis was found to increase with a larger molar excess of sodium hydroxide (Table C-4, Entries 1-4). Substitution of the base by

potassium hydroxide did not have a considerable impact on the conversion (Table C-4, Entry 5). Raising the water content in the reaction solution to 55 v% slightly decelerated the conversion (Table C-4, Entry 6) and a further increase to 60 v% caused solubility issues.

Table C-4: Optimization of reaction conditions of step 3 in batch.

Entry	Solvent	Base	Mol eq. base	Conversion[a] [%]
1	Dioxane:H_2O=1:1	NaOH	2.5	29.5
2	Dioxane:H_2O=1:1	NaOH	5.0	46.1
3	Dioxane:H_2O=1:1	NaOH	10.0	67.3
4	Dioxane:H_2O=1:1	NaOH	20.0	81.3
5	Dioxane:H_2O=1:1	KOH	10.0	67.7
6	Dioxane:H_2O=45:55	NaOH	10.0	61.3

[a] Conversion of **5** at 80 °C after 5 min (determined by HPLC)

2.2 Optimization of sequential steps 1 and 2 in batch

For Pd-catalyzed Suzuki-Miyaura cross-couplings, the presence of a base is essential for the reaction to occur [35]. Hence, the pH of the reaction environment affects the rate of C-C bond formation [36]. In view of the performance of the Suzuki coupling subsequently to step 1, different influencing factors on the pH of the reaction mixture have to be considered. These include the formation of hydrogen chloride during the *N*-acylation step and hydrolysis of the excess acid chloride to the corresponding carboxylic acid upon addition of water. Consequently, the pH of the reaction mixture after step 1 is acidic and part of potassium carbonate, which is added for the Suzuki coupling, gets neutralized. In order to study the effect of the pH on the Suzuki coupling step and to identify the necessary amount of potassium carbonate to be added, we performed steps 1 and 2 in a sequential fashion in one-pot (Scheme C-4).

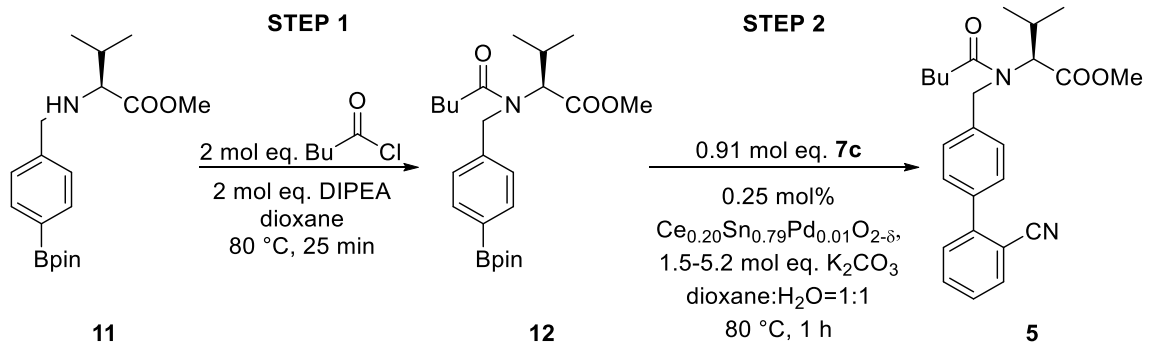

Scheme C-4: Steps 1 and 2 sequentially performed in one-pot fashion in batch.

For the sequential performance of steps 1 and 2, *N*-acylation of **11** was accomplished using 2 mol eq. of both valeryl chloride and DIPEA in dioxane at 80 °C. Upon completion of the reaction, the reaction mixture was quenched with an equal volume of water. Then, potassium carbonate, 2-iodobenzonitrile **7c** and Pd catalyst $Ce_{0.20}Sn_{0.79}Pd_{0.01}O_{2-\delta}$ were added to the reaction flask in order to achieve formation of **5**. We compared the Suzuki coupling step performed in one-pot with the optimized separate Suzuki coupling, exhibiting a pH of 11.3 in the presence of 1.5 mol eq. of potassium carbonate (Table C-5, Entry 1). When the same amount of base was used in the one-pot experiment, a pH of only 9.7 was obtained and the conversion in the Suzuki coupling step was considerably lower (Table C-5, Entry 2). Therefore, another 0.17 mmol of K_2CO_3 were added, corresponding to the employed amount of valeryl chloride reagent in step 1. In doing so, the pH approaches the reference value and conversion was enhanced significantly (Table C-5, Entry 3). Further increasing the amount of base in the reaction mixture gave comparable conversion (Table C-5, Entry 4). Upon addition of 0.39 mmol of base, formation of a second liquid phase was observed (Table C-5, Entry 5), which was confirmed by following the reaction with the Crystalline (Technobis) [37]. The device is designed for studying crystallization processes by turbidity measurements but also allows real time monitoring of reactions via a particle view camera. Regarding obtained results and in view of the sequential performance of steps 1 and 2 in the multistep continuous setup for the synthesis of **13**, the use of 3.7 mol eq. potassium carbonate in the Suzuki coupling step was considered as most appropriate.

Table C-5: Effect of K_2CO_3 addition on pH and conversion of the Suzuki coupling step when performed after *N*-acylation in a one-pot fashion.

Entry	K_2CO_3 [mmol]	K_2CO_3 [mol eq.][a]	pH[b]	Conversion Step 2[c] [%]
1[d]	0.11	1.5	11.3	97.7
2	0.11	1.5	9.7	33.7
3	0.28	3.7	10.9	82.4
4	0.33	4.4	11.0	83.4
5	0.39	5.2	11.1	n.d.[e]

n.d.= not determined

[a] Relative to **7c**

[b] pH determined with a Mettler Toledo FiveEasy™ pH meter equipped with a Mettler Toledo LE409 probe after performance of step 1 (55 mM **11**, 2 mol eq. valeryl chloride, 2 mol eq. DIPEA, 1.5 mL dioxane, 80 °C, 25 min) and addition of 1.5 mL H_2O and K_2CO_3

[c] Conversion of **7c** after 30 min (determined by HPLC)

[d] Optimized separate Suzuki coupling (25 mM **7c**, 1.1 mol eq. **12**, 1.5 mol eq. K_2CO_3, 3 mL dioxane:H_2O=1:1)

[e] Formation of two liquid phases (monitored via Crystalline, Technobis)

2.3 Continuous setups for the individual steps

After optimization of the individual steps in batch, we first targeted the realization of *N*-acylation as well as saponification in continuous flow. As both transformations exhibit a monophasic reaction solution, we decided to utilize a stainless steel coil (L x O.D. x I.D. 3.0 m x 1/16 in. x 0.030 in., V= 1.368 mL) as reactor in combination with a split-and-recombine unit (V= 0.565 mL) as static mixer (Scheme C-5). The mixing efficiency of the latter and its applicability for rapid chemical transformations has been demonstrated lately for the aerobic oxidation of Grignard reagents in continuous flow [38]. The reactor comprises a precooling section, after which the two reagent streams are merged and introduced into a split-and-recombine section for enhanced mixing.

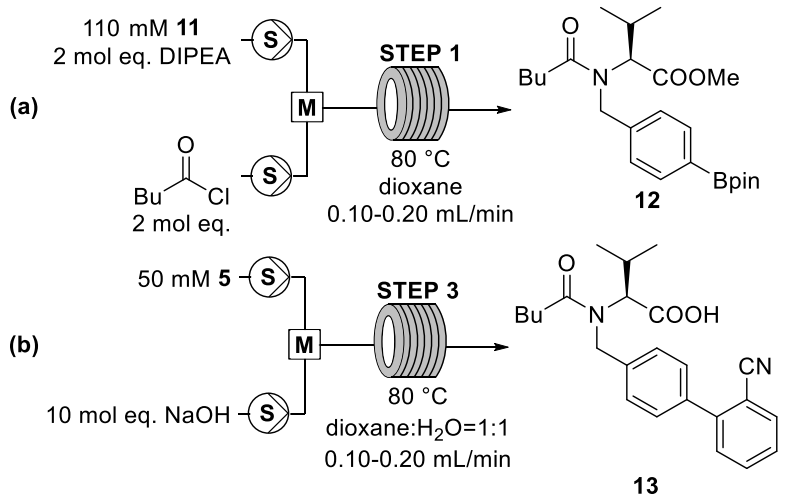

Scheme C-5: Continuous setup for (a) *N*-acylation as well as (b) methyl ester hydrolysis using a coil reactor at ambient pressure (S= syringe pump, M= split-and-recombine reactor as static mixer).

Regarding the continuous performance of steps 1 and 3, a dual syringe infusion pump (LA-120, Landgraf) was utilized for steady reagent delivery into the reactor setup (V=1.933 mL), which was assembled using standard HPLC fittings. The performance of the continuous setup at ambient pressure was determined at three different total flow rates based on the conversion of **11** and **5,** respectively (for details see Supporting information). In both cases, substrate conversion of >99% was obtained at the lowest flow rate of 0.10 mL/min, which corresponds to a calculated residence time of τ~19 min (Table C-6, Entry 1). Whereas the *N*-acylation step proved to be similarly efficient at higher flow rates of 0.15 and 0.20 mL/min, for methyl ester hydrolysis conversion decreased noticeably (Table C-6, Entries 2-3). However, the observed general trend of higher conversion at lower flow rates suggests that the mixing obtained with the split-and-recombine reactor is sufficient for both transformations.

Table C-6: Conversion of step 1 and step 3 when performed in continuous flow using different flow rates.

Entry	V(reactor) [mL]	Flow rate [mL/min]	τ [a] [min]	Conversion Step 1[b] [%]	Conversion Step 3[c] [%]
1	1.93	0.10	19.3	99.9	99.5
2	1.93	0.15	12.9	99.7	97.2
3	1.93	0.20	9.7	99.6	92.6

[a] Calculated residence time

[b] Conversion of **11** after 2.5τ (determined by HPLC)

[c] Conversion of **7c** after 2.5τ (determined by HPLC)

Next, we focused on the continuous setup for the second step of our cascade towards **13**, Suzuki-Miyaura cross-coupling. The applicability of our heterogeneous Pd catalyst for the continuous Suzuki coupling of various substituted bromoarenes with phenylboronic utilizing the plug & play reactor has already been reported by our group [29,30]. Therefore, we decided to adopt this approach for the C-C cross-coupling of boronic acid ester **12** with aryl halide **7c**. In view of the performance of our three-step reaction cascade, we based the experiment design on the preceding *N*-acylation step. For step 1 quantitative conversion of **11** is targeted, which is achieved in dioxane using a flow rate of 0.10 mL/min. As we identified an equivolume dioxane-water mixture as optimal for subsequent Suzuki coupling, we intended to merge the reagent stream of step 1 with an aqueous stream of the same flow rate. Consequently, for testing step 2 separately in a continuous fashion, we chose a flow rate of 0.20 mL/min. In the experiment, a pre-mixed reagent solution containing both coupling partners as well as potassium carbonate was pumped through the plug & play reactor [30], which was equipped with an HPLC column (L x I. D. 120 x 8 mm) filled with catalyst particles (4.7 g) (Scheme C-6, for details see Supporting information). Due to the backpressure of the catalyst bed (2-3 bar) and incompatibility of the solvent mixture with the available HPLC pump, a high-pressure syringe pump (VIT-FIT HP, LAMBDA Instruments) in combination with stainless steel syringes was utilized. At the chosen flow rate of 0.2 mL/min, the mean residence time inside the HPLC column containing the catalytic species was determined by measurement of a tracer-determined residence time distribution curve to be 22.3 min. Utilizing the abovementioned setup, step 2 of the targeted reaction cascade was successfully performed in a continuous fashion. After an initial equilibration phase of 50 min (consuming 10 mL of stock solution), the target compound **5** was obtained with an average 95% yield (Figure C-1).

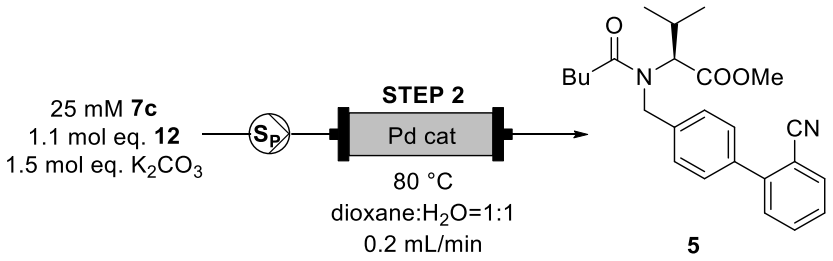

Scheme C-6: Continuous setup for the Suzuki coupling utilizing the plug & play reactor equipped with an HPLC column filled with particles of $Ce_{0.20}Sn_{0.79}Pd_{0.01}O_{2-\delta}$ (S_P= high-pressure syringe pump).

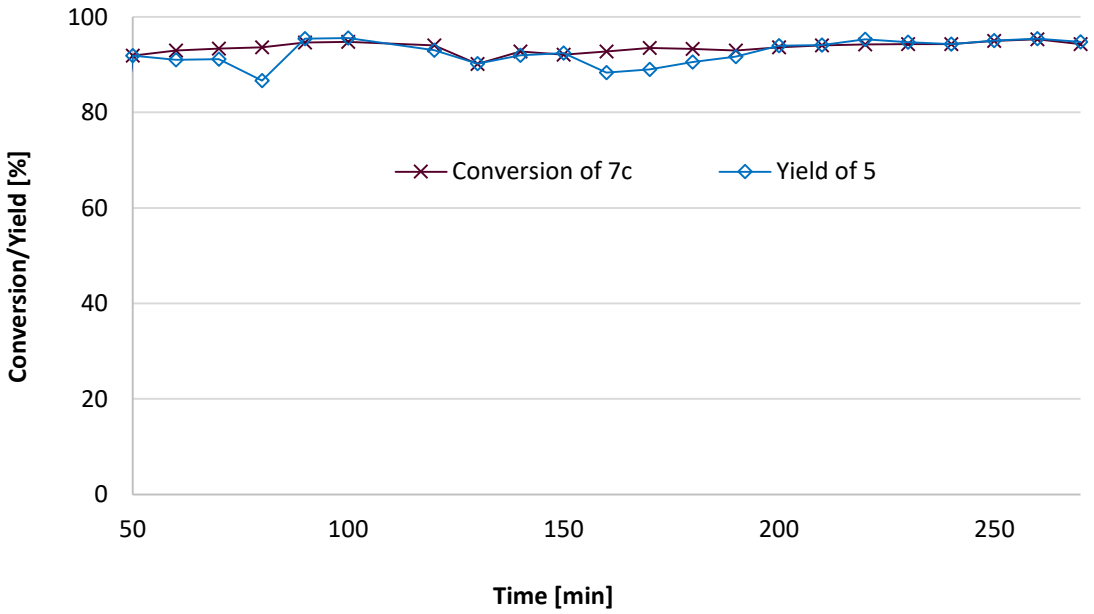

Figure C-1: Conversion of **7c** and yield of **5** in continuous Suzuki-Miyaura cross-coupling utilizing the plug & play reactor.

Regarding the performance of Suzuki cross-coupling reactions in continuous flow, leaching of catalytically active Pd species from the solid support into the reaction solution is known to be a major issue [39,40]. Therefore, the contents of palladium, cerium and tin in the outlet flow of the continuous experiment were measured by ICP-MS after certain time points (Table C-7). As already observed in the batch experiments, the amount of tin in the reaction solution was found to be negligible in all samples (<0.02 mg/kg). The concentration of cerium in the outlet flow instead was determined to decrease over the course of the continuous experiment and was quantified to be 0.70 mg/kg after 4 h. As already reported previously [29], the heterogeneous catalysts with the molecular formula $Ce_{0.99-x}Sn_xPd_{0.01}O_{2-\delta}$ show a significant loss of palladium during the initial phase (0-120 min) of the Suzuki cross-coupling in continuous flow (literature conditions: 1.10 g of Pd catalyst, flow rate 0.45 mL/min). However, after equilibration of the system the palladium content drops below the limit of quantification [29]. Likewise, considerable leaching of palladium into the reaction solution was also observed in the continuous Suzuki coupling step for the synthesis of valsartan precursor **5** over the entire runtime of the experiment. Presumably, due to the lower flow rate of 0.2 mL/min and the larger amount of catalyst compared to mentioned literature experiment [29], the applied system has not reached its steady-state within the duration of the experiment, which was limited by the availability of boronic acid ester **12**. However, in view of a possible application of the reaction setup

for continuous Suzuki coupling on a larger scale, the implementation of a palladium scavenging strategy is advisable. Galaffu et al. reported the successful use of different sulfur-based silica scavengers for the removal of palladium from a variety of advanced synthetic intermediates including valsartan precursor **5** [19]. In their study, after the Suzuki coupling step (1 mol% $Pd(PPh_3)_4$, DME/EtOH/H_2O, Na_2CO_3) the residual amount of palladium in product **5** was effectively decreased from 2100 ppm to <1 ppm by the utilization of respective functionalized silica frameworks [19].

Table C-7: Leaching of Pd, Ce and Sn into the reaction solution in the continuous Suzuki coupling determined by ICP-MS.

Entry	Time [min]	Ce [mg/kg]	Sn [mg/kg]	Pd [mg/kg]
1	50-60	4.1±0.2	<0.02	31.6±0.6
2	120-130	10±1	<0.02	84.2±0.8
3	170-180	2.7±0.2	<0.02	189±1
4	230-240	0.70±0.02	<0.02	207±4

2.4 Multistep continuous setup for the synthesis of 13

After confirming the feasibility of the three single steps of the reaction cascade in continuous flow, an integrated setup for their consecutive performance was developed by simple combination of the individual reaction modules (Scheme C-7). The *N*-acylation step was performed in the coil reactor setup already described using a flow rate of 0.10 mL/min by means of high-pressure syringe pumps (VIT-FIT HP, Lambda Instruments). The outlet stream was then quenched with an aqueous potassium carbonate solution delivered by an HPLC pump (0.10 mL/min, P4.1S, Knauer) using a T-mixing element. For the key step of the reaction cascade, Suzuki-Miyaura cross-coupling, the reaction solution was introduced at resulting 0.20 mL/min into the plug & play reactor [30] equipped with a fixed bed of heterogeneous Pd catalyst $Ce_{0.20}Sn_{0.79}Pd_{0.01}O_{2-\delta}$. Finally, the process stream was merged with a sodium hydroxide solution supplied by a syringe pump (0.1 mL/min, LA-120, Landgraf) to achieve methyl ester hydrolysis. For this step, a longer reactor coil (PTFE, L x O.D. x I.D. 10.0 m x 1/16 in. x 0.031 in.) was chosen in comparison to the individual setup in order to compensate for the higher flow

rate of 0.3 mL/min and to achieve a similar residence time. With this setup exhibiting an estimated total residence time of roughly 1 h, the three steps of the reaction cascade were successfully performed continuously in a consecutive fashion for over 6 h. After an initial equilibration phase (260 min), quantitative conversion of 2-iodobenzonitrile **7c** was achieved and the target compound **13** was obtained with up to 96% yield (90±4% yield, values fluctuating around the mean) and 73% enantiomeric excess (determined by achiral and chiral HPLC, respectively; see Supporting information). Performing the analogous three-step reaction sequence from **11** to **13** in batch including purification of intermediates **5** and **12**, the obtained overall yield was only 28% (see Supporting information for the performance of the individual steps in batch). Therefore, translation of the multistep cascade from batch to continuous flow allowed a significant increase in yield of valsartan precursor **13**. Addressing the moderate enantiopurity of compound **13** synthesized in continuous flow, racemization apparently occurred during the saponification step as intermediates **5** and **12** were shown to be enantiopure (see Supporting information for determination of enantiopurity of **5** and **12**). Consequently, in view of a potential application of the developed continuous approach for actual API production, further process optimization is required to achieve the synthesis of an enantiomerically pure compound.

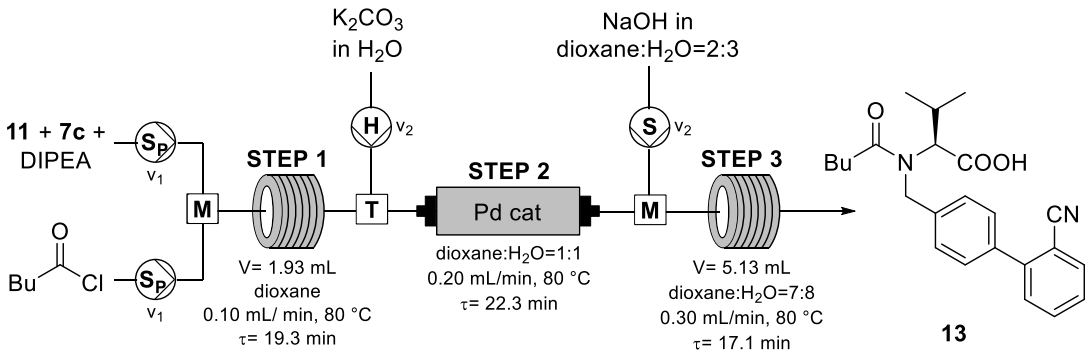

Scheme C-7: Three-step continuous setup for the synthesis of valsartan precursor **13** (S_P= high-pressure syringe pump, S= syringe pump, H= HPLC pump, M= split-and-recombine reactor, T= T-mixer, v_1= 0.05 mL/min, v_2= 0.10 mL/min).

Regarding the selectivity of the reaction steps, in $Ce_{0.99-x}Sn_xPd_{0.01}O_{2-\delta}$ catalyzed Suzuki cross-coupling oxidation and homocoupling of the boronic acid species were reported to cause minor side product formation upon depletion of the aryl halide coupling partner [27]. Therefore, only a slight excess of 1.10 mol eq. of boronic acid ester **12** was employed to minimize formation of the respective by-products, which were presumably present in the reaction mixture

and can be removed by chromatographic techniques. Apart from that, *N*-acylation as well as methyl ester hydrolysis proved to be rather clean reaction steps. This is supported by the fact that HPLC analysis of the outlet flow of the thee-step continuous process revealed side products to the extent of 9 area% compared to the product peak (λ= 230 nm), which most likely originate from the 10% excess of **12**.

3 Conclusion

In conclusion, we developed an approach for the integrated multistep synthesis of a late-stage precursor of the active pharmaceutical ingredient valsartan using a modular continuous setup composed of two coil reactor units and a fixed bed reactor. After equilibration of the multistep setup, it was demonstrated to successfully yield the target compound **13** with up to 96% yield with a moderate enantiomeric excess. Whereas in published approaches for the continuous synthesis of a valsartan precursor in a packed bed reactor little functionalized biphenyls were obtained [21,22], with our described setup we were able to perform the synthesis of a more advanced valsartan precursor, in this way highlighting the broad functional-group tolerance of the employed heterogeneous palladium catalyst. However, leaching of palladium into the reaction solution was observed for the heterogeneous catalyst employed in the Suzuki-Miyaura cross-coupling step. Hence, there is room for improvement of the process, for example by implementation of a Pd scavenger or by utilization of a more leaching-resistant Pd catalyst. Nevertheless, with the development of the three-step continuous setup, the applicability of continuous flow techniques for the synthesis of advanced chemical intermediates has been proven once more and hopefully encourages research in this field.

4 Experimental section

4.1 General information

Chemicals and solvents were purchased from commercial suppliers and used as received [**Ark Pharm**: 2-(4-(bromomethyl)phenyl)-4,4,5,5-tetramethyl-1,3,2-dioxaborolane (97%); **Fluorochem**: L-valine methyl ester hydrochloride (99%), 2-iodobenzonitrile (98%); **Sigma Aldrich**: potassium carbonate (99%), valeryl chloride (98%), anisole (99%); **Carl Roth**: dioxane (>99.5%), NaOH (>99%)]. Analytical thin layer chromatography was performed on pre-coated aluminium

plates (Merck, silica gel 60, F_{254}) and spots were visualized with UV light (254 nm) and potassium permanganate stain. Column chromatography purifications were carried out using MN silica gel 60 (70-230 mesh). For monitoring of the reaction progress and determination of enantiomeric excess, an Agilent 1100 series HPLC system was utilized (for HPLC parameters see Supporting information). HPLC-MS measurements were performed on a Waters Acquity H-Class system equipped with a Waters Acquity SQD detector. For ICP-MS measurements, an Agilent 7700x ICP-MS system was employed after microwave assisted acidic digestion of the samples. Measurement of the pH was achieved using a Mettler Toledo FiveEasy^{TM} pH bench meter equipped with a Mettler Toledo LE409 probe. NMR-measurements were recorded using a Bruker Avance III 300 MHz spectrometer (^{1}H: 300 MHz, ^{13}C: 75 MHz, for NMR-data see Supporting information)

4.2 Batch experiments for optimization of step 1

In a typical *N*-acylation experiment, borate **11** (82.5 µmol, 55 mM), DIPEA (1.05-2.00 mol eq.) and anisole (133 mM, internal standard) were dissolved in dioxane to achieve a total volume of 1.5 mL. To start the reaction, valeryl chloride (1.05-2.00 mol eq.) was added at room temperature and the reaction was kept stirring (2000 rpm) with a magnetic stirrer at elevated temperature (40-80 °C) for 20 min. To examine the reaction progress, an aliquot (20 µL) was withdrawn from the reaction solution, quenched with MeOH:H_3PO_4=50:50 (400 µL) and analyzed by HPLC (Method A, see Supporting information for details).

4.3 Batch experiments for optimization of step 2

For optimization of Suzuki-Miyaura cross-coupling reaction, 2-halobenzonitrile **7b-c** (75-150 µmol, 25 mM), borate **12** (1.1-1.5 mol eq.), K_2CO_3 (1.5 mol eq.) and anisole (67 mM, internal standard) were dissolved in the respective reaction solvent to achieve a total volume of 3-6 mL. Then, $Ce_{0.99-x}Sn_xPd_{0.01}O_{2-\delta}$ (2.1-21.4 mg, corresponding to 0.05-1 mol% Pd) was added and the reaction mixture was stirred (2000 rpm) at elevated temperature (65-85 °C) for 90-120 min. For investigation of the reaction progress, an aliquot (40 µL) was withdrawn from the reaction solution, quenched with MeOH:H_3PO_4 buffer=55:45 (400 µL) and analyzed by HPLC (Method B for reactions with **7c**, method C for reactions with **7b**, see Supporting information for details). For determination of leaching of Pd, Ce and Sn, the reaction solution was

filtered, the filter washed with the reaction solvent and the solvent was evaporated. Obtained solid residue was then analyzed by ICP-MS after microwave assisted acidic digestion of the samples.

4.4 Batch experiments for optimization of step 3

In a typical methyl ester hydrolysis experiment, biphenyl compound **5** (60 µmol, 20 mM) and anisole (67 mM, internal standard) were dissolved in the respective reaction solvent to achieve a total volume of 2.95 mL. To initiate the reaction, aqueous base (NaOH or KOH, 50 µL, 2.5-20 mol eq.) was added and the reaction mixture was stirred (2000 rpm) at 80 °C for 30 min. To monitor the reaction progress, an aliquot (40 µL) was quenched with MeOH:H_3PO_4 buffer=55:45 (400 µL) and analyzed by HPLC (Method B, see Supporting information for details).

4.5 Batch experiments for optimization of sequential steps 1 and 2

For optimization of the sequential performance of steps 1 and 2 in batch, borate **11** (82.5 µmol, 55 mM), DIPEA (2.00 mol eq.) and anisole (185 mM, internal standard) were dissolved in dioxane to achieve a total volume of 1.5 mL. To start the reaction, valeryl chloride (2.00 mol eq.) was added at room temperature and the reaction was kept stirring (2000 rpm) at 80 °C. After 20 min of reaction, deionized water (1.5 mL), potassium carbonate (0.11-0.50 mmol) and 2-iodobenzonitrile **7c** (75 µmol) were added to the reaction solution. Then, $Ce_{0.20}Sn_{0.79}Pd_{0.01}O_{2-\delta}$ (2.7 mg, corresponding to 0.25 mol% Pd) was added and the reaction mixture was stirred (2000 rpm) at 80 °C for 60 min. For investigation of the reaction progress, an aliquot (40 µL) was withdrawn from the reaction solution, quenched with MeOH:H_3PO_4 buffer=55:45 (400 µL) and analyzed by HPLC (Method B, see Supporting information for details).

4.6 Integrated synthesis of 13 in continuous flow

Solution A [boronic acid ester **11** (110 mM, 1.1 mol eq.), 2-iodobenzonitrile **7c** (100 mM), DIPEA (220 mM, 2.2 mol eq.), anisole (240 mM) as internal standard] and solution B [valeryl chloride (220 mM, 2.2 mol eq.)] were prepared in dioxane and degassed in an ultrasonic bath

for 15 min. After equilibration of the reactor system, the two reagent solutions were introduced into the first part of the reactor for *N*-acylation (step 1, split-and-recombine reactor + 3 m PEEK coil L x O.D. x I.D. 3.0 m x 1/16 in. x 0.030 in., V_{total}= 1.93 mL, τ= 19.3 min) by means of high-pressure syringe pumps (VIT-FIT HP, Lambda Instruments) at 80 °C using a flow rate of 0.05 mL/min (resulting in a total flow rate of 0.1 mL/min for step 1). The outlet stream was quenched with an aqueous solution of potassium carbonate (185 mM, 3.7 mol eq.) delivered by an HPLC pump (P4.1S, Knauer) with a flow rate of 0.1 mL/min using a T-mixing element. The resulting reaction solution was then pumped through the plug & play reactor [30] equipped with a preparative HPLC column (L x I.D. 120 x 8 mm) filled with Pd catalyst $Ce_{0.20}Sn_{0.79}Pd_{0.01}O_{2-\delta}$ (4.3 g) for Suzuki-Miyaura cross-coupling (τ= 22.3 min). Subsequently, the process stream was merged with a sodium hydroxide solution (750 mM, 15 mol eq., dioxane:H_2O=2:3) with a flow rate of 0.1 mL/min delivered by a syringe pump (LA-120, Landgraf) and introduced into the final part of the reactor to achieve methyl ester hydrolysis (step 3, split-and-recombine reactor + 10 m PEEK coil L x O.D. x I.D. 10.0 m x 1/16 in. x 0.030 in., V_{total}= 5.13 mL, τ= 17.1 min) to obtain targeted valsartan precursor **13**. After certain time points, an aliquot of the outlet flow (50 µL) was quenched with MeOH:H_3PO_4=55:45 (400 µL) and analyzed by HPLC (Method B).

5 References

1. Cardiovascular diseases (2017) World Health Organization. http://www.who.int/news-room/fact-sheets/detail/cardiovascular-diseases-(cvds). Accessed 4 Sept 2018
2. Oparil S, Schmieder RE (2015) Circ Res 116:1074-1095
3. Goossen LJ, Melzer B (2007) J Org Chem 72:7473-7476
4. Kloss F, Neuwirth T, Haensch VG, Hertweck C (2018) Angew Chem Int Ed Engl 57:14476-14481
5. Siddiqui N, Husain A, Chaudhry L, Alam MS, Mitra M, Bhasi PS (2011) J Appl Pharm Sci 01:12-19
6. Li JJ, Corey EJ (2013) Drug Discovery: Practices, Processes, and Perspectives. Wiley-VCH, New Jersey
7. Davis J, Oparil S (2018) Curr Hypertens Rep 20:90
8. Vilela-Martin JF (2016) Drug Des, Dev Ther 10:1627-1639

9. Bühlmayer P, Ostermayer F, Schmidlin T (1991) Acyl compounds. Eur Patent EP 1991-810098, Aug 28, 1991; (1992) Chem Abstr 116:151772

10. Lamberth C, Dinges J (2016) Bioactive Carboxylic Compound Classes. Wiley-VCH, New Jersey

11. Verardo G, Geatti P, Castaldi G, Toniutti N, Allegrini P (2005) A process for the preparation of valsartan and intermediates thereof. Eur Patent Application EP 1 533 305 A1, Mar 25, 2005; (2005) Chem Abstr 142:482034

12. Sedelmeier G (2013) Process for the preparation of tetrazole derivatives from organo boron and organo aluminium azides. US Patent US 8,569,528 B2, Oct 29, 2013; (2016) Chem Abstr 166:362689

13. Villa M, Allegrini P, Arrighi K, Paiocchi M (2001) Ortho-metalation process for the synthesis of 2-substituted-1-(tetrazol-5-yl)benzenes. US Patent US 6,271,375 B1, Aug 7, 2001; (1999) Chem Abstr 130:125215

14. Zhang CX, Zheng GJ, Bi FQ, Li YL (2008) Chin Chem Lett 19:759-761

15. Zhang C, Zheng G, Fang L, Li Y (2006) Synlett 03:475-477

16. Tsiperman E, Fine S, Yurkovsky S, Braude V (2007) Process for preparing valsartan. PCT Int Appl WO 2007/005967 A2, Jan 11, 2007; (2007) Chem Abstr 146:122299

17. Seki M, Nagahama M (2011) J Org Chem 76:10198-10206

18. Ghosh S, Kumar AS, Mehta GN (2010) Beilstein J Org Chem 6:4-7

19. Galaffu N, Man SP, Wilkes RD, Wilson JRH (2007) Org Process Res Dev 11:406-413

20. Bessa Belmunt J, Huguet Clotet J, Perez Andres JA, Dalmases Barjoan P (2005) Process for the preparation of valsartan and precursors thereof. PCT Int Appl WO 2005/102987 A1, Nov 3, 2005; (2005) Chem Abstr 143:406147

21. Pandarus V, Gingras G, Béland F, Ciriminna R, Pagliaro M (2014) Org Process Res Dev 18:1550-1555

22. Nagaki A, Hirose K, Tonomura O, Taniguchi S, Taga T, Hasebe S, Ishizuka N, Yoshida J-i (2016) Org Process Res Dev 20:687-691

23. Newman SG, Jensen KF (2013) Green Chem 15:1456-1472

24. FDA Perspective on Continuous Manufacturing (2012) US Food and Drug Administration. https://www.fda.gov/downloads/AboutFDA/CentersOffices/OfficeofMedicalProductsandTobacco/CDER/UCM341197.pdf. Accessed 21 Jan 2019

25. Statement from FDA (2018) US Food and Drug Administration. https://www.fda.gov/NewsEvents/Newsroom/PressAnnouncements/ucm619024.htm. Accessed 30 Oct 2018

26. ONE-FLOW Research Project Home Page. https://one-flow.org. Accessed 20 Feb 2019

27. Lichtenegger GJ, Maier M, Hackl M, Khinast JG, Gössler W, Griesser T, Kumar VSP, Gruber-Woelfler H, Deshpande PA (2017) J Mol Catal A: Chem 426:39-51

28. Roh J, Vávrová K, Hrabálek A (2012) Eur J Org Chem 2012:6101-6118

29. Lichtenegger GJ, Maier M, Khinast JG, Gruber-Wölfler H (2016) J Flow Chem 6:244-251

30. Lichtenegger GJ, Tursic V, Kitzler H, Obermaier K, Khinast JG, Gruber-Wölfler H (2016) Chem Ing Tech 88:1518-1523

31. Huang F, Yip H-L, Cao Y (2016) Polymer Photovoltaics: Materials, Physics, and Device Engineering. Royal Society of Chemistry, Cambridge

32. Smith MD, Stepan AF, Ramarao C, Brennan PE, Ley SV (2003) Chem Commun 3:2652-2653

33. Smith MD, Mostofian B, Petridis L, Cheng X, Smith JC (2016) J Phys Chem B 120:740-747

34. Duefert MA, Billingsley KL, Buchwald SL (2013) J Am Chem Soc 135:12877-12885

35. Suzuki A (2002) J Organomet Chem 653:83-90

36. Hoffmann I, Blumenröder B, Onodi neé Thumann S, Dommer S, Schatz J (2015) Green Chem 17:3844-3857

37. Technobis Crystallization Systems Homepage. https://www.crystallizationsystems.com/Crystalline. Accessed 8 May 2019

38. Maier MC, Lebl R, Sulzer P, Lechner J, Mayr T, Zadravec M, Slama E, Pfanner S, Schmölzer C, Pöchlauer P, Kappe CO, Gruber-Woelfler H (2019) React Chem Eng 4:393-401

39. Bourouina A, Meille V, de Bellefon C (2018) J Flow Chem 8:117-121

40. Barreiro EM, Hao Z, Adrio LA, van Ommen JR, Hellgardt K, Hii KK (2018) Catal Today 308:64-70

6 Supporting information

6.1 $^{1}H/^{13}C$-NMR spectra of 5, 11, 12 and 13

NMR-measurements were recorded using a Bruker Avance III 300 MHz spectrometer (^{1}H: 300 MHz, ^{13}C: 75 MHz). The chemical shift (δ [ppm]) was reported relatively to the corresponding solvent $CDCl_3$ (7.26, s). For designation of multiplicities of observed coupling patterns, following abbreviations were used: s (singlet), d (doublet), dd (duplicated doublet), t (triplet), q (quartet), qi (quintet), m (multiplet), brs (broad signal).

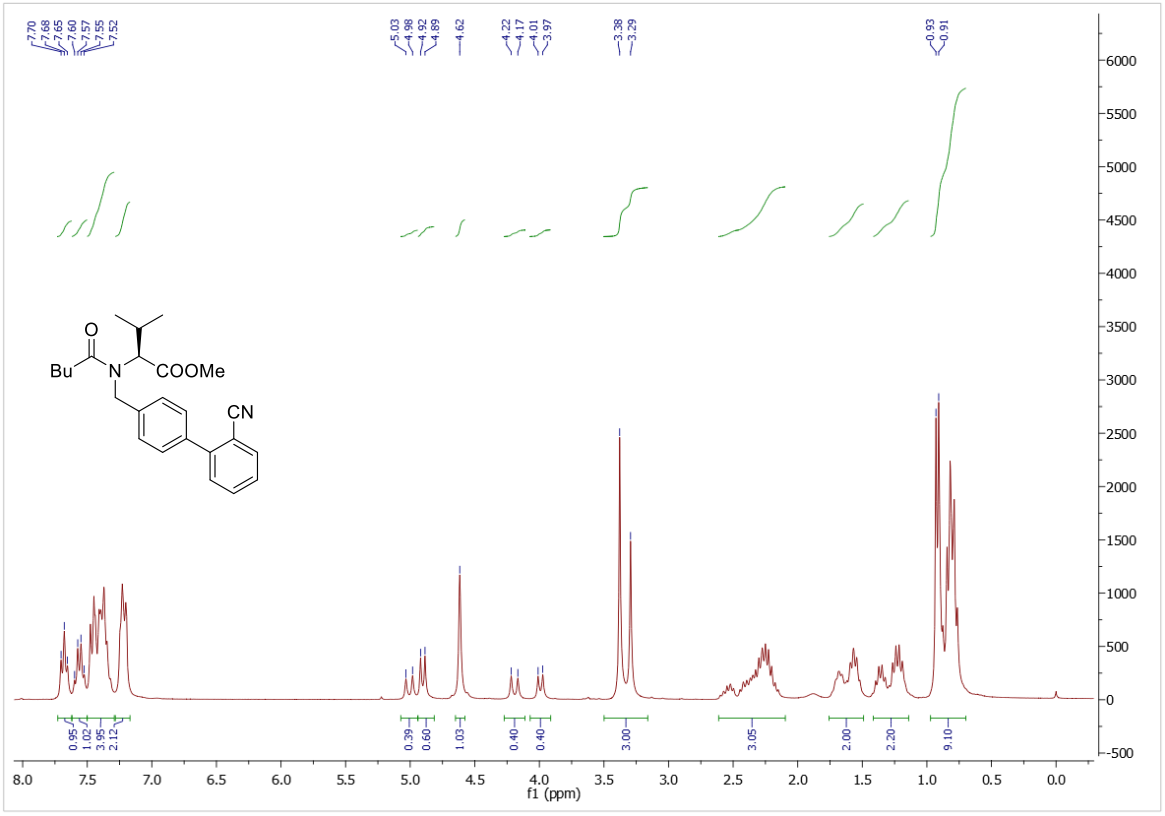

Figure C-S1: ^{1}H-NMR of **5** in $CDCl_3$.

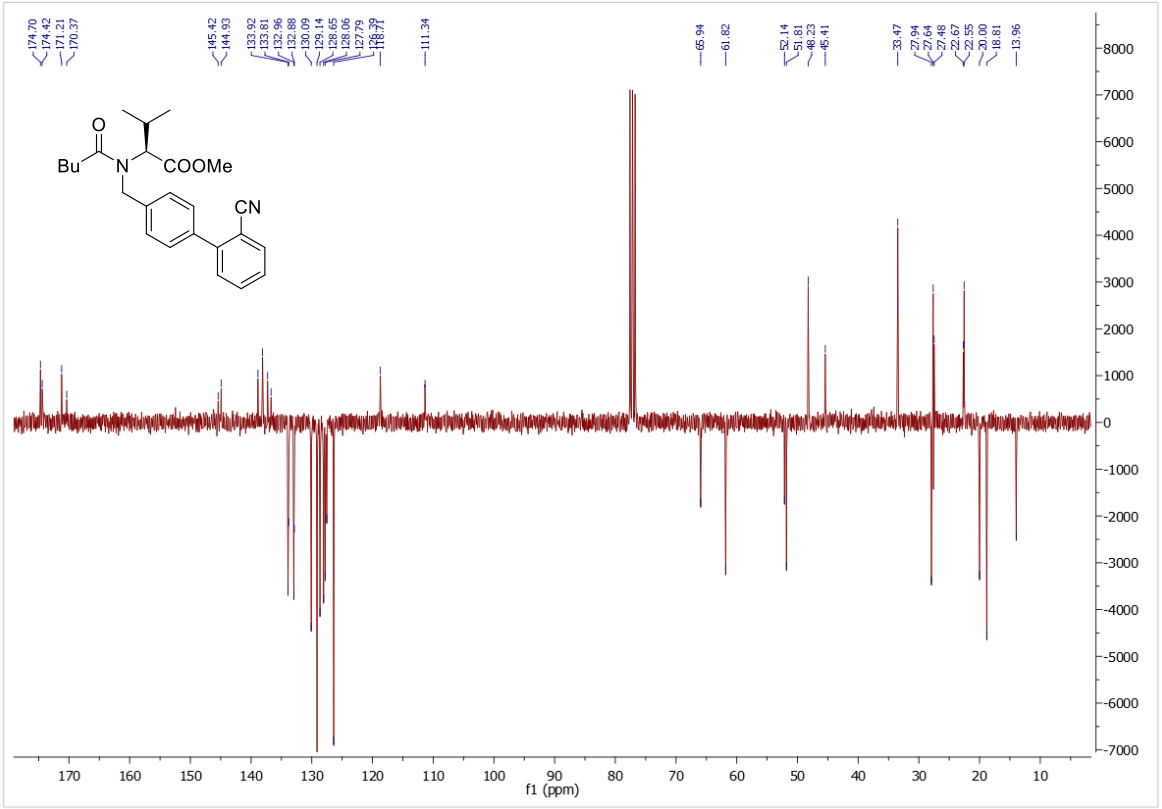

Figure C-S2: ^{13}C-NMR of **5** in $CDCl_3$.

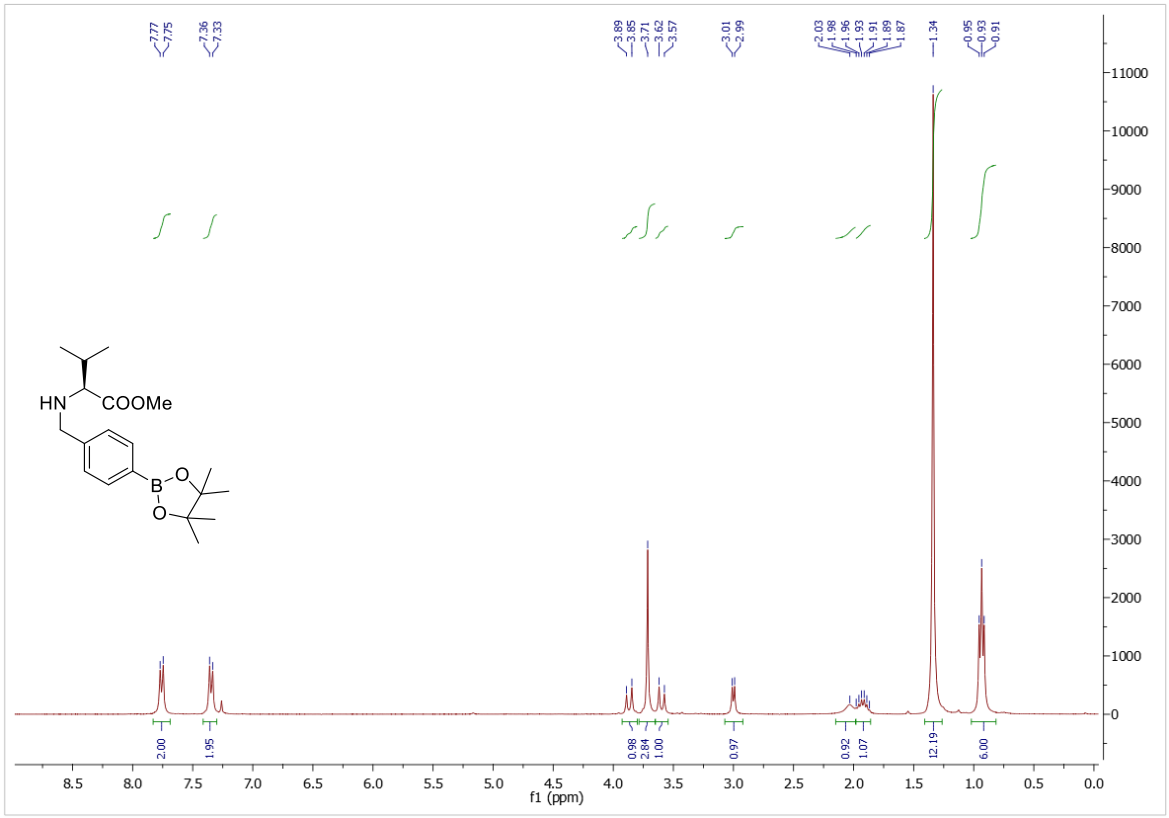

Figure C-S3: ^{1}H-NMR of **11** in $CDCl_3$.

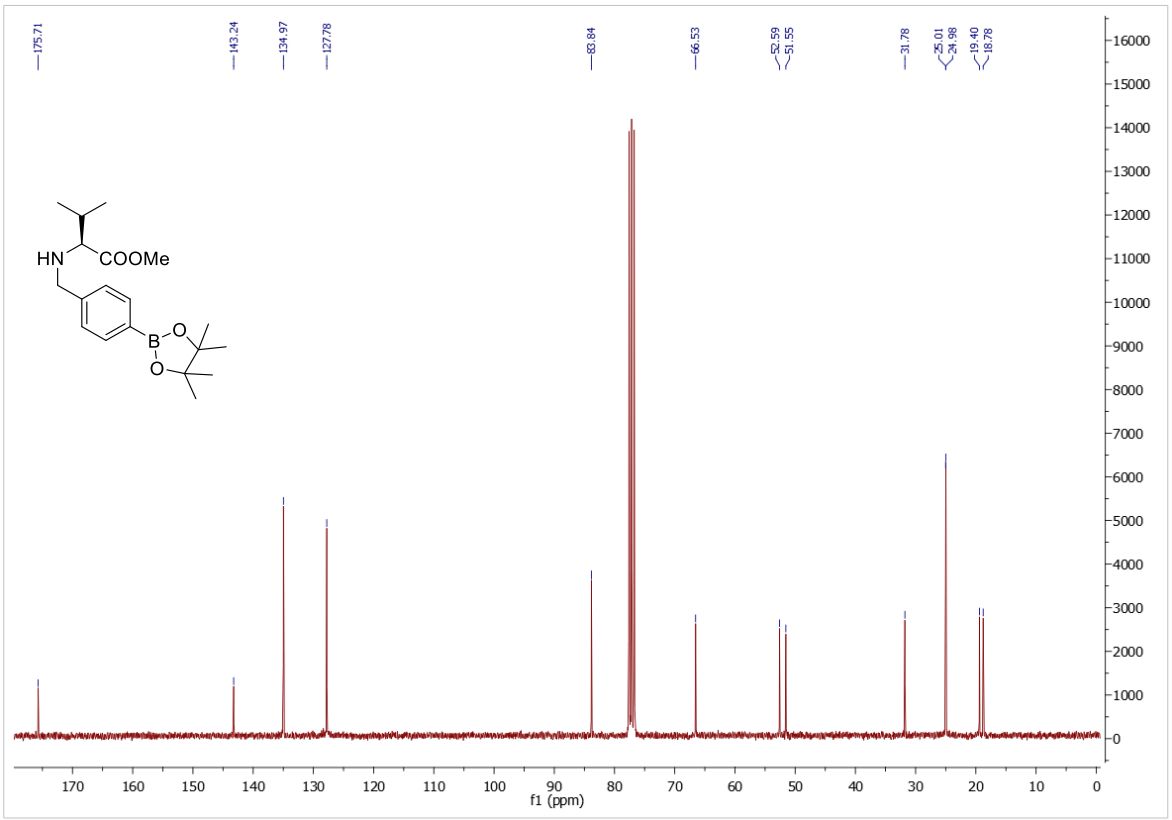

Figure C-S4: ^{13}C-NMR of **11** in $CDCl_3$.

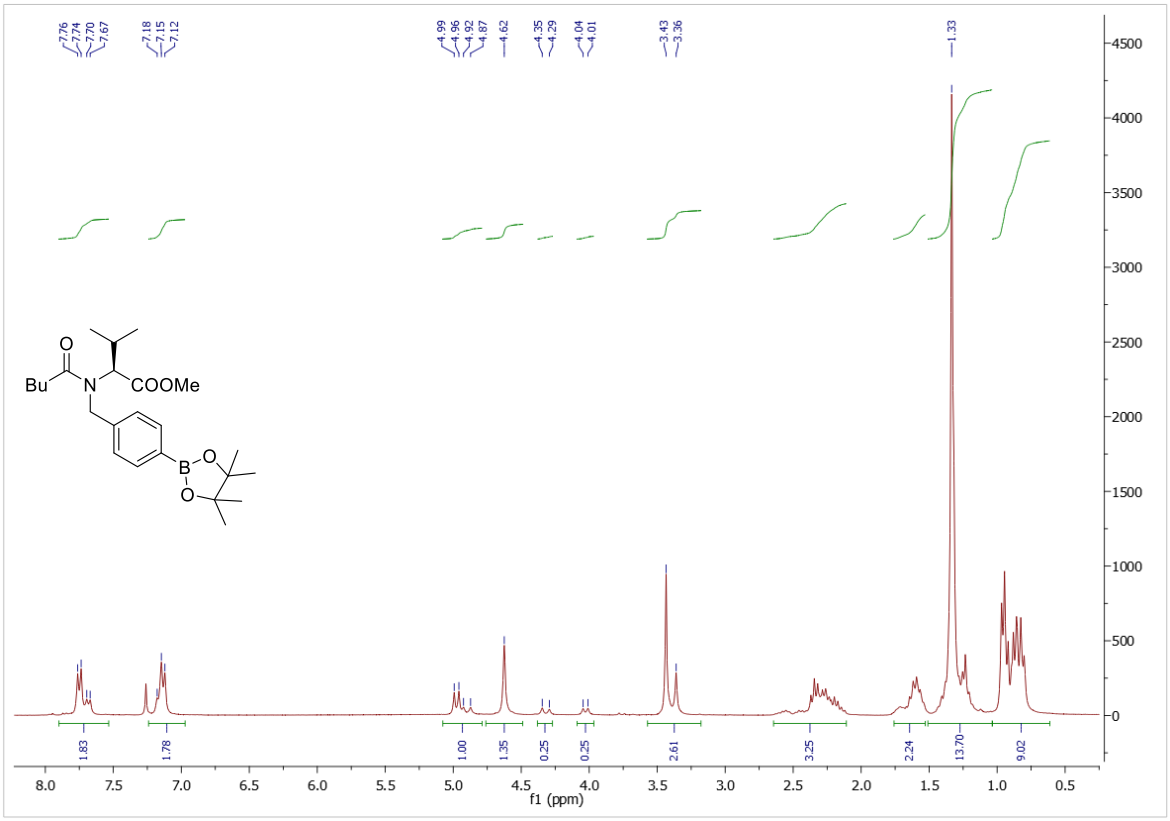

Figure C-S5: ^{1}H-NMR of **12** in $CDCl_3$.

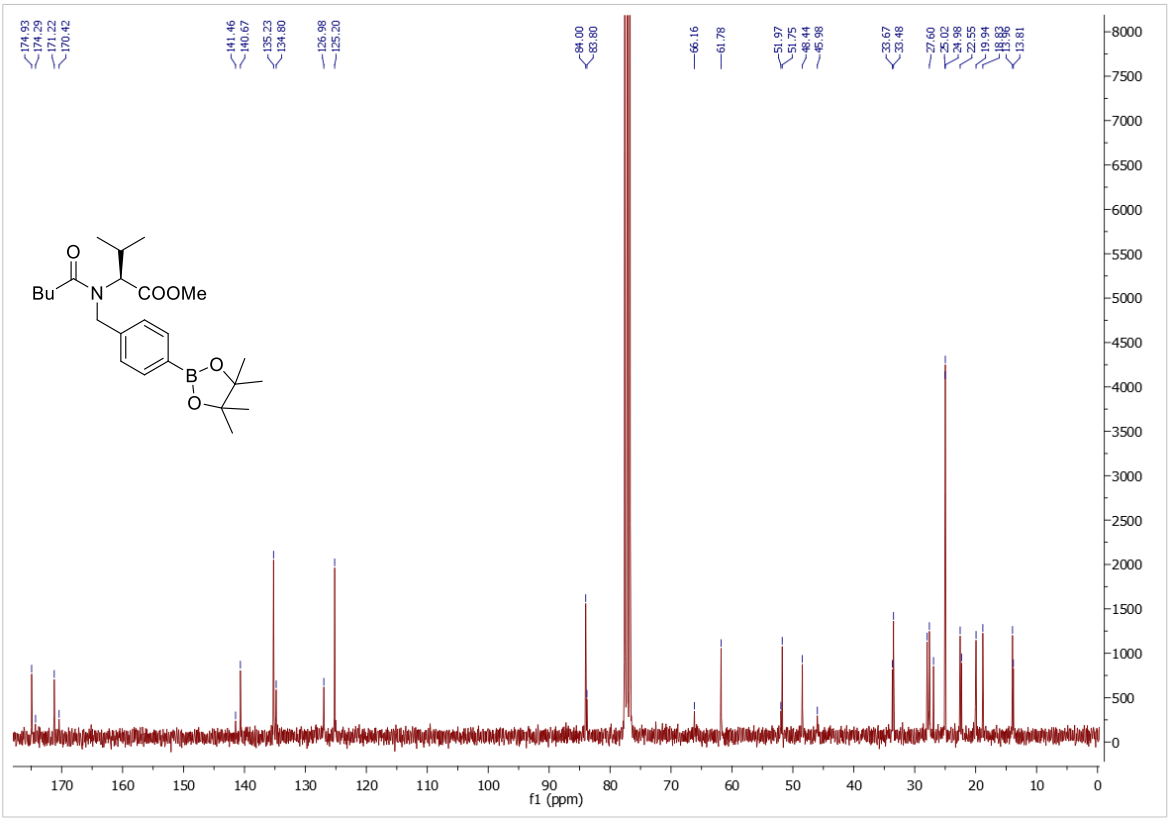

Figure C-S6: ^{13}C-NMR of **12** in $CDCl_3$.

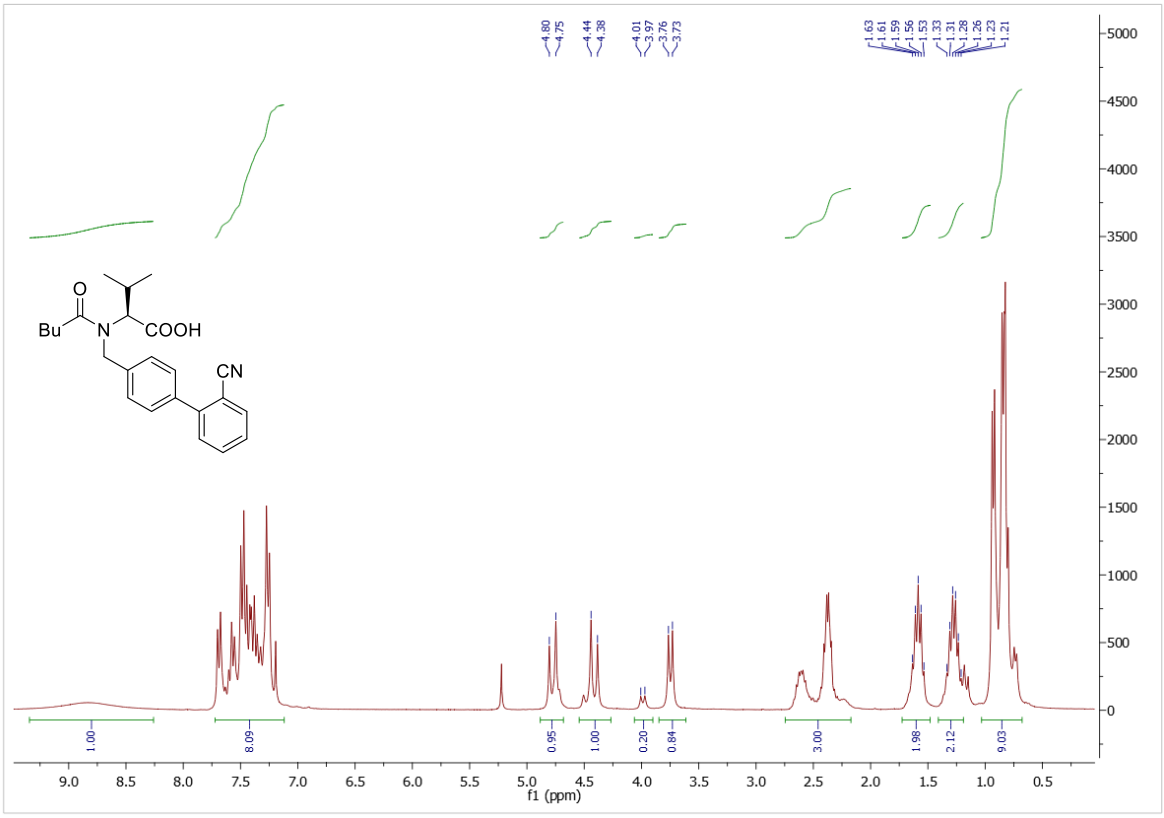

Figure C-S7: ^{1}H-NMR of **13** in $CDCl_3$.

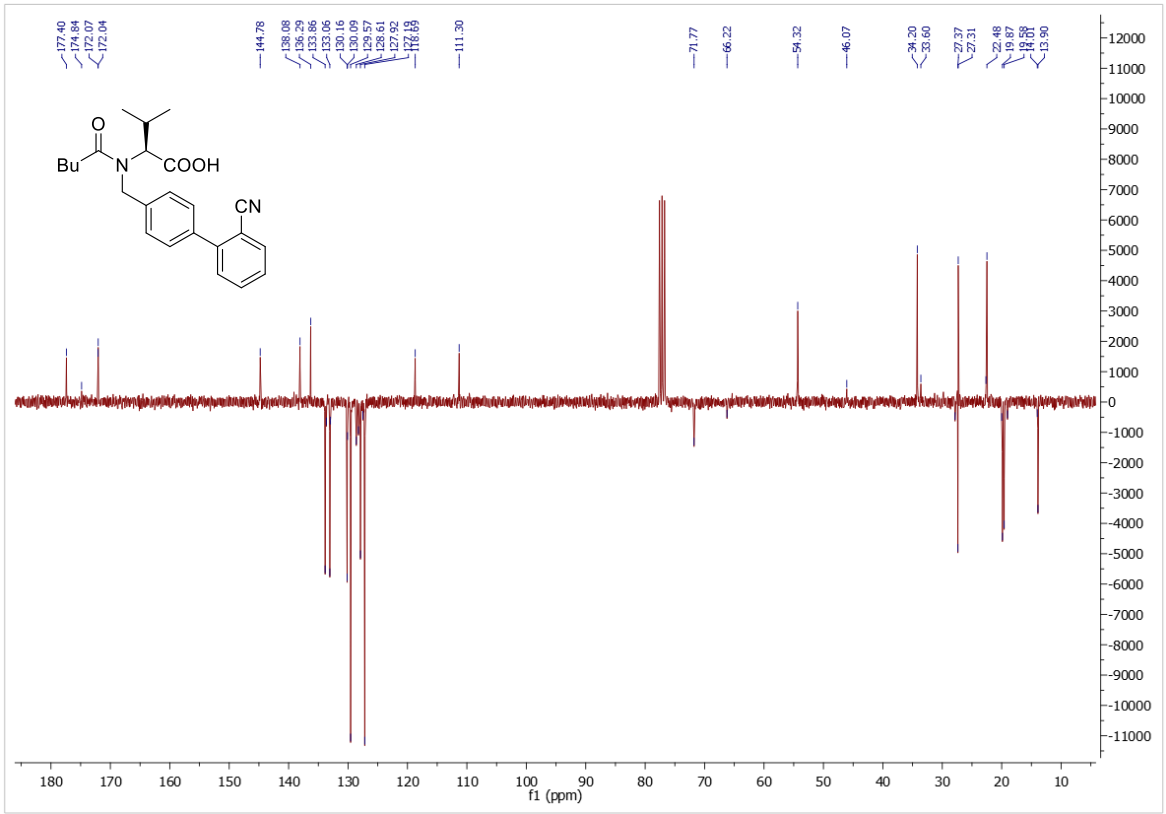

Figure C-S8: ^{13}C-NMR of **13** in $CDCl_3$.

6.2 High performance liquid chromatography (HPLC)

For monitoring of the reaction progress, reaction samples were analyzed using an Agilent 1100 series HPLC system equipped with an online degasser, quaternary pump, autosampler, thermostated column compartment and UV-visible diode array detector. As mobile phases, MeOH (solvent A) and aq. phosphoric acid (H_2O:H_3PO_4=300:1 v/v; solvent B) were used. Compounds were separated using a ThermoFischer Scientific Accucore^{TM} C18 reversed phase column (50 x 4.6 mm; 2.6 µm) at 25 °C with a flow rate of 1 mL/min and detected by UV-absorption over the run time of 15 min. Used elution methods are summarized in Table C-S1.

Table C-S1: HPLC methods (% A = % MeOH, % B = % H_2O:H_3PO_4=300:1 v/v) for monitoring of the reaction progress.

Method	Time [min]	% A (v/v)	% B (v/v)	Sample diluent	Flow [mL/min]
A	0	50	50	MeOH:H_2O=50:50	1
	10	80	20		
	12	50	50		
B	0	55	45	MeOH:H_2O=55:45	1
	10	80	20		
	12	55	45		
C	0	60	40	MeOH:H_2O=60:40	1
	10	80	20		
	12	60	40		

Retention times (t_R) of the respective compounds are apparent from Table C-S2.

Table C-S2: Retention times of compounds separated by HPLC.

Compound	Method	λ [nm]	t_R [min]
5	B	230	7.0
	C		5.3
7b	C	230	1.0
7c	B	230	1.4
11	A	230	0.5 (free acid)
12	A	230	4.4 (free acid)
	B		3.5 (free acid)
	C		2.3 (free acid)
13	B	230	5.4
anisole	A	270	2.1
	B		1.7
	C		1.3

6.3 Determination of enantiomeric purity

*6.3.1 Determination of enantiomeric purity of **12** and **13** by chiral HPLC*

For determination of enantiomeric excess of compounds **12** and **13**, an Agilent 1100 Series HPLC system equipped with a temperature-controlled oven and a UV detector was employed. As mobile phase, n-hexane (solvent A) and 2-propanol (solvent B) containing trifluoroacetic acid (TFA) as modifier if necessary was used. Compounds were separated using a Daicel Chiralpak® AD-H column (250 x 4.6 mm) with a flow rate of 0.8-1 mL/min kept at 30 °C over a time period of 20-25 min and detected by UV-absorption (λ= 230 nm). Used elution methods are summarized in Table C-S3. The chromatographic elution order of the stereoisomers was determined by comparison with synthesized reference compounds **(*S*)-12** and **(*R*)-12** as well as **(*S*)-13** and **(*R*)-13**, respectively. Due to lacking literature values of optical rotation of **(*S*)-12** and **(*S*)-13**, no polarimetric measurements were performed.

Table C-S3: HPLC methods (% A = % n-hexane, % B = % 2-propanol) for determination of enantiomeric purity of **12** (Method A) and **13** (Method B).

Method	% A (v/v)	% B (v/v)	Run time [min]	Flow rate [mL/min]	Modifier
A	90	10	20	0.8	-
B	85	15	25	1.0	0.1 v% TFA

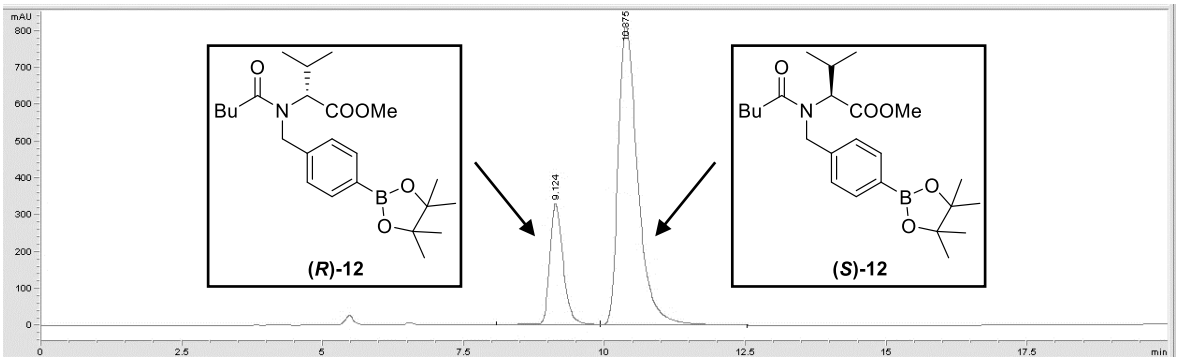

Figure C-S9: Chiral separation of **(*R*)-** and **(*S*)-12** by HPLC (λ= 230 nm, Method A).

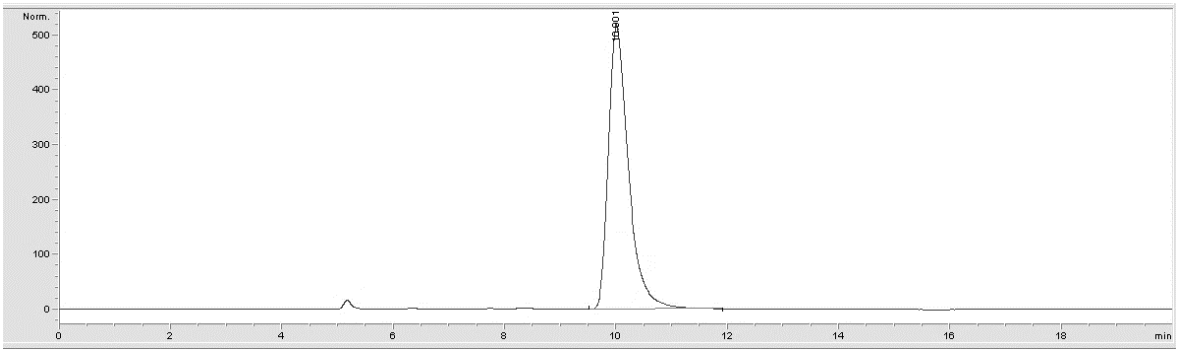

Figure C-S10: Determination of enantiomeric excess of compound **12** (λ= 230 nm, Method A).

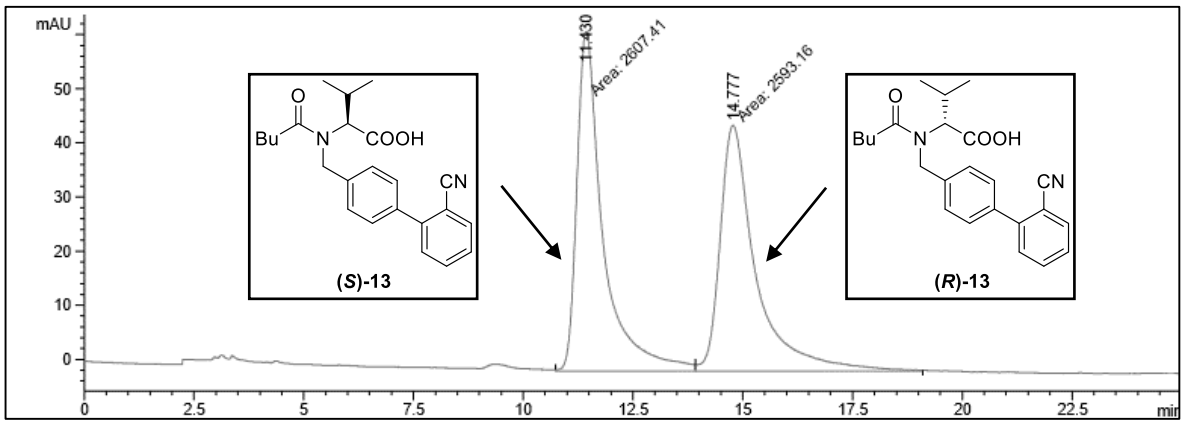

Figure C-S11: Chiral separation of **(*R*)-** and **(*S*)-13** by HPLC (λ= 230 nm, Method B).

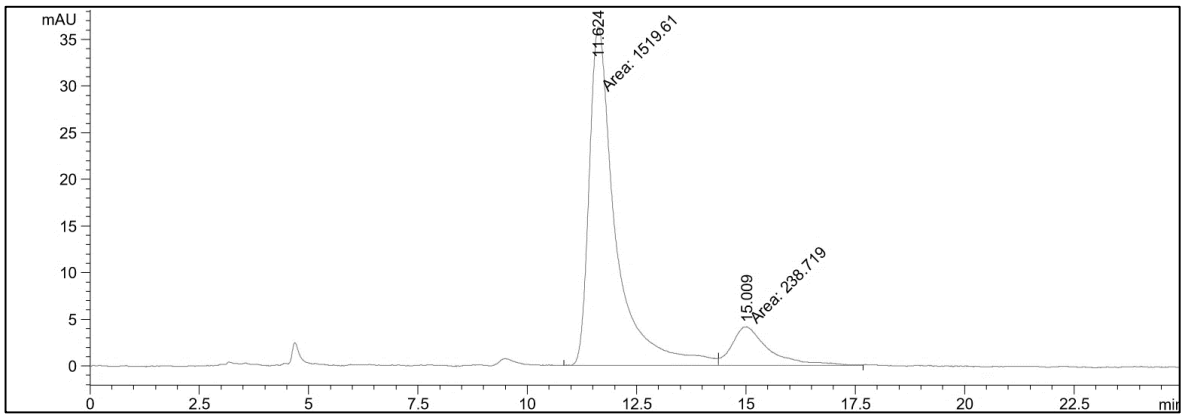

Figure C-S12: Determination of enantiomeric excess of compound **13** synthesized in the multistep flow process (λ= 230 nm, Method B).

*6.3.2 Determination of enantiomeric purity of **5** by optical rotation*

According to the measured optical rotation of compound **5** of $[\alpha]_D^{20}$= -44.0 (*c*= 3.5, $CHCl_3$) [Lit.: $[\alpha]_D^{20}$= -38.0 (*c*= 3.5, $CHCl_3$)] [S1], no significant racemization seems to take place during the Suzuki coupling step. For measurement of optical rotation of compound **5**, a thermostatically controlled Polarimeter MCP 500 equipped with a 1 dm cuvette was utilized. Used wavelength of the sodium halogen lamp was 589 nm and the temperature during measurement was kept constant at 25 °C. The pure sample was diluted in $CHCl_3$ and for calculation of optical rotation following formula was employed:

$$[\alpha]_{\mathrm{D}}^{\mathrm{temperature}} = \frac{[\alpha]}{[\mathrm{c}] * [\mathrm{l}]} \text{ in } \frac{\mathrm{mL}}{\mathrm{dm} * \mathrm{g}}$$

6.4 Optimization of reaction conditions in batch

6.4.1 Step 1 - Batch

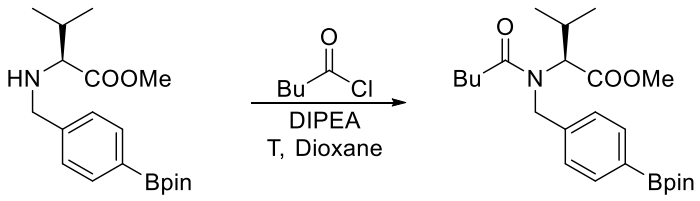

11 **12**

Scheme C-S1: Batch reaction for optimization of the *N*-acylation step.

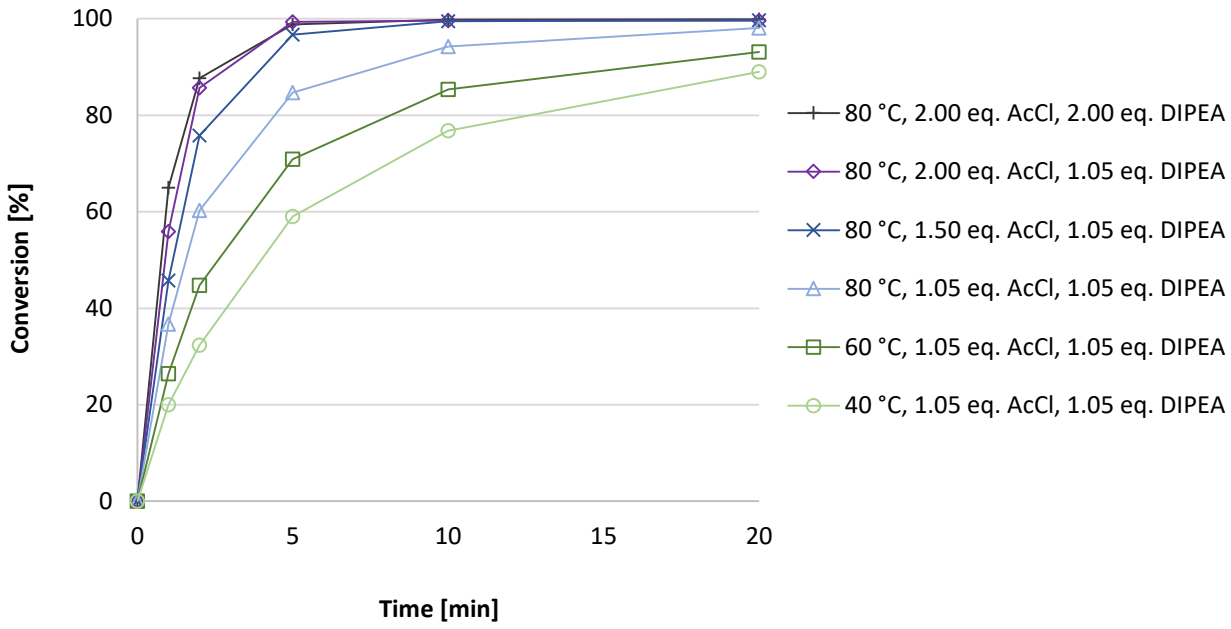

Figure C-S13: Effect of temperature and molar equivalents of valeryl chloride (AcCl) as well as DIPEA on the conversion of **11** in batch.

6.4.2 Step 2 - Batch

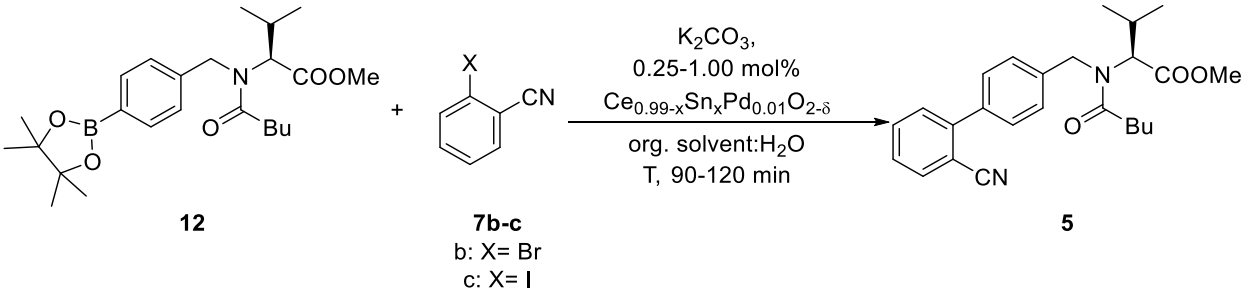

12 **7b-c** b: X= Br c: X= I **5**

Scheme C-S2: Batch reaction for optimization of the Suzuki-Miyaura cross-coupling step.

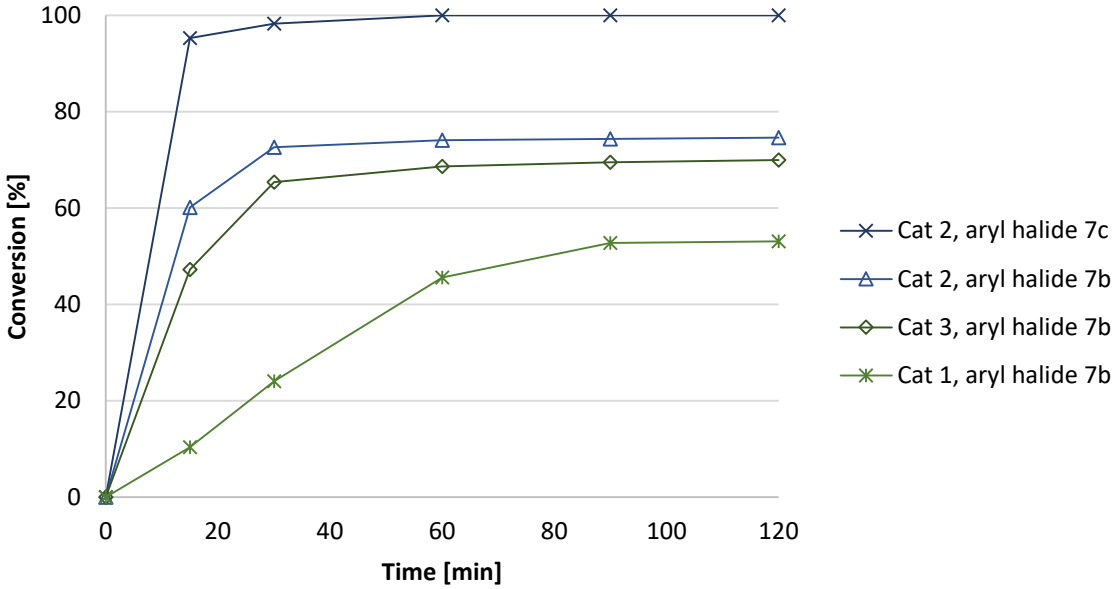

Figure C-S14: Effect of catalyst and aryl halide coupling partner on the conversion of aryl halide **7b-c** in Suzuki-Miyaura cross-coupling with **12** in EtOH:H_2O=7:3.

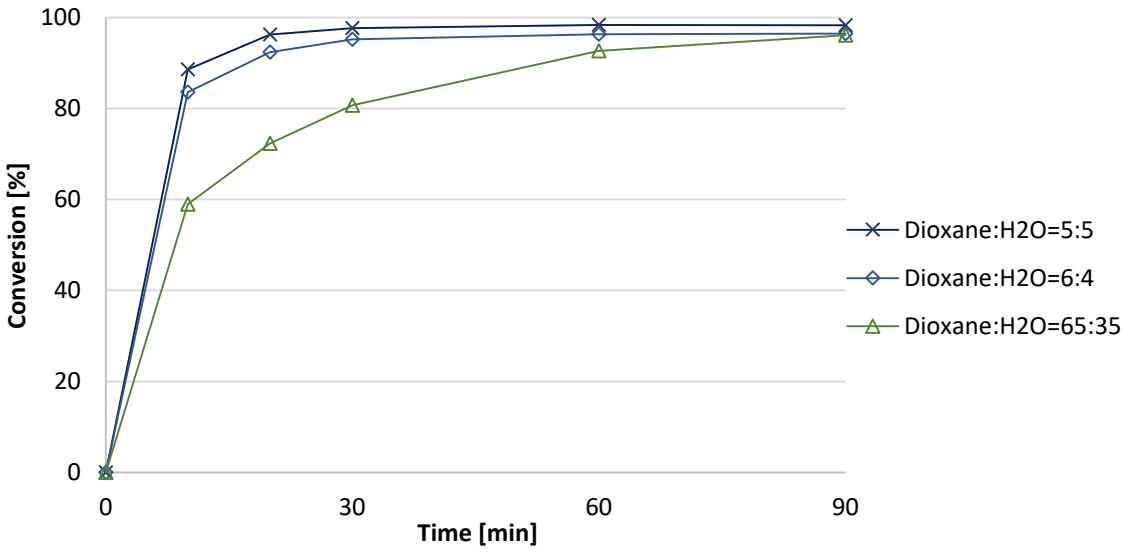

Figure C-S15: Effect of different solvent compositions of dioxane:H_2O on the conversion of **7c** in Suzuki-Miyaura cross-coupling with **12**.

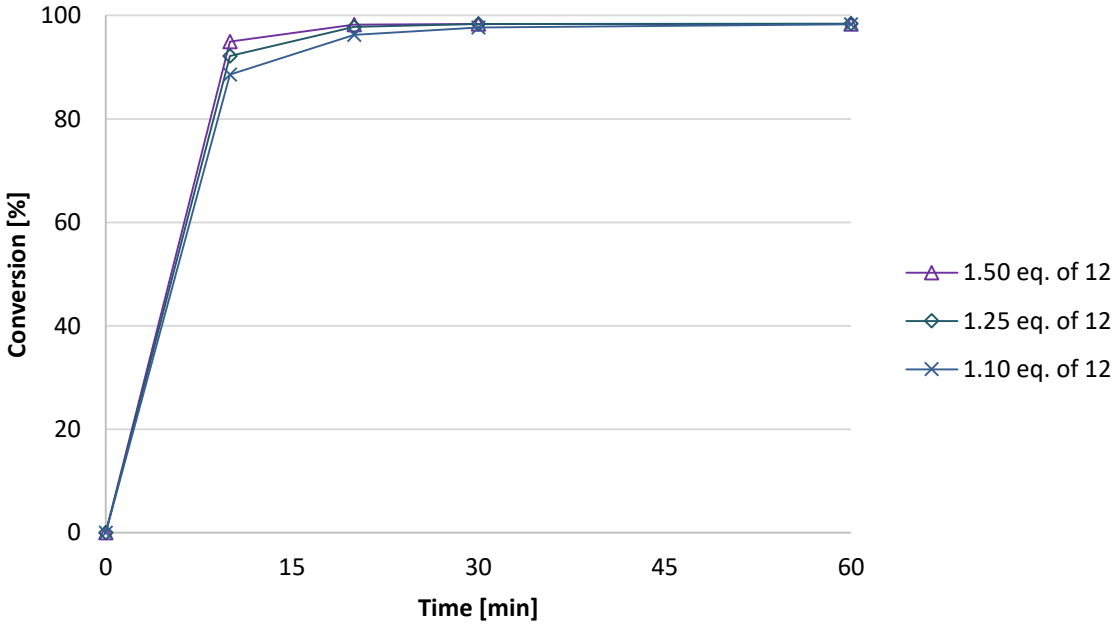

Figure C-S16: Effect of different molar equivalents of **12** on the conversion of **7c** in Suzuki-Miyaura cross-coupling with **12** in dioxane:H_2O=1:1.

6.4.3 Step 3 - Batch

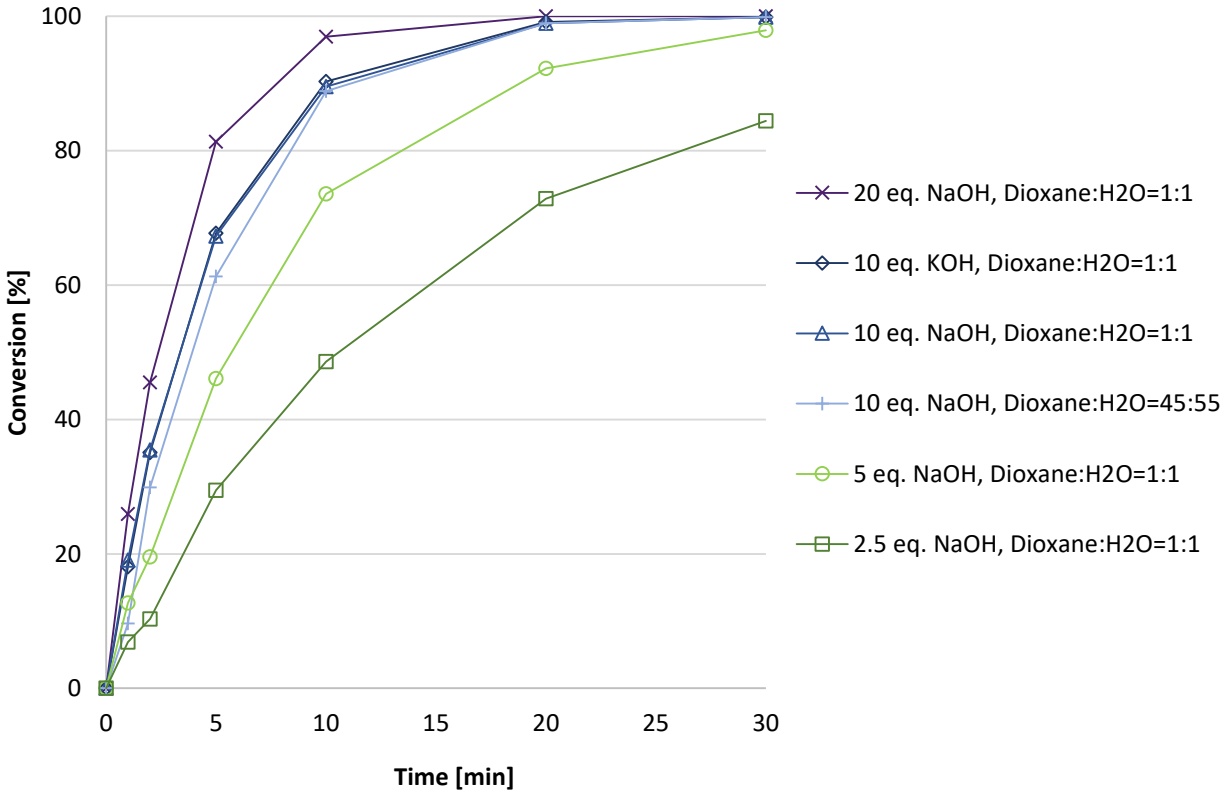

Figure C-S17: Effect of hydroxide source, molar equivalents of base and solvent composition on the conversion of **5** in methyl ester hydrolysis.

6.4.4 Sequential steps 1 + 2 in one-pot in batch

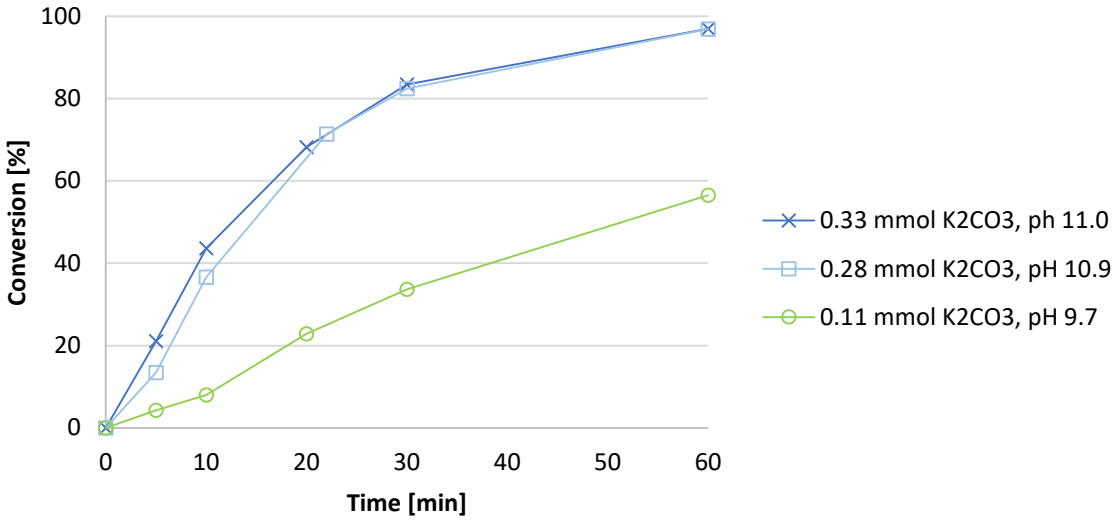

Figure C-S18: Effect of the pH on the conversion of **7c** in Suzuki coupling with **12** performed after *N*-acylation in one-pot.

6.5 Individual continuous setups

6.5.1 Step 1 – Continuous flow

For the continuous performance of the *N*-acylation step, a stainless steel coil (L x O.D. x I.D. 3.0 m x 1/16 in. x 0.030 in.) in combination with a split-and-recombine static mixer [S2] was utilized. A solution containing boronic acid ester **11** (110 mM), DIPEA (220 mM, 2 mol eq.) as well as anisole as internal standard (264 mM) and another solution containing valeryl chloride (220 mM, 2 mol eq.) were prepared in dioxane. Then the two reagent solutions were filled into separate syringes and introduced into the reactor setup at 80 °C with the same flow rate (0.05-0.10 mL/min for each syringe, corresponding to 0.10-0.20 mL/min total flow rate) using a dual-syringe infusion pump (LA-120, Landgraf). At the outlet, the product stream was collected and after certain time points, an aliquot (20 µL) was quenched with MeOH:H_3PO_4=50:50 (400 µL) and analyzed by HPLC (Method A).

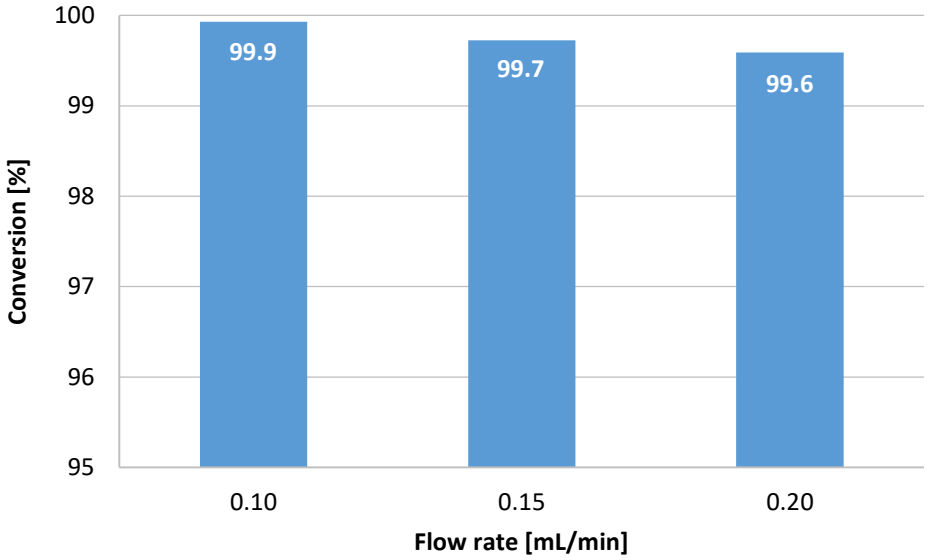

Figure C-S19: Effect of different flow rates on the conversion of **11** during the *N*-acylation step.

6.5.2 Step 2 – Continuous flow

Continuous Suzuki coupling of boronic acid ester **12** with 2-iodobenzonitrile **7c** was performed utilizing the plug & play reactor [S3]. A preparative HPLC column (L x I.D. 120 x 8 mm) was filled with the Pd catalyst $Ce_{0.20}Sn_{0.79}Pd_{0.01}O_{2-\delta}$ (4.7 g) and introduced into the reactor at 80 °C. Then the reactor setup was flushed with solvent for equilibration of the system and removal of air bubbles. A solution containing 2-iodobenzonitrile **7c** (25 mM), boronic acid ester **12** (27.5 mM, 1.1 mol eq.), potassium carbonate (37.5 mM, 1.5 mol eq.) and anisole (67 mM) as internal standard was prepared in dioxane:H_2O=1:1, degassed in an ultrasonic bath for 30 minutes and filtered through a 0.2 µm membrane filter. The reagent solution was transferred into a stainless steel syringe and pumped through the reactor setup with a flow rate of 0.2 mL/min utilizing a high-pressure syringe pump (VIT-FIT HP, Lambda Instruments). At the outlet, the product stream was collected and after certain time points, an aliquot (40 µL) was quenched with MeOH:H_3PO_4=55:45 (400 µL) and analyzed by HPLC (Method B). For determination of leaching of Pd, Ce and Sn, the reaction solution was acidified (10% HNO_3/HCl, 1+1, v/v) and then analyzed by ICP-MS after microwave assisted acidic digestion.

6.5.3 Step 3 – Continuous flow

For the continuous performance of the methyl ester hydrolysis, a stainless steel coil (L x O.D. x I.D. 3.0 m x 1/16 in. x 0.030 in.) in combination with a split-and-recombine static mixer was

utilized. A solution containing biphenyl **5** (50 mM) as well as anisole (60 mM) as internal standard and another solution containing NaOH (500 mM, 10 mol eq.) were prepared in dioxane:H_2O=1:1. Then the two reagent solutions were filled into separate syringes and introduced into the reactor setup at 80 °C with the same rate (0.05-0.10 mL/min for each syringe, corresponding to 0.10-0.20 mL/min total flow rate) using a dual-syringe infusion pump (LA-120, Landgraf). At the outlet, the product stream was collected and after certain time points, an aliquot (40 µL) was quenched with MeOH:H_3PO_4=55:45 (400 µL) and analyzed by HPLC (Method B).

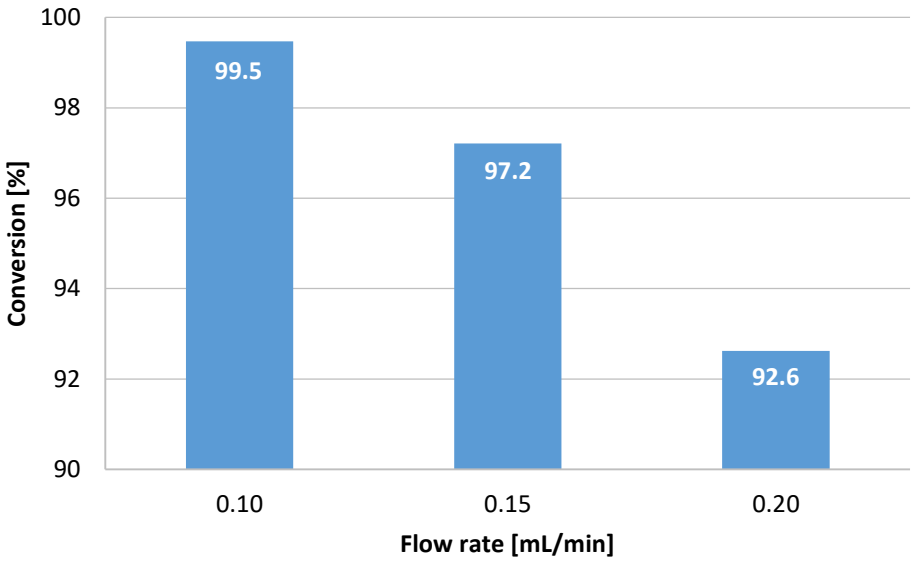

Figure C-S20: Effect of different flow rates on the conversion of **5** during the methyl ester hydrolysis step.

6.6 Multistep continuous setup

The course of yield over time obtained in the multistep continuous process for formation of **13** is apparent from Figure C-S21.

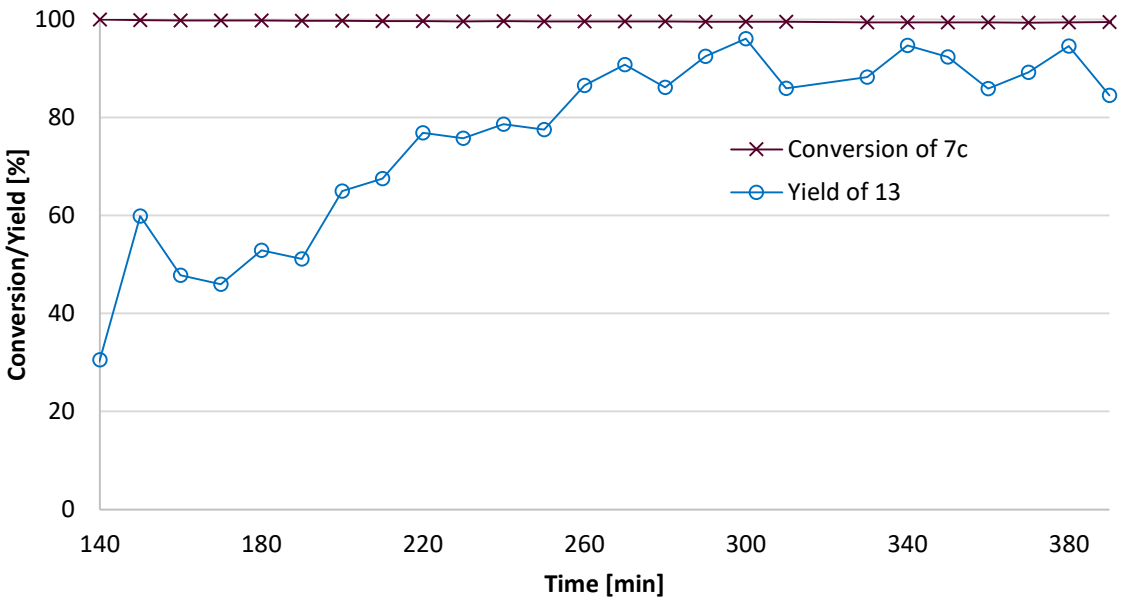

Figure C-S21: Conversion of **7c** and yield of **13** obtained using the multistep continuous setup for the synthesis of valsartan precursor **13**.

6.7 Chemical syntheses of 5, 11, 12, 13 and $Ce_{0.99-x}Sn_xPd_{0.01}O_{2-\delta}$

*6.7.1 Synthesis of **5***

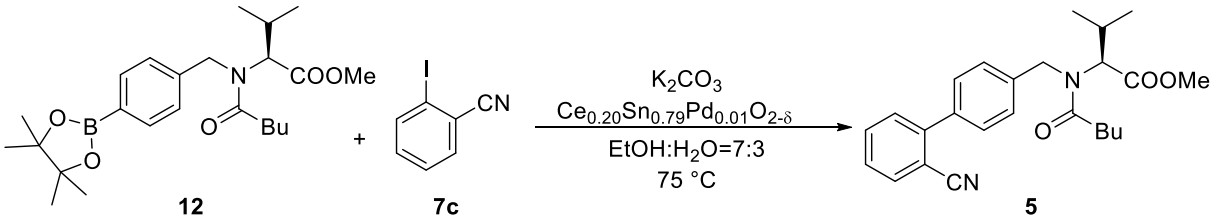

For synthesis of compound **5**, (*S*)-*N*-(1-oxopentyl)-*N*-[[4-(4,4,5,5-tetramethyl-1,3,2-dioxaborolan-2-yl)phenyl]methyl]-L-valine methyl ester **12** (0.28 g, 0.66 mmol), 2-iodobenzonitrile **7c** (0.17 g, 0.73 mmol, 1.1 mol eq.) and potassium carbonate (0.14 g, 0.99 mmol, 1.5 mol eq.) were dissolved in EtOH:H_2O=7:3 (20 mL). Then, the catalyst $Ce_{0.20}Sn_{0.79}Pd_{0.01}O_{2-\delta}$ (50 mg, 0.5 mol%) was added and the reaction mixture was stirred at 75 °C for 1 h. After cooling to room temperature, the solvent was evaporated and diluted with ethyl acetate (25 mL). The Pd catalyst was removed by filtration and the organic phase was washed with deionized water (2x15 mL) and brine (1x10 mL) successively. Combined organic phases were dried over sodium sulfate and solvent was removed by rotary evaporation. The crude product was purified by column chromatography on silica gel (toluene:ethyl acetate=9:1, R_f= 0.31) to obtain **5** as

slightly yellow oil with 70% yield (0.19 mg, 0.46 mmol). ^{1}H- and ^{13}C-NMR data (mix of rotamers) are in accordance with literature [S4,S5].

^{1}H-NMR (300 MHz, $CDCl_3$): δ_H [ppm]= 7.68 (t, *J*= 7.4 Hz, 1H), 7.56 (q, *J*= 7.4 Hz, 1H), 7.50-7.29 (m, 4H), 7.28-7.17 (m, 2H), 5.01 and 4.91 (2d, J_{d1}=15.5 Hz, J_{d2}=10.3 Hz, 1H), 4.62 (s, 1 H), 4.20 (d, *J*= 15.5 Hz, 0.4 H), 3.99 (d, *J*= 10.8 Hz, 0.4 H), 3.38 and 3.29 (2s, 3H), 2.62-2.10 (m, 3H), 1.76-1.49 (m, 2H), 1.41-1.14 (m, 2H), 0.92 and 0.97-0.70 (d+m, *J*= 6.4 Hz, 9H).

^{13}C-NMR (75 MHz, $CDCl_3$): δ_C [ppm]= 174.7, 174.4, 171.2, 170.4, 145.4, 144.9, 138.9, 138.1, 137.3, 136.7, 133.9, 133.8, 133.0, 132.9, 130.1, 129.1, 128.7, 128.1, 127.8, 127.5, 126.4, 118.7, 111.3, 65.9, 61.8, 52.1, 51.8, 48.2, 45.4, 33.5, 27.9, 27.6, 27.5, 22.7, 22.6, 20.0, 18.8, 14.0.

HPLC/MS-ES (*m/z*) found 407, calcd for $[M+H]^+$ 407.52

*6.7.2 Synthesis of **11***

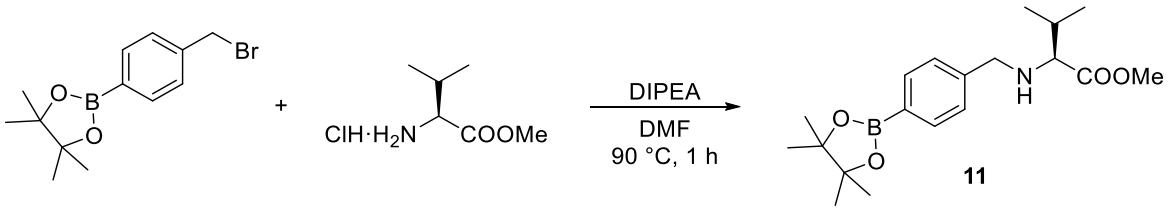

Compound **11** was synthesized based on a reported literature procedure [S6]. 2-(4-(bromomethyl)phenyl)-4,4,5,5-tetramethyl-1,3,2-dioxaborolane (2.00 g, 6.73 mmol) and L-valine methyl ester hydrochloride (1.35 g, 8.08 mmol, 1.2 mol eq.) were suspended in *N*,*N*-dimethylformamide (1.6 mL) and *N*,*N*-diisopropylethylamine (2.59 mL, 14.9 mmol, 2.21 mol eq.) was added. The reaction mixture was heated to 90 °C for 1 h. After cooling to room temperature, toluene (20 mL) was added and the organic phase was washed with deionized water (4x10 mL) and dried over sodium sulfate. The solvent was evaporated and obtained crude product was purified by column chromatography on silica gel (n-hexane:ethyl acetate:toluene=50:12:50; R_f= 0.36). The target compound **11** was obtained as colorless oil with 64% yield (1.50 g, 4.32 mmol). ^{1}H- and ^{13}C-NMR data are in accordance with literature [S5].

^{1}H-NMR (300 MHz, $CDCl_3$): δ_H [ppm]= 7.76 (d, *J*= 7.7 Hz, 2H), 7.35 (d, *J*= 7.7 Hz, 2H), 3.87 (d, *J*= 13.4 Hz, 1H), 3.71 (s, 3H), 3.60 (d, *J*= 13.4 Hz, 1H), 3.00 (d, *J*= 6.0 Hz, 1H), 2.03 (brs, 1H), 1.92 (sex, *J*= 6.6 Hz, 1H), 1.34 (s, 12H), 0.93 (t, *J*= 6.2 Hz, 6H).

^{13}C-NMR (75 MHz, $CDCl_3$): δ_C [ppm]= 175.7, 143.2, 135.0, 127.8, 83.8, 66.5, 52.6, 51.6, 31.8, 25.0, 19.4, 18.8.

HPLC/MS-ES (*m/z*) found 348, calcd for $[M+H]^+$ 348.27

*6.7.3 Synthesis of **12***

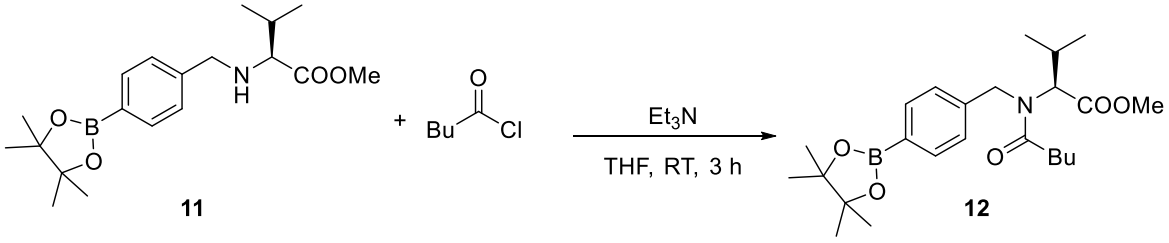

The synthesis of **12** was performed according to published literature procedure [S5]. (*S*)-*N*-[[4-(4,4,5,5-tetramethyl-1,3,2-dioxaborolan-2-yl)phenyl]methyl]-L-valine methyl ester **11** (1.00 g, 2.88 mmol) was dissolved in dry tetrahydrofurane (25 mL) and triethylamine (0.41 mL, 2.94 mmol, 1.02 mol eq.) was added dropwise. After cooling to 0 °C, valeryl chloride (0.68 mL, 5.76 mmol, 2.0 mol eq.) was added dropwise and the reaction mixture was stirred at room temperature for 3 h. The solvent was removed by rotary evaporation and the residue was diluted with ethyl acetate (50 mL). The organic phase was washed with deionized water (3x20 mL) and brine (1x20 mL) successively, dried over sodium sulfate and the solvent was evaporated. The crude product was purified by column chromatography on silica gel (eluent petrol ether:ethyl acetate=9:1 to 8:2, $R_{f\ 9:1}$= 0.35). Product **12** was obtained with 64% yield (0.80 g, 1.84 mmol) as slightly yellow oil. ^{1}H- and ^{13}C-NMR data (mix of rotamers) are in accordance with literature [S5].

^{1}H-NMR (300 MHz, $CDCl_3$): δ_H [ppm]= 7.75 and 7.69 (2d, *J*= 7.7 Hz, 2H), 7.22-7.05 (m, 2H), 4.98 and 4.90 (2d, J_{d1}=10.4 Hz, J_{d2}=15.4 Hz, 1H), 4.62 (s, 1.5 H), 4.32 (d, *J*= 15.8 Hz, 0.25 H), 4.03 (d, *J*= 10.6 Hz, 0.25 H), 3.43 and 3.36 (2s, 3H), 2.65-2.10 (m, 3H), 1.80-1.52 (m, 2H), 1.51-1.15 (m+s, 14H), 1.03-0.70 (m, 9H).

^{13}C-NMR (75 MHz, $CDCl_3$): δ_C [ppm]= 174.9, 174.3, 171.2, 170.4, 141.5, 140.7, 135.2, 134.8, 127.0, 125.2, 84.0, 83.8, 66.2, 61.8, 52.0, 51.8, 48.4, 46.0, 33.7, 33.5, 28.0, 27.6, 26.9, 25.0, 22.6, 22.3, 19.9, 18.8, 14.0, 13.8.

HPLC/MS-ES (*m/z*) found 432, calcd for $[M+H]^+$ 432.38

6.7.4 Synthesis of 13

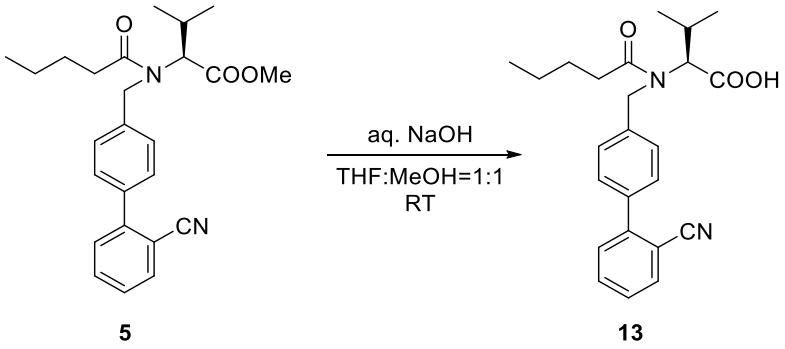

5 **13**

The synthesis of **13** was performed according to a chemical ester hydrolysis procedure stated in literature [S7]. *(S)-N*-[(2'-cyano[1,1'-biphenyl]-4-yl)methyl]-*N*-(1-oxopentyl)-L-valine methyl ester **5** (25 mg, 0.06 mmol) was dissolved in tetrahydrofuran (0.5 mL) and methanol (0.5 mL) and aqueous sodium hydroxide solution (1 M, 0.62 mL, 10 mol eq.) was added. The reaction mixture was stirred at room temperature for 23 h. Then, organic solvents were removed by rotary evaporation and the reaction mixture was acidified using an aqueous hydrogen chloride solution (6 M) until a pH of ~3 was reached. The aqueous phase was extracted with ethyl acetate (3 x 3 mL), dried over sodium sulfate and solvent was removed. Purification of the crude product by column chromatography on silica gel (petrol ether:ethyl acetate:acetic acid=69.5:70:0.5, R_f= 0.33) gave the product **13** as yellowish solid with 67% yield (16 mg, 0.04 mmol).^{1}H- and ^{13}C-NMR data (mix of rotamers) are in accordance with literature [S8].

^{1}H-NMR (300 MHz, $CDCl_3$): δ_H [ppm]= 9.35-8.25 (brs, 1H), 7.72-7.15 (m, 8H), 4.78 (d, *J*= 17.0 Hz, 1H), 4.41 (d, *J*=17.0 Hz, 1H), 3.99 (d, *J*= 10.8 Hz, 0.2H), 3.75 (d, *J*= 10.5 Hz, 0.8H), 2.70-2.17 (m, 3H), 1.72-1.50 (m, 2H), 1.41-1.19 (m, 2H), 0.68-1.03 (m, 9H).

^{13}C-NMR (75 MHz, $CDCl_3$): δ_C [ppm]= 177.4, 174.8, 172.0, 144.8, 138.1, 136.3, 133.9, 133.7, 133.1, 133.0, 130.2, 130.1, 129.6, 128.6, 128.3, 127.9, 127.5, 127.2, 118.7, 111.3, 71.8, 66.2, 54.3, 46.1, 34.2, 33.6, 27.9, 27.4, 27.3, 22.7, 22.5, 20.0, 19.9, 19.6, 19.0, 14.0, 13.9.

HPLC/MS-ES (*m/z*) found 393, calcd for $[M+H]^+$ 393.50

6.7.5 Synthesis of $Ce_{0.99-x}Sn_xPd_{0.01}O_{2-\delta}$

Catalysts of formula $Ce_{0.99-x}Sn_xPd_{0.01}O_{2-\delta}$ (x= 0.20, 0.79, 0.99) were synthesized using a modification of the solution combustion method reported by Baidya et al. [S9]. For the synthesis of 3 g catalyst, the respective amounts of ammonium cerium(IV) nitrate, tin(II) oxalate, palladium(II) chloride and glycine (Table C-S4) were pestled in a mortar to achieve a fine powder. Then, HPLC-grade water (2 mL) was added and the mixture was subjected to ultrasonic radiation for 30 min. After combustion in the oven (350 °C, 1 h), the particle size of the catalyst was again reduced by a mortar and resulting yellow powder was dried in the oven (350 °C) over night. The catalyst was obtained quantitatively and used as such for Suzuki-Miyaura cross-coupling reactions.

Table C-S4: Amounts of catalyst precursors and fuel used for the synthesis of 3 g Pd catalyst.

x	Molecular formula	$(NH_4)_2Ce(NO_3)_6$	SnC_2O_4	$PdCl_2$	glycine
0.2	$Ce_{0.79}Sn_{0.20}Pd_{0.01}O_{2-\delta}$	7.758 g	0.741 g	0.032 g	3.445 g
0.79	$Ce_{0.20}Sn_{0.79}Pd_{0.01}O_{2-\delta}$	2.124 g	3.164 g	0.034 g	3.345 g
0.99	$Sn_{0.99}Pd_{0.01}O_{2-\delta}$	-	4.077 g	0.035 g	3.307 g

6.8 References

S1. Revell JD, Ganesan A (2004) Chem Commun:1916-1917

S2. Maier MC, Lebl R, Sulzer P, Lechner J, Mayr T, Zadravec M, Slama E, Pfanner S, Schmölzer C, Pöchlauer P, Kappe CO, Gruber-Woelfler H (2019) React Chem Eng 4:393-401

S3. Lichtenegger GJ, Tursic V, Kitzler H, Obermaier K, Khinast JG, Gruber-Wölfler H (2016) Chem Ing Tech 88:1518-1523

S4. Goossen LJ, Melzer B (2007) J Org Chem 72:7473-7476

S5. Spencer J, Baltus CB, Patel H, Press NJ, Callear SK, Male L, Coles SJ (2011) ACS Comb Sci 13:24-31

S6. Bessa Belmunt J, Huguet Clotet J, Perez Andres JA, Dalmases Barjoan P (2005) Process for the preparation of valsartan and precursors thereof. PCT Int Appl WO 2005/102987 A1, Nov 3, 2005; (2005) Chem Abstr 143:406147

S7. Levin JI, Rush TS, Lovering F, Hu Y, Li J, Li W, Wu JJ, Hotchandani R, Xiang JS, Du X, Cole DC, Tam SY (2005) Biaryl sulfonamides and methods for using same. US Pat Appl 2005/0143422 A1, Jun 30, 2005; (2005) Chem Abstr 143:97637

S8. Wang Y, Zheng G, Cai G, Chen B, Li H (2009) Process for preparation of valsartan. CN Patent 101450917, Jun 10, 2009; (2009) Chem Abstr 151:124004

S9. Baidya T, Gupta A, Deshpandey PA, Madras G, Hegde MS (2009) J Phys Chem C 113:4059-4068

D Development of a multistep reaction cascade for the synthesis of a sacubitril precursor in continuous flow

The following chapter is taken from the same-titled journal article published in Journal of Flow Chemistry by Hiebler et al. [Hiebler K, Dertnig C, Soritz S, Maier MC, Hörmann TR, Grabner B, Gruber-Woelfler H (2020) J Flow Chem 10:259-270].

The active pharmaceutical ingredient (API) sacubitril acts as a neprilysin inhibitor in the body and is administered to patients suffering from high blood pressure and chronic heart failure. In this paper, we report the development of a three-step setup for the synthesis of an advanced sacubitril precursor in continuous flow. The key transformation of our cascade is a Suzuki-Miyaura coupling facilitated by a heterogeneous palladium catalyst. Its implementation in a packed bed reactor and the application of continuous flow methodologies allow intensification of the cross-coupling reaction compared to batch processing. The subsequent steps for the synthesis of the target molecule involve Boc-deprotection as well as N-succinylation, which have been optimized using the statistical "Design of Experiments" (DoE) approach. In this way, the individual as well as interactive effects of selected parameters on the output of the reactions could be investigated very efficiently. The consecutive performance of the three reaction steps using an integrated setup enabled the synthesis of a late-stage sacubitril precursor in continuous flow with 81% overall yield.

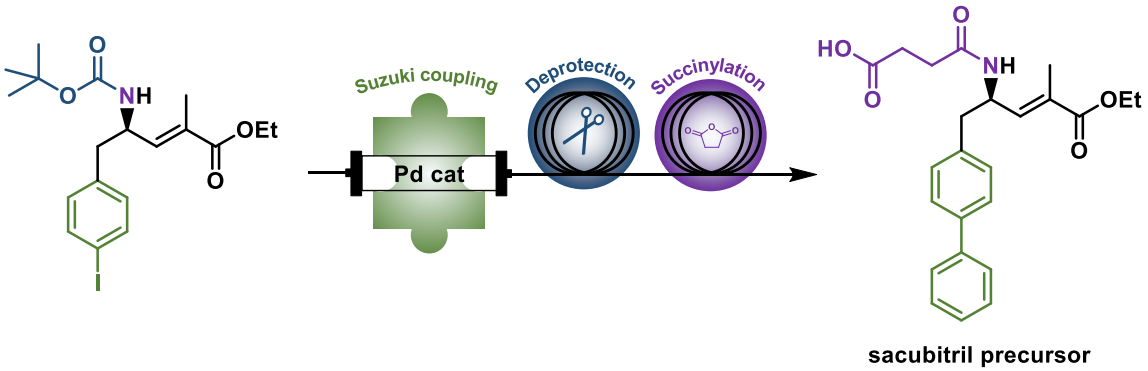

sacubitril precursor

1 Introduction

Among the different medication options for the treatment of hypertension and related cardiovascular complaints [1], drugs affecting the renin-angiotensin-aldosterone system have proved to be highly effective [1]. One prominent representative of this class of agents is LCZ696 (Novartis International AG, Basel, Switzerland), which was approved by the Food and Drug Administration (FDA) in 2015 for the treatment of heart failure in patients with reduced ejection fraction [2]. The fixed-dose combination drug marketed under the brand name Entresto® comprises the active pharmaceutical ingredient valsartan, an angiotensin-II-receptor antagonist, and the prodrug sacubitril **1** [3]. The latter compound is metabolized in the body to an active neprilysin inhibitor upon cleavage of its ethyl ester moiety [2]. The synthesis of sacubitril **1** was first reported by Ksander et al. [4] in 1995, starting from an unnatural D-amino acid derivative **3**. Formation of the main chiral intermediate **2** was achieved in 8 linear steps and involved a Wittig reaction as well as stereoselective hydrogenation (Scheme D-1, a). An alternative route, also running via formation of intermediate **2**, was developed by Hook et al. [5], who used L-pyroglutamic acid methyl ester **4** as chiral pool for the synthesis of **2** in batch (Scheme D-1, b). Recently, Ley et al. [6] published a novel approach applying the concept of continuous flow technology and integrating machine-assisted methods for the synthesis of hydrochloride salt **2*HCl**. In contrast to the other groups, their strategy employs exclusively achiral starting materials **5-7** and the two chiral centers are installed by both Rh-catalyzed stereoselective hydrogenation and diastereoselective Reformatsky-type carbethoxyallylation. By a combination of two batch steps and five transformations in continuous flow, they obtained the target molecule in 54% overall yield (Scheme D-1, c).

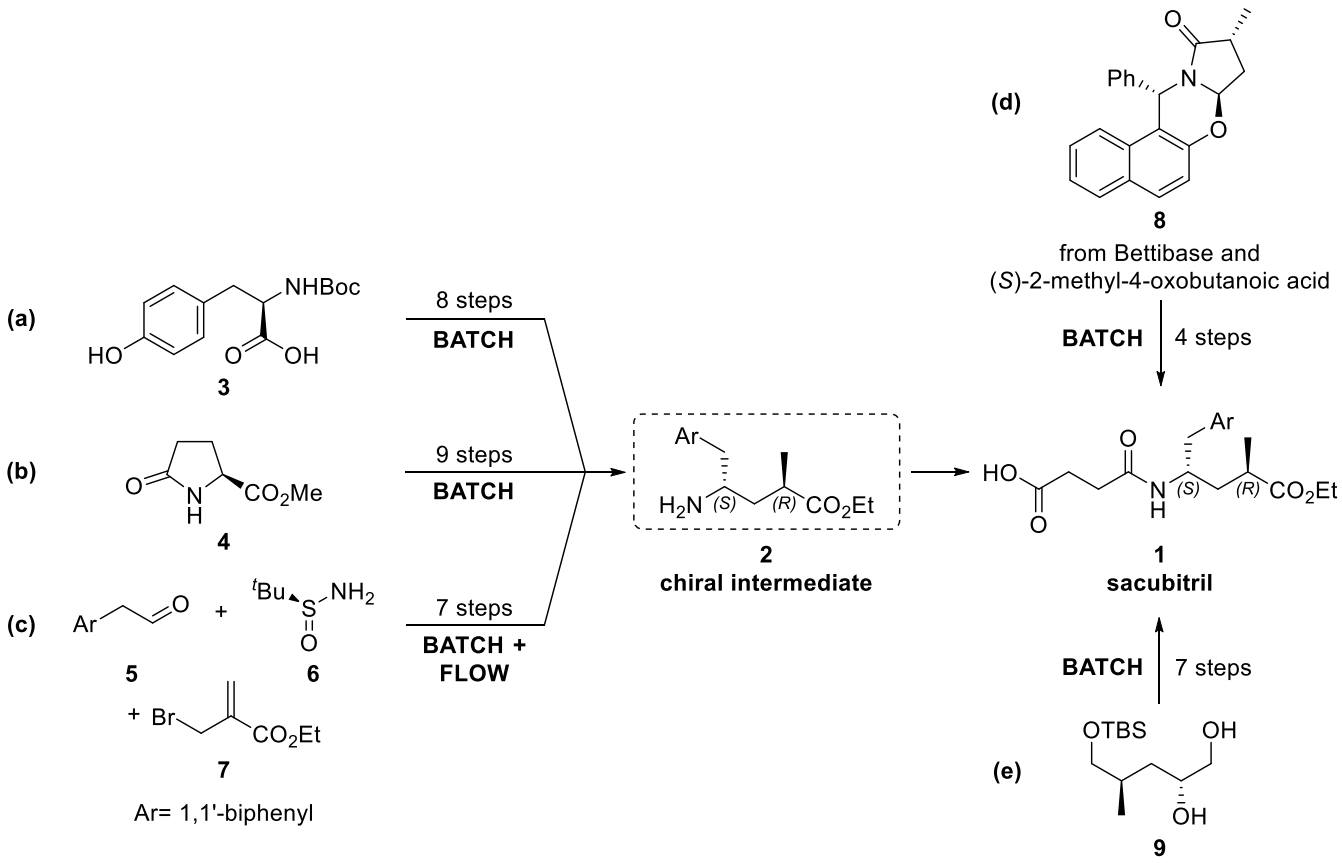

Scheme D-1: Published literature routes for the synthesis of sacubitril **1** [4-8].

Apart from the mentioned approaches involving the formation of chiral intermediate **2**, two alternative strategies for the synthesis of sacubitril **1** have been reported in literature. Firstly, Xu et al. [7] achieved formation of **1** starting from Bettibase and (*S*)-2-methyloxobutanoic acid, which yielded oxazolidine **8**. Upon stereoselective addition of a Grignard reagent to the obtained chiral intermediate **8**, the biphenyl motif is installed and 3 more steps finally give the active pharmaceutical ingredient **1** (Scheme D-1, d). Secondly, the group of Wang [8] developed a chiron-based approach relying on the protected triol **9**. The key transformations of their process are epoxide formation as well as a one-flask Staudinger reduction/succinic amide formation, which facilitate formation of sacubitril **1** in a total of 7 steps (Scheme D-1, e).

Regarding the synthesis of sacubitril **1** on an industrial scale, Novartis International AG (Basel, Switzerland) holds various patents covering different synthetic routes. Their earlier patents comprise chiral pool approaches, similar to the cascades established by Ksander [9] and Hook [10], for formation of the two chiral centers present in the API **1**. However, researchers at the Swiss pharmaceutical company have recently developed a novel organocatalytic strategy for

installation of the stereocenters [11]. The first option described in the patent involves the reaction of Michael acceptor **10** with propionaldehyde employing a proline-derived organocatalyst, which is high-yielding but unsatisfactory in terms of diastereoselectivity (Scheme D-2, a). Formation of the desired diastereomer **12** could be improved by the use of nucleophile **11** in combination with methacrolein and a thiourea-derived catalyst (Scheme D-2, b). However, in view of the potential application of organocatalysis for the synthesis of sacubitril **1** on a large scale, diastereoselectivity still needs to be improved to meet the requirements of the pharmaceutical industry.

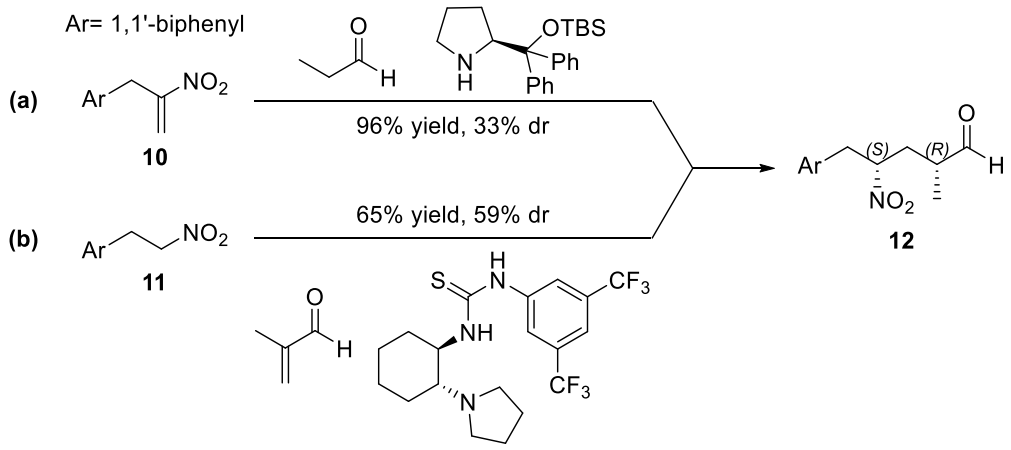

Scheme D-2: Recent organocatalytic approaches for the synthesis of sacubitril **1** via chiral intermediate **12** patented by Novartis [11].

Although apparently a number of different strategies for the synthesis of sacubitril **1** have been developed in the past years, it is conspicuous that almost every approach relies on traditional batch chemistry. As mentioned above, the sole exception is the combined batch and flow process published by Ley and his group [6], involving 5 transformations in continuous flow. Continuous flow methodology offers a plethora of opportunities for the pharmaceutical industry in terms of both process optimization and economics. On the one hand, flow processes benefit from a rapid heat and mass transfer as well as the opportunity for automation and process intensification [exemplarily 12,13], in this way opening novel process windows [14]. Furthermore, improved energy efficiency, high safety and reduced waste generation associated with continuous processing [13,15,16] align with the principles of green and sustainable chemistry [17]. On the other hand, flow chemistry allows to reduce development times and to monitor the product quality in-line, thus saving up to 30% costs in comparison with an equivalent batch process [18-20]. In view of the numerous arguments speaking in favor for

the implementation of continuous flow operations, it is not surprising that continuous manufacturing becomes an increasingly important topic for the pharmaceutical industry [21-24] and is also supported by the FDA [25,26].

Accordingly, as part of the ONE-FLOW research project [27], we are aiming for the development of catalyzed cascade reactions for the formation of active pharmaceutical ingredients. Recently, our group has demonstrated the applicability of flow methodology for the multistep synthesis of an advanced valsartan precursor in a continuous fashion [28]. Hence, our next goal was to prove our concept also for the integrated synthesis of a late-stage sacubitril intermediate **16** in continuous flow, which we report in this paper. The key step of our envisaged reaction scheme, inspired by the paper of Ksander et al. [4], is Suzuki-Miyaura cross-coupling of functionalized sacubitril intermediate **13** (obtained via a three-step batch synthesis procedure, see Supporting information for experimental details) with phenylboronic acid facilitated by the heterogeneous palladium catalyst $Ce_{0.99-x}Sn_xPd_{0.01}O_{2-\delta}$ [28-31]. Subsequently, deprotection of the obtained biphenyl compound **14** and *N*-amidation of the free amine **15** with succinic anhydride yielded the targeted sacubitril precursor **16** (Scheme D-3).

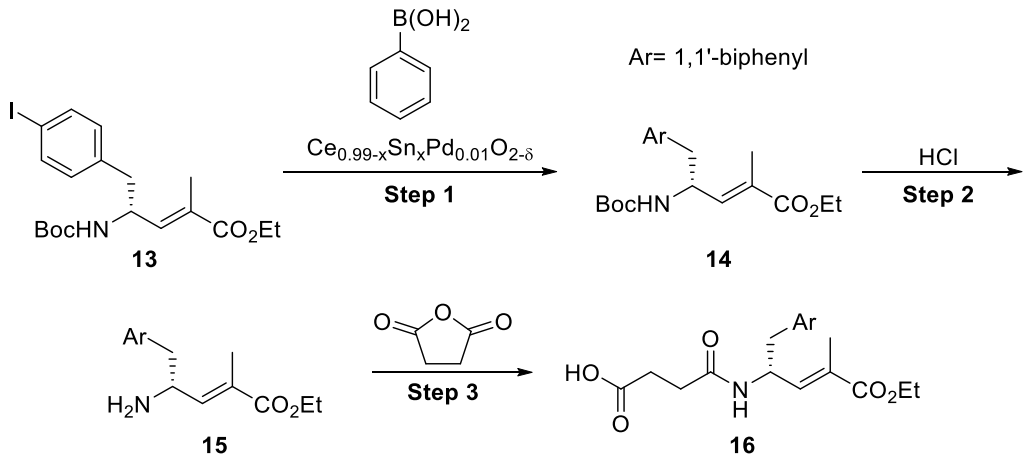

Scheme D-3: Targeted three-step approach for the integrated synthesis of sacubitril precursor **16** in continuous flow.

2 Results and discussion

2.1 Optimization of the individual steps in continuous flow

Palladium-catalyzed C-C cross-coupling reactions have become indispensable in modern organic chemistry [32-34]. Due to its remarkable versatility, functional-group tolerance as well as selectivity, palladium catalysis is long since a key component in the toolbox of the pharmaceutical industry [35-37]. In particular, the Suzuki-Miyaura reaction between aryl halides and boronic acid derivatives plays an important role for the formation of biphenyl motifs [38-40]. In the past couple of years, our group has gained experience with Suzuki-Miyaura reactions in continuous flow facilitated by heterogeneous Ce-Sn-Pd oxides [28-31]. Reviewing published literature procedures for the synthesis of sacubitril **1**, only the route developed by Ksander et al. [4] comprises a Suzuki coupling step and served as our point of reference. First, we aimed for the identification of a successful cross-coupling reaction facilitated by the class of heterogeneous palladium catalysts with the molecular formula $Ce_{0.99-x}Sn_xPd_{0.01}O_{2-\delta}$ (x= 0, 0.20, 0.495, 0.79, 0.99) [29] developed and available in our lab. Their successful utilization for the Suzuki coupling of aryl halides with boronic acid derivatives in batch as well as in continuous flow has already been reported by our group [28-31]. In previous studies and preliminary experiments, the catalyst $Ce_{0.20}Sn_{0.79}Pd_{0.01}O_{2-\delta}$ proved to be the best choice for the Suzuki cross-coupling of advanced chemical intermediates [28]. Therefore, we tested the applicability of the respective palladium catalyst (standard reaction conditions: 1 mol eq. aryl halide, 1.5 mol eq. phenylboronic acid, 1.5 mol eq. K_2CO_3, iPrOH:H_2O=7:3, 75 °C) for Suzuki couplings employing different cross-coupling partners. In doing so, the C-C bond formation between functionalized aryl iodide **13** and phenylboronic acid (Scheme D-3, step 1) emerged to be superior and was chosen to be the key step of our reaction cascade for formation of a sacubitril precursor. Our reaction scheme was completed by Boc-deprotection of the resulting biphenyl derivative **14** as well as reaction of amine **15** with succinic anhydride, giving the sacubitril precursor **16** (Scheme D-3).

Next, we had to select a suitable solvent for our targeted reaction cascade, meeting different requirements for the individual reaction steps. Concerning the Suzuki coupling step using the chosen type of catalyst, the presence of water is crucial for the reaction to occur [28,41]. In

particular, we experienced that our catalyst favors an aqueous single-phase reaction environment [28]. Regarding the solubility of substrates and reaction intermediates as well as stability of the succinic anhydride reagent in the third step, an aprotic organic cosolvent was needed. For that purpose, acetonitrile (MeCN), tetrahydrofuran as well as dioxane came into question. For toxicity as well as miscibility reasons [42,43], we decided to use acetonitrile:water as the reaction medium for the synthesis of sacubitril precursor **16**. For the first step of our cascade, Suzuki cross-coupling, a ratio of acetonitrile:water=65:35 (v/v) turned out to provide sufficient solubility of substrate **13** (25 mM) while keeping the present potassium carbonate dissolved.

After having identified the preferred reaction medium for our targeted synthesis of sacubitril precursor **16**, we aimed to optimize the individual steps of our reaction cascade in continuous flow. Initially, we focused on the first step of the reaction cascade, the Suzuki cross-coupling reaction. Previous studies [28-31] showed that Suzuki couplings employing catalyst $Ce_{0.20}Sn_{0.79}Pd_{0.01}O_{2-\delta}$ work best using the respective aryl halide in combination with both 1.5 mol eq. of boronic acid species and potassium carbonate. Hence, we adopted that approach for the targeted reaction of sacubitril intermediate **13** with phenylboronic acid in a continuous fashion. More specifically, we wanted to study the effect of the reaction temperature on measured conversion of substrate **13**. For the experiment, a solution containing the cross-coupling partners and the inorganic base potassium carbonate in a mixture of acetonitrile:water=65:35 (v/v) was pumped through an HPLC column (L x I.D. 50 x 4.6 mm) filled with particles of palladium catalyst $Ce_{0.20}Sn_{0.79}Pd_{0.01}O_{2-\delta}$ (Scheme D-4, see Experimental section for details). Using a flow rate of 0.05 mL/min, the mean residence time inside the packed bed reactor was determined to be 18.4 min regarding the measurement of a tracer-determined residence time distribution curve. According to literature [44], the employed reaction solvent starts boiling at a temperature of approximately 77 °C. However, one of the major benefits of flow chemistry compared to batch processing is the ability to heat the reaction mixture above its boiling point in a pressurized system and thus to accelerate the reaction rate [12,13]. Hence, we evaluated the performance of our setup at 75, 100 and 125 °C, maintaining a stable pressure of 75 psi with a back pressure regulator. In doing so, a significant increase in measured conversion could be observed with higher temperature. Whereas at a temperature of 75 °C conversion of **13** was determined to be only 59% (Entry 1, Table D-1), an increase to 100 °C led to an improved conversion of 84% (Entry 2, Table D-1). Best results were obtained

at a reaction temperature of 125 °C, giving almost quantitative conversion of **13** using the abovementioned setup (96%, Entry 3, Table D-1). Isolation of biphenyl **14** synthesized in continuous flow at a temperature of 125 °C proved that only minor racemization of the chiral center occurs under the employed reaction conditions (95% enantiomeric excess, see Supporting information for determination of enantiomeric excess by chiral HPLC).

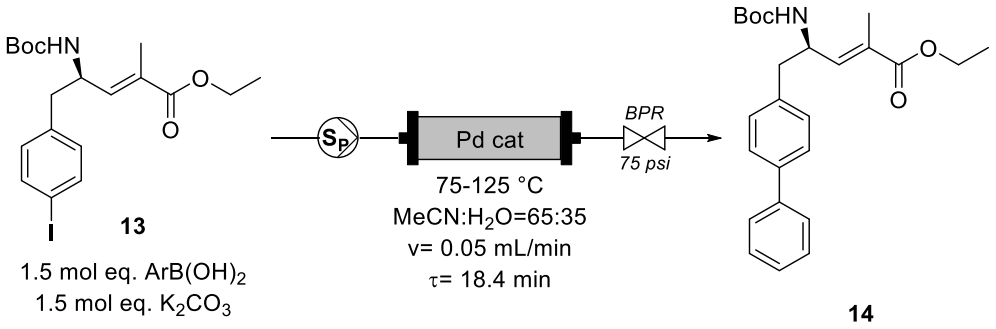

Scheme D-4: Suzuki-Miyaura cross-coupling for formation of sacubitril intermediate **14** in continuous flow facilitated by Pd catalyst $Ce_{0.20}Sn_{0.79}Pd_{0.01}O_{2-\delta}$

Table D-1: Optimization of the reaction temperature of step 1 in continuous flow.

Entry	T [°C]	Conversion[a] [%]
1	75	59
2	100	84
3	125	96

[a] Conversion of **13** after system reached steady state (determined by HPLC)

After having demonstrated the applicability of our packed bed reactor setup for the key Suzuki coupling reaction of our targeted cascade for the synthesis of **16**, we turned our attention to the subsequent steps Boc-deprotection and *N*-amidation. Since we did not have a substantial amount of biphenyl intermediate **14** in hand, we wanted to keep its consumption to a minimum. Therefore, we decided to use readily available surrogate substrates for the optimization of steps 2 and 3 in continuous flow, comprising similar core structures as sacubitril precursor **14**. Thus, we chose to study the Boc-deprotection of Boc-L-phenylalanine methyl ester **17** (Figure D-1) as well as *N*-amidation of L-phenylalanine methyl ester **18** (Figure D-2) using a coil reactor setup. Considering the fact that the outcome (e.g. conversion, yield) of a chemical transformation is the result of a number of interacting reaction parameters, the traditional

one-variable-at-a-time optimization is not the most effective method to investigate the experimental space [45,46]. For this reason, we decided to use an alternative optimization approach employing “Design of Experiments” (DoE), which is a branch of applied statistics. DoE allows the determination of individual as well as combined effects of different influencing factors on the output of an experiment. Furthermore, using DoE the required information for optimization of a given process can be obtained with the minimum amount of experimentation [46]. Being developed already in the 1920s based on the work of R. A. Fisher [47], DoE has been used extensively in various sectors including car manufacturing, biotech and steel industry [46]. In recent years, also the pharmaceutical industry has increasingly taken advantage of DoE for the efficient identification of optimal process parameters for their manufacturing processes [45,48-50].

Regarding the Boc-deprotection of compound **17**, we first had to define how we wanted to achieve the removal of the protecting group. In view of the performance of the deprotection step in targeted cascade for the continuous synthesis of sacubitril precursor **16** after the Suzuki coupling step, the transformation had to be performed in an acetonitrile:water solution. Preliminary batch experiments showed that the deprotection of **17** utilizing commonly employed trifluoroacetic acid [51,52] is relatively slow in aqueous media. Likewise, published deprotection on a strongly acidic ion exchange resin [53,54] did not prove to be satisfyingly successful in water-containing solvent mixtures. In our case, best results were obtained using aqueous hydrochloric acid for removal of the protecting group. The same strategy has also been reported for achieving Boc-removal on a large scale for the synthesis of APIs in batch [55] as well as in continuous flow [24].

Considering the optimization of our Boc-deprotection step, we decided to examine the influence of the factors *temperature* as well as *mol eq. hydrochloride (HCl)* on the conversion of compound **17**. Applying the Design of Experiments approach, we performed the Boc-deprotection of **17** in continuous flow at three different temperatures (70, 75, 80 °C) and varied the amount of hydrochloric acid (5, 10, 15 mol eq.) in the experiments. As we decided to utilize a full factorial DoE, we determined the conversion of **17** resulting of every possible combination of the two selected reaction parameters. Analysis of the collected experimental data with the software MODDE Pro revealed a statistically significant impact of the two interacting variables

on the conversion of **17**, which is visualized in Figure D-1. As expected, the contour plot illustrates an increase in conversion both at higher reaction temperature and using a larger excess of hydrochloric acid. However, the reaction temperature seems to influence the outcome of the reaction more strongly than the excess of hydrochloric acid. Exemplarily, the model suggests that using 5 mol eq. HCl the conversion can be increased from 50% to 80% by raising the temperature only by about 8 °C. To achieve the same boost in conversion at a given temperature of 70 °C, more than double the HCl concentration would be necessary. Regarding our multistep cascade for the synthesis of **16**, we wanted to achieve quantitative conversion utilizing 10 mol eq. of acid. The obtained DoE model led us to expect that quantitative conversion of **17** using 10 mol eq. of HCl could be realized at a temperature of 85 °C. Indeed, the performance of an additional experiment (T= 85 °C, 10 mol eq. HCl) confirmed this assumption (see Supporting information for a detailed description of conducted DoE study, model parameters as well as experimental data).

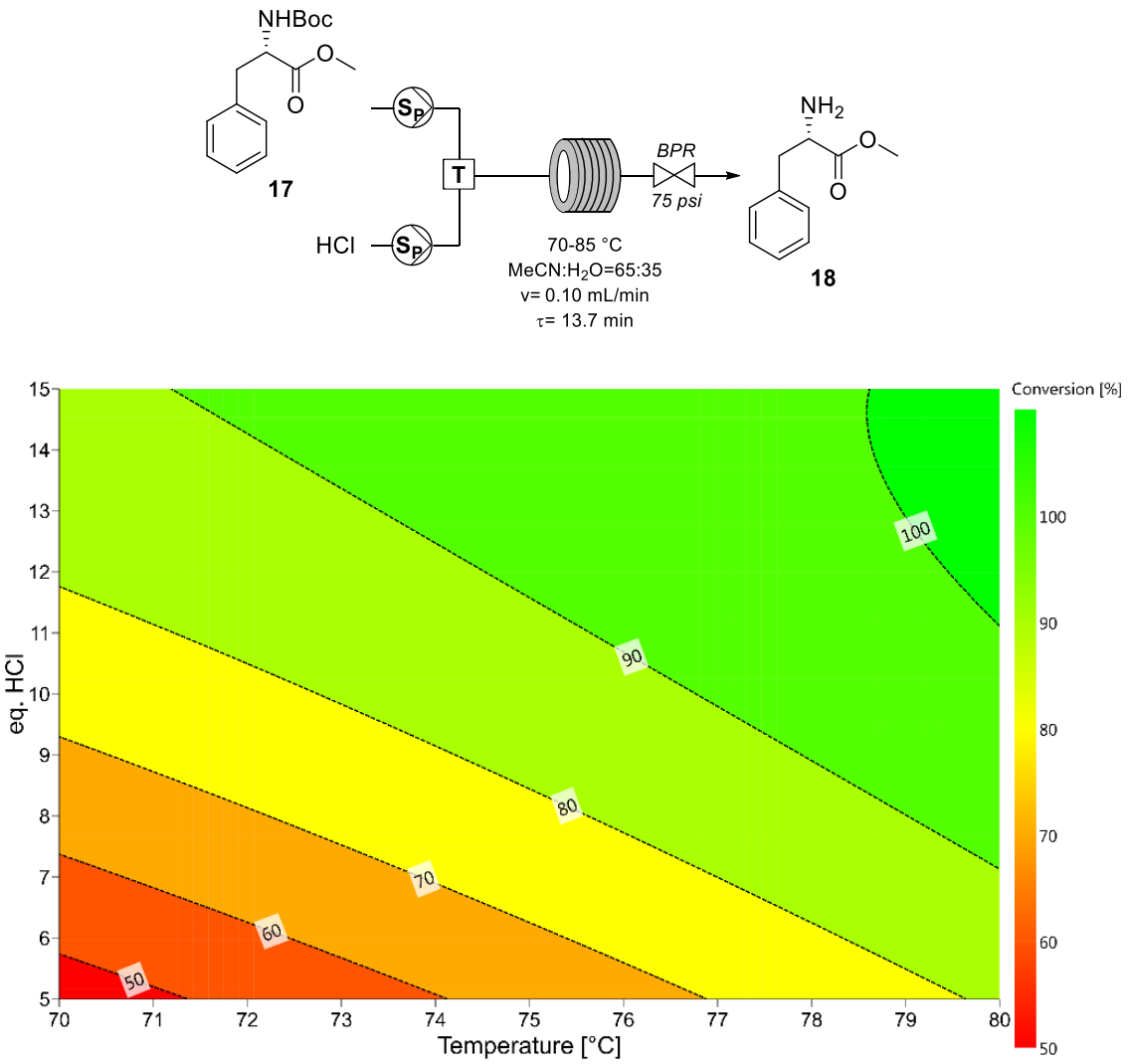

Figure D-1: Reaction scheme and contour plot obtained by DoE analysis of Boc-deprotection of Boc-L-phenylalanine methyl ester **17** in continuous flow with MODDE Pro.

In terms of the continuous *N*-amidation of **18** in an acetonitrile:water medium at room temperature, we chose to determine the impact of the variables *mol eq. succinic anhydride* as well as *mol eq. diisopropylethylamine (DIPEA)* on the reaction outcome. In compliance with full-factorial DoE, we measured the conversion of **18** resulting from every combination of the two influencing factors (1, 1.5, 2 mol eq. succinic anhydride; 0.5, 1, 1.5 mol eq. DIPEA). Evaluation of collected data with MODDE Pro suggested a statistical relevant influence of both parameters on the conversion and revealed also interactive effects. The visual illustration of the calculated mathematical model is depicted in Figure D-2. Within the covered experimental range, maximum conversion is obtained using 2 mol eq. of succinic anhydride along with 1 mol eq. of DIPEA (see Supporting information for a detailed description of conducted DoE study, model parameters as well as experimental data).

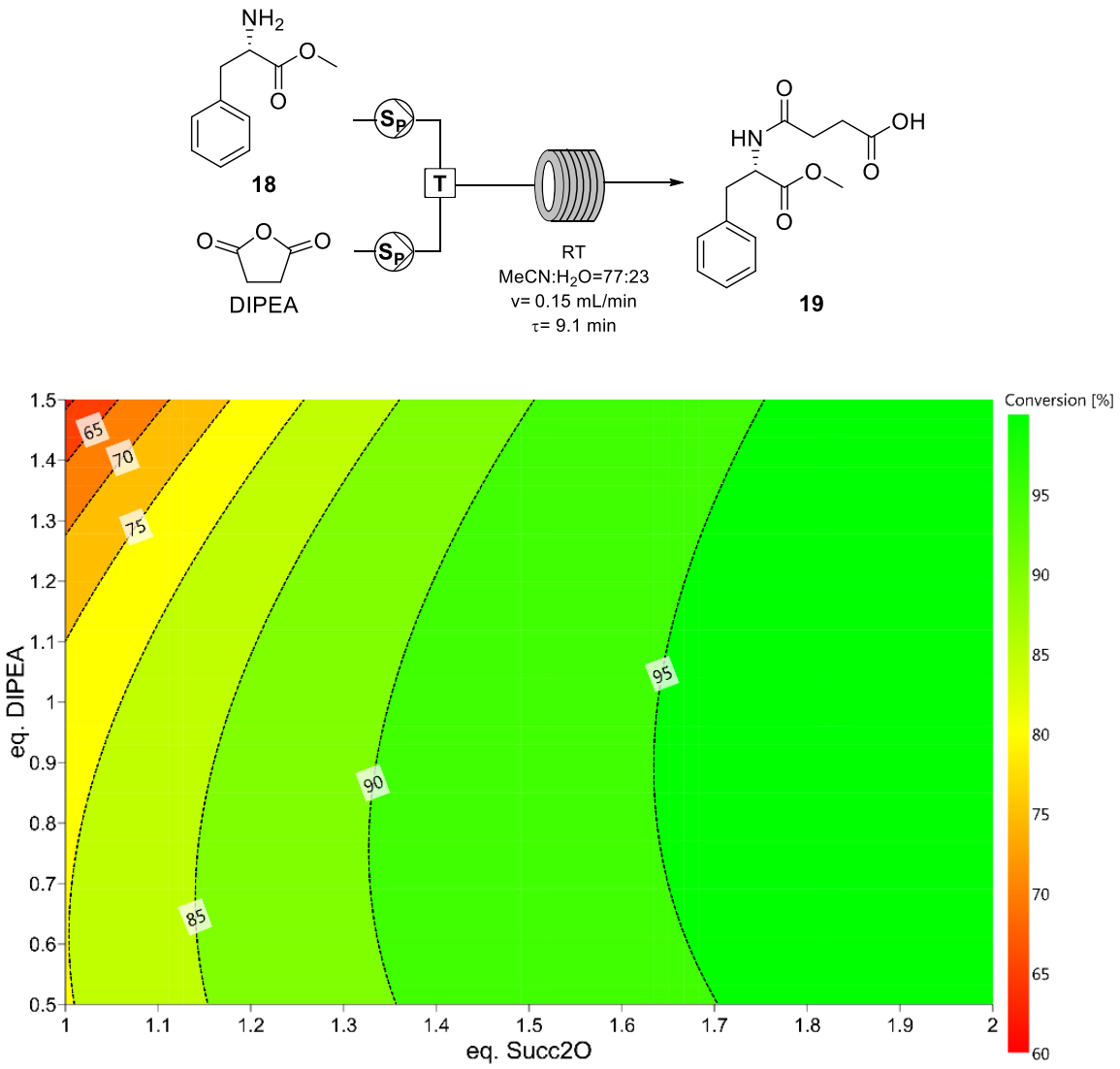

Figure D-2: Reaction scheme and contour plot obtained by DoE analysis of *N*-amidation of L-phenylalanine methyl ester **18** in continuous flow with MODDE Pro.

2.2 Multistep continuous setup for the synthesis of 16

Following the intensification of the Suzuki coupling of sacubitril precursor **13** as well as proving the feasibility of Boc-deprotection and *N*-amidation in a continuous fashion, we targeted the integrated synthesis of sacubitril precursor **16** in a fully continuous setup (Scheme D-5). As outlined above, Suzuki-Miyaura cross-coupling of **13** was performed at a temperature of 125 °C employing a packed bed reactor (L x I.D. 50 x 4.6 mm) containing the heterogeneous palladium catalyst $Ce_{0.20}Sn_{0.79}Pd_{0.01}O_{2-\delta}$. Subsequently, Boc-deprotection of obtained biphenyl intermediate **14** was achieved by merging the reaction stream with a solution of hydrochloric acid and introducing it into a coil reactor (L x O.D. x I.D. 3.0 m x 1/16 in. x 0.030 in.). According to the optimization of Boc-removal by DoE, the free amine **15** was generated using 10 mol eq.

HCl and a reaction temperature of 85 °C. To take the partial neutralization of hydrochloric acid by present potassium carbonate (1.5 mol eq.) into account, a stock solution containing 11.5 mol eq. HCl was utilized for this purpose. Since the large excess of hydrochloric acid in the reaction solution is detrimental for the following third step of the reaction cascade, the acid was removed deploying anion exchange resin Amberlyst A21 implemented in an HPLC column (L x I.D. 120 x 8 mm). The same approach has already been reported in literature for the removal of trifluoroacetic acid from organic solvents in batch [61]. Finally, as suggested by DoE analysis, *N*-amidation of **15** was accomplished in a coil reactor (L x O.D. x I.D. 3.0 m x 1/16 in. x 0.030 in.) after addition of 2 mol eq. succinic anhydride as well as 1 mol eq. DIPEA. Using this multistep setup (Scheme D-5) exhibiting a total residence of about 90 min (including tubing), the synthesis of the late-stage sacubitril precursor **16** was successfully performed for over 5 h yielding the targeted compound with up to 98% yield. After a steady increase in the beginning, the yield of sacubitril precursor **16** was observed to slowly decrease over the course of the experiment and stabilized at approximately 81% (corresponding to a space-time-yield of 4 g/L*h) after 370 min (see Supporting information for graphic representation). This can probably be contributed to an initial loss of palladium due to leaching from the employed heterogeneous catalyst, which has already been reported in literature [28,30]. Determination of the residual levels of palladium, cerium and tin in the reaction solution by ICP-MS strongly support this hypothesis (Table D-2). Whereas the reaction outlet collected at t= 160-180 min exhibits a palladium content of 563±13 µg/kg (Entry 1, Table D-2), the concentration of the metal was found to significantly decrease over the course of the continuous experiment. After a run time of 400 min, the amount of palladium was determined to be reduced to 105±3 µg/kg (Entry 4, Table D-2), which renders our developed multistep process highly promising to meet the strict regulatory guidelines for the production of pharmaceutical products [62]. Concerning the leaching behavior of tin from the employed heterogeneous catalyst, the residual levels in the outlet flow were measured to be ≤30 µg/kg (Entries 1-4, Table D-2) in all samples. Likewise, the concentration of cerium was very low in analyzed samples (≤9.7 µg/kg, Entries 1-4, Table D-2).

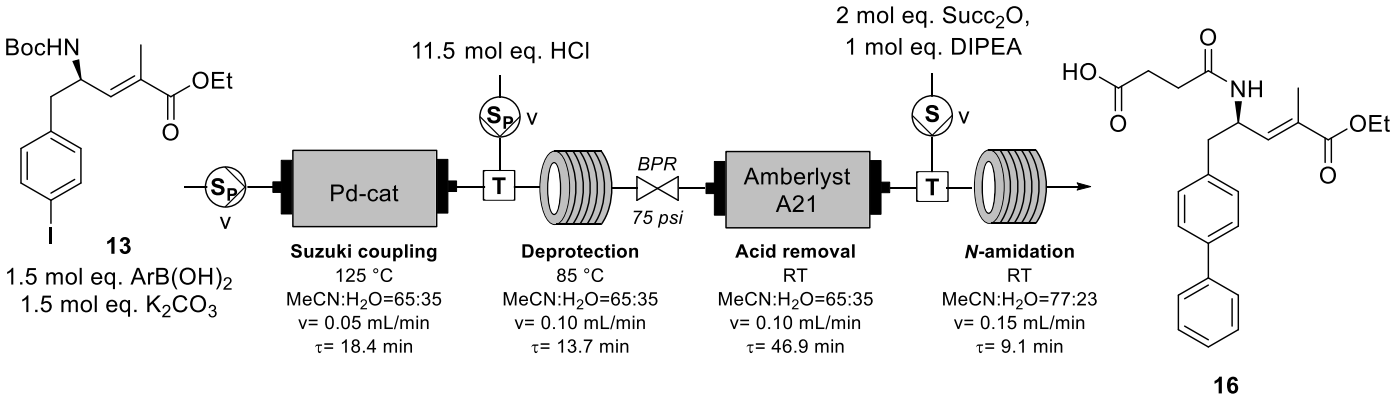

Scheme D-5: Multistep setup for the synthesis of sacubitril precursor **16** in continuous flow (S_P= high-pressure syringe pump, S= syringe pump, T= T-mixer, v= 0.05 mL/min).

Table D-2: Levels of Pd, Ce and Sn in the outlet flow of the three-step cascade for the synthesis of **16** in continuous flow (determined by ICP-MS).

Entry	Time [min]	Pd [µg/kg]	Sn [µg/kg]	Ce [µg/kg]
1	160-180	563±13	24±5	9.7±0.3
2	240-260	312±2	22±12	7.2±0.5
3	320-340	145±5	30±13	9.4±0.8
4	400-420	105±3	29±8	8.9±0.4

Apart from that, also the constant reduction of acid scavenging capacity of the deployed ion exchange resin might account for observed course of yield. As far as starting material **13** is concerned, HPLC measurements revealed full conversion throughout the whole experiment. However, it has to be noted that **13** can as well undergo Boc-deprotection and in further consequence *N*-amidation. Regarding the formation of by-products in the three-step continuous cascade, oxidation and homocoupling of phenylboronic acid are reported to occur upon depletion of the aryl halide coupling partner in the Suzuki coupling step [29]. In fact, the HPLC chromatogram of the outlet flow showed a small peak corresponding to biphenyl resulting from the coupling of two molecules of phenylboronic acid. Apart from that, the reaction steps seemed to be rather clean and only small peaks attributable to unidentified side-products could be detected by HPLC (λ= 237 nm) at first. However, after an experiment run time of 260 min HPLC analysis showed the appearance of a peak at 0.7 min, which seemed to increase with decreasing yield. The molecular structure of the corresponding compound could not have been elucidated so far.

Concerning the absence of other significant by-product peaks in HPLC chromatogram, the use of weakly basic anion exchange resin Amberlyst A21 for the adsorption of excess hydrochloric acid can also be regarded as an in-line purification step. It removes various kinds of acidic materials from the process stream including potentially formed hydroiodic acid [63] resulting from the use of an aryl iodide coupling partner in the Suzuki reaction as well as phenol originating from the oxidation of phenylboronic acid [64]. In addition, we observed that in our multistep continuous cascade Amberlyst A21 acts as a scavenger of unreacted phenylboronic acid too. Moreover, the respective anion exchange resin was reported to adsorb Pd(II) from aqueous solutions [65,66] and might therefore contribute to the observed low levels of palladium in the outlet flow of the continuous setup.

Besides the reaction yield, another important quality attribute of pharmaceutical processes is the enantiopurity of the obtained target molecule. Enantiomeric excess of compound **16** synthesized in continuous flow utilizing the described integrated setup was determined to be moderate 43% (see Supporting information for determination of enantiomeric excess by chiral HPLC). As biphenyl intermediate **14** obtained in continuous Suzuki cross-coupling was shown to be almost enantiopure, the partial racemization of the chiral center most likely occurred during the removal of the protecting group. Boc-deprotection was performed in an aqueous and strongly acidic environment at elevated temperature, conditions which presumably caused racemization of the sacubitril precursor to some extent [67,68]. Therefore, in order to provide a process suitable for pharmaceutical industry, future work will focus on improving the enantiomeric excess of sacubitril precursor **16** obtained in developed continuous cascade by applying milder conditions for the Boc-deprotection step.

3 Conclusion

In summary, we have successfully applied continuous flow techniques for the synthesis of a late-stage sacubitril precursor in three steps. The optimization of interacting reaction parameters was demonstrated to be efficiently performed using statistical “Design of Experiments”. Furthermore, the use of a continuous setup comprising a packed bed reactor as well as coil reactor modules allowed intensification of the multistep process compared to batch. After an initial equilibration phase, the target molecule was obtained with a steady 81% overall yield and moderate enantiomeric excess using an integrated continuous setup. Moreover, levels of

residual palladium in the outlet flow were determined to be in the ppb range, thus proving our developed process to be attractive for pharmaceutical applications. However, in view of a conceivable implementation of developed reaction cascade into an industrial process for API production, its optimization in terms of enantiomeric excess of the final product is indispensable. Nevertheless, we could prove once more that with relatively simple equipment it is possible to synthesize advanced chemical intermediates in continuous flow. With our work, we hope to contribute to the establishment of continuous flow methodologies for process development and operation in pharmaceutical industry.

4 Experimental section

4.1 General information

Chemicals and solvents were purchased from commercial suppliers and used as received unless stated otherwise [**Sigma Aldrich**: potassium carbonate (99%), anisole (99%); $LiAlH_4$ (1 M in diethyl ether), trifluoroacetic acid (99%), Boc-L-phenylalanine methyl ester (98%), L-phenylalanine methyl ester hydrochloride (98%), Amberlyst A21 (4.6 eq./kg dry weight); **BLDpharm:** Boc-4-iodo-D-phenylalanine (98%); **Fluorochem:** *O*,*N*-dimethylhydroxylamine hydrochloride (98%), 1-ethyl-3-(3-dimethylaminopropyl)carbodiimide hydrochloride (99%), ethyl(hydroxyimino)cyanoacetate (98%), (carbethoxyethylidene)triphenylphosphorane (94%), succinic anhydride (99%); **Carl Roth:** triethylamine (99.5%), hydrochloric acid (37%); **Oxchem:** phenylboronic acid (95%); **ACROS organics:** diisopropylethylamine (98%); **ChemLab:** acetonitrile (HPLC grade)]. According to a reported literature procedure [69], L-phenylalanine methyl ester hydrochloride was neutralized by addition of sodium carbonate in water and extraction of the aqueous phase with ethyl acetate yielded free L-phenylalanine methyl ester. Analytical thin layer chromatography was performed on pre-coated aluminium plates (Merck, silica gel 60, F_{254}) and spots were visualized with UV light (254 nm) or potassium permanganate stain. Column chromatography purifications were carried out using MN silica gel 60 (70-230 mesh). An Agilent 1100 series HPLC system was utilized for monitoring of the reaction progress as well as determination of enantiomeric excess (see Supporting information for HPLC parameters). HPLC-MS measurements were performed on a Waters Acquity H-Class system equipped with a Waters Acquity SQD detector. For determination of Pd, Ce and Sn in the outlet flow of the multistep reaction cascade in continuous flow, an Agilent 7700x ICP-MS system was employed

after microwave assisted acidic digestion of the samples. NMR-data were recorded on a Bruker Avance III 300 MHz spectrometer (^{1}H: 300 MHz, ^{13}C: 75 MHz, see Supporting information for NMR-data). For the DoE analysis of Boc-deprotection and *N*-amidation in continuous flow, the software MODDE Pro (Version 12.1.0.5491, Copyright © Sartorius Stedim Data Analytics AB) was utilized.

4.2 Optimization of Suzuki cross-coupling in continuous flow

For the Suzuki coupling of intermediate **13** with phenylboronic acid in continuous flow, a packed bed reactor setup was utilized. Therefore, an HPLC column (L x I.D. 50 x 4.6 mm) was filled with dry Pd catalyst $Ce_{0.20}Sn_{0.79}Pd_{0.01}O_{2-\delta}$ (602 mg, containing 0.04 mmol Pd) and connected to a back pressure regulator (IDEX BPR Cartridge 75 psi Gold Coat). After equilibration of the reactor setup with the reaction solvent (MeCN:H_2O=65:35), the packed bed reactor was heated to elevated temperature (75-125 °C) in an oil bath. Then, a solution containing intermediate **13** (25 mM), phenylboronic acid (37.5 mM, 1.5 mol eq.), potassium carbonate (37.5 mM, 1.5 mol eq.) and anisole (62.5 mM) as internal standard was prepared in MeCN:H_2O=65:35, degassed in an ultrasonic bath and filtered through a 0.2 µm membrane filter. Obtained stock solution was pumped through the reactor with a flow rate of 0.05 mL/min (τ= 18.4 min) utilizing a high-pressure syringe pump (VIT-FIT HP, Lambda Instruments). For monitoring of the reaction progress, every 10 minutes an aliquot (40 µL) was quenched with MeOH:H_3PO_4=75:25 (400 µL) and analyzed by HPLC (Method B).

4.3 Optimization of Boc-deprotection in continuous flow

The influence of temperature and equivalents of acid on Boc-deprotection was studied using Boc-L-phenylalanine methyl ester **17** as surrogate substrate utilizing a coil reactor setup. Solution A [Boc-L-phenylalanine methyl ester (25 mM), anisole (62.5 mM) as internal standard] and solution B [HCl (125-375 mM, 5-15 mol eq.)] were prepared in the reaction solvent MeCN:H_2O=65:35 and degassed by ultrasonic irradiation. The setup comprising a PEEK coil (L x O.D. x I.D. 3.0 m x 1/16 in. x 0.030 in., V= 1.37 mL) connected to a back pressure regulator (IDEX BPR Cartridge 75 psi Gold Coat) was equilibrated with solvent and heated to elevated temperature in a water bath (70-85 °C). The two reagent solutions were merged using a T-mixing element and pumped through the reactor by means of high-pressure syringe pumps

(VIT-FIT HP, Lambda Instruments) at a flow rate of 0.05 mL/min each, giving a total flow rate of 0.10 mL/min (τ= 13.7 min). After certain time points (3τ / 3.5 τ / 4 τ), aliquots (80 µL) of the outlet flow were quenched with MeOH:H_3PO_4=55:45 (400 µL) and analyzed by HPLC (Method A).

4.4 Optimization of *N*-amidation in continuous flow

The influence of different equivalents of succinic anhydride as well as DIPEA on *N*-amidation of L-phenylalanine methyl ester **18** was examined in a coil reactor setup. Solution A [L-phenylalanine methyl ester (12.5 mM), anisole (31.3 mM) as internal standard] was prepared in MeCN:H_2O=65:35, whereas solution B [succinic anhydride (25-50 mM, 1-2 mol eq.), DIPEA (12.5-37.5 mM, 0.5-1.5 mol eq.)] was prepared in anhydrous MeCN to avoid hydrolysis of the anhydride reagent. The stock solutions were degassed in an ultrasonic bath and the reactor setup composed of a PEEK coil (L x O.D. x I.D. 3.0 m x 1/16 in. x 0.030 in., V= 1.37 mL) was equilibrated with the reaction solvent at ambient pressure and temperature. Stock A (flow rate 0.10 mL/min) and stock B (flow rate of 0.05 mL/min) were merged using a T-mixing element and the reaction solution was pumped through the reactor coil at a total flow rate of 0.15 mL/min (τ= 9.1 min) using high-pressure syringe pumps (VIT-FIT HP, Lambda Instruments). After certain time points (3τ / 3.5 τ / 4 τ), aliquots (120 µL) of the outlet flow were quenched with MeOH:H_3PO_4=55:45 (400 µL) and analyzed by HPLC (Method A).

4.5 Integrated synthesis of 16 in continuous flow

For the multistep synthesis of sacubitril precursor **16** in continuous flow, a modular setup comprising a packed bed reactor and reactor coils was utilized. Stock A [(intermediate **13** (25 mM), phenylboronic acid (37.5 mM, 1.5 mol eq.), potassium carbonate (37.5 mM, 1.5 mol eq.) and anisole (62.5 mM) as internal standard] was prepared in MeCN:H_2O=65:35, dissolved by ultrasonic irradiation and filtered through a 0.2 µm membrane filter. Stock B [HCl (287.5 mM, 11.5 mol eq.)] and stock C [succinic anhydride (50 mM, 2 mol eq.), DIPEA (25 mM, 1 mol eq.)] were prepared in MeCN:H_2O=65:35 and MeCN, respectively, and degassed in an ultrasonic bath. After equilibration of the reactor system, stock A was pumped through the packed bed reactor (L x I.D. 50 x 4.6 mm) filled with Pd catalyst $Ce_{0.20}Sn_{0.79}Pd_{0.01}O_{2-\delta}$ (594 mg, containing 0.04 mmol Pd) at a flow rate of 0.05 mL/min (τ= 18.4 min) and a temperature of

125 °C using a high-pressure syringe pump (VIT-FIT HP, Lambda Instruments) for Suzuki-Miyaura cross-coupling. Then, the outlet flow was mixed with stock B, delivered by a second high-pressure syringe pump (VIT-FIT HP, Lambda Instruments), at a flow rate of 0.05 mL/min using a T-mixing element. The resulting reaction solution was introduced into the first coil reactor (PEEK coil, L x O.D. x I.D. 3.0 m x 1/16 in. x 0.030 in., V= 1.37 mL) at a total flow rate of 0.10 mL/min and a temperature of 85 °C (τ= 13.7 min) for Boc-deprotection. After the first reaction coil, a backpressure regulator (IDEX BPR Cartridge 75 psi Gold Coat) was installed to be able to heat above the boiling point (~77 °C, [44]) of the reaction solution. For removal of excess HCl, the reagent stream was then pumped through a preparative HPLC column (L x I.D. 120 x 8 mm, τ= 46.9 min) filled with the anion exchange resin Amberlyst A21 (2 g dry weight) at ambient temperature and pressure. Subsequently, the process stream was mixed with stock C, which was pumped into the setup by means of a dual-syringe infusion pump (LA-120, Landgraf) at a flow rate of 0.05 mL/min. *N*-amidation was then performed in a second coil reactor (PEEK coil, L x O.D. x I.D. 3.0 m x 1/16 in. x 0.030 in., V= 1.37 mL) at a total flow rate of 0.15 mL/min (τ= 9.1 min) to obtain targeted sacubitril precursor **16** (calculated total residence time= 90.2 min). For monitoring of the reaction progress, every 10 min an aliquot of the outlet flow (120 µL) was quenched with MeOH:H_3PO_4=75:25 (400 µL) and analyzed by HPLC (Method B). To determine the residual levels of Pd, Ce and Sn in the outlet flow of the continuous setup for synthesis of **16** aliquots of the reaction solution were acidified with equal volumes of 20% HNO_3/HCl (1+1, v/v) and analyzed by ICP-MS after microwave assisted acidic digestion.

5 References

1. Dahlöf B (2000) JRAAS 1:14-16
2. Vilela-Martin JF (2016) Drug Des, Dev Ther 10:1627-1639
3. Andersen MB, Simonsen U, Wehland M, Pietsch J, Grimm D (2016) Basic Clin Pharmacol Toxicol 118:14-22
4. Ksander GM, Ghai RD, deJesus R, Diefenbacher CG, Yuan A, Berry C, Sakane Y, Trapani A (1995) J Med Chem 38:1689-1700
5. Hook D, Riss B, Kaufmann D, Napp M, Bappert E, Polleux P, Medlock J, Zangotti-Gerosa A (2009) New processes for γ-amino-δ-biphenyl-α-methylalkanoic acid or acid ester. PCT Int. Appl. WO 2009/090251, Jul 23, 2009; (2009) Chem Abstr 151:198239

6. Lau SH, Bourne SL, Martin B, Schenkel B, Penn G, Ley SV (2015) Org Lett 17:5436-5439
7. Xu X-N (2015) A preparation method of sacubitril. CN Patent CN 104557600 A, Apr 29, 2015; (2015) Chem Abstr 162:603569
8. Wang Y, Chen F-E, Shi Y, Tian W-S (2016) Tetrahedron Lett 57:5928-5930
9. Ksander G (1993) Biaryl substituted 4-amino-butyric acid amides. US Patent 5,217,996, Jun 8, 1993
10. Hook D, Ruch T, Riss B, Wietfeld B, Sedelmaier G, Napp M, Bänzinger M, Hawker S, Ciszewski L, Waykole L (2008) New process for preparation of 5-(4-biphenylylmethyl) pyrrolidin-2-one derivatives. PCT Int. Appl. WO 2008/083967 A2, Jul 17, 2008; (2008) Chem Abstr 149:176170
11. Martin B, Mandrelli F, Venturoni S-L (2018) Process and Intermediates for the preparation of NEP inhibitors. U.S. Pat. Appl. US 2018/0022690 A1, Jan 25, 2018; (2005) Chem Abstr 165:298456
12. Plutschack MB, Pieber B, Gilmore K, Seeberger PH (2017) Chem Rev 117:11796-11893
13. Newman SG, Jensen KF (2013) Green Chem 15:1456-1472
14. Hessel V (2009) Chem Eng Technol 32:1655-1681
15. Ley SV (2012) Chem Rec 12:378-390
16. Wiles C, Watts P (2014) Green Chem 16:55-62
17. Anastas P, Eghbali N (2010) Chem Soc Rev 39:301-312
18. Roberge DM, Zimmermann B, Rainone F, Gottsponer M, Eyholzer M, Kockmann N (2008) Org Process Res Dev 12:905-910
19. Benaskar F, Ben-Abdelmoumen A, Patil NG, Rebrov EV, Meuldijk J, Hulshof LA, Hessel V, Krtschil U, Schouten JC (2011) J Flow Chem 1:74-89
20. Schaber SD, Gerogiorgis DI, Ramachandran R, Evans JMB, Barton PI, Trout BL (2011) Ind Eng Chem Res 50:10083-10092
21. Gutmann B, Cantillo D, Kappe CO (2015) Angew Chem Int Ed Engl 54:6688-6728
22. Porta R, Benaglia M, Puglisi A (2016) Org Process Res Dev 20:2-25
23. Baumann M, Baxendale IR (2015) J Org Chem 11:1194-1219
24. Heider PL, Born SC, Basak S, Benyahia B, Lakerveld R, Zhang H, Hogan R, Buchbinder L, Wolfe A, Mascia S, Evans JMB, Jamison TF, Jensen KF (2014) Org Process Res Dev 18:402-409
25. FDA Perspective on Continuous Manufacturing (2012) US Food and Drug Administration. https://www.fda.gov/downloads/AboutFDA/CentersOffices/OfficeofMedicalProductsandTobacco/CDER/UCM341197.pdf. Accessed 21 Jan 2019

26. Statement from FDA (2018) US Food and Drug Administration. https://www.fda.gov/NewsEvents/Newsroom/PressAnnouncements/ucm619024.htm. Accessed 30 Oct 2018
27. ONE-FLOW Research Project Home Page. https://one-flow.org. Accessed 20 Feb 2019
28. Hiebler K, Soritz S, Gavric K, Birrer S, Maier MC, Grabner B, Gruber-Woelfler H (2019) J Flow Chem 10:283–294
29. Lichtenegger GJ, Maier M, Hackl M, Khinast JG, Gössler W, Griesser T, Kumar VSP, Gruber-Woelfler H, Deshpande PA (2017) J Mol Catal A: Chem 426:39-51
30. Lichtenegger GJ, Maier M, Khinast JG, Gruber-Wölfler H (2016) J Flow Chem 6:244-251
31. Lichtenegger GJ, Tursic V, Kitzler H, Obermaier K, Khinast JG, Gruber-Wölfler H (2016) Chem Ing Tech 88:1518-1523
32. Bäckvall J-E (2010) Sci Backgr Nobel Prize Chem 50005:1-12
33. Buchwald SL (2008) Acc Chem Res 41:1439-1439
34. Magano J, Dunetz JR (2011) Chem Rev 111:2177-2250
35. Selander N, Szabo KJ (2011) Chem Rev 111:2048-2076
36. Beletskaya IP, Cheprakov AV (2009) Chem Rev 100:3009-3066
37. Wu XF, Anbarasan P, Neumann H, Beller M (2010) Angew Chem Int Ed Engl 49:9047-9050
38. Suzuki A (2002) J Organomet Chem 653:83-90
39. Miyaura N, Suzuki A (1995) Chem Rev 95:2457-2483
40. Kotha S, Lahiri K, Kashinath D (2002) Tetrahedron 58:9633-9695
41. Smith MD, Stepan AF, Ramarao C, Brennan PE, Ley SV (2003) Chem Commun 3:2652-2653
42. Alfonsi K, Colberg J, Dunn PJ, Fevig T, Jennings S, Johnson TA, Kleine HP, Knight C, Nagy MA, Perry DA, Stefaniak M (2008) Green Chem 10:31-36
43. Smith MD, Mostofian B, Petridis L, Cheng X, Smith JC (2016) J Phys Chem B 120:740-747
44. Othmer DF, Josefowitz S (1947) Ind Eng Chem 39:1175-1177
45. Gooding OW (2004) Curr Opin Chem Biol 8:297-304
46. Eriksson L, Johansson E, Kettaneh-Wold N, Wikström C, Wold S (2008) Design of Experiments: Principles and Applications. 3rd edn. Umetrics AB, Umea
47. Mead R (1988) The design of experiments - Statistical principles for practical applications. Cambridge University Press, Cambridge
48. Multivariate analysis in the pharmaceutical industry (2018). 1st edn. Academic Press, Cambridge Mass

49. Rubin AE, Tummala S, Both DA, Wang C, Delaney EJ (2006) Chem Rev 106:2794-2810

50. Politis SN, Colombo P, Colombo G, Rekkas DM (2017) Drug Dev Ind Pharm 43:889-901

51. López SE, Salazar J (2013) J Fluorine Chem 156:73-100

52. Qian Z, Baxendale IR, Ley SV (2010) Chemistry 16:12342-12348

53. Liu Y-S, Zhao C, Bergbreiter DE, Romo D (1998) J Org Chem 63:3471-3473

54. Zhang CX, Zheng GJ, Bi FQ, Li YL (2008) Chin Chem Lett 19:759-761

55. Coffey DS, Hawk MKN, Pedersen SW, Ghera SJ, Marler PG, Dodson PN, Lytle ML (2004) Org Process Res Dev 8:945-947

56. Gilmore K, Kopetzki D, Lee JW, Horvath Z, McQuade DT, Seidel-Morgenstern A, Seeberger PH (2014) Chem Commun (Camb) 50:12652-12655

57. Dulla B, Vijayavardhini S, Rambau D, Anuradha V, Rao MVB, Pal M (2014) Curr Green Chem 1:73-79

58. Sumida Y, Iwai S, Nishiya Y, Kumagai S, Yamada T, Azuma M (2016) Adv Synth Catal 358:2041-2046

59. Cailla HL, Racine-Weisbuch MS, Delaage MA (1973) Anal Biochem 56:394-407

60. Bunton CA (1963) J Chem Soc:2918-2926

61. Srinivasan N, Yurek-George A, Ganesan A (2005) Mol Divers 9:291-293

62. ICH guideline Q3D (R1) on elemental impurities (2019) European Medicines Agency. https://www.ema.europa.eu/en/documents/scientific-guideline/international-conference-harmonisation-technical-requirements-registration-pharmaceuticals-human-use_en-32.pdf. Accessed 27 Sep 2019

63. Ion Exchange Resins - Removing acid from a solution (2019) DuPont Water Solutions Customer Help. https://water.custhelp.com/app/answers/detail/a_id/144/related/1. Accessed 8 May 2019

64. Amberlyst™ A21 Product Data Sheet (2016) The Dow Chemical Company. http://www.faran-water.ir/userfiles/files/resin/chemical/0901b803808d3096.pdf. Accessed 8 May 2019

65. Nagireddi S, Golder AK, Uppaluri R (2018) J Water Process Eng 22:227-238

66. Hubicki Z, Wołowicz A (2009) Hydrometallurgy 96:159-165

67. Kaiser K, Benner R (2005) Limnol Oceanograph: Methods 3:318-325

68. Yamada S, Hongo C, Yoshioka R, Chibata I (1983) J Org Chem 48:843-846

69. Zhang X, Cividino P, Poisson JF, Shpak-Kraievskyi P, Laurent MY, Martel A, Dujardin G, Py S (2014) Org Lett 16:1936-1939

6 Supporting information

6.1 $^{1}H/^{13}C$-NMR spectra of 13, 14 and 16

NMR-measurements were performed using a Bruker Avance III 300 MHz spectrometer (^{1}H: 300 MHz, ^{13}C: 75 MHz). The chemical shift (δ [ppm]) was reported relatively to the used solvent $CDCl_3$ (7.26, s). For designation of multiplicities of observed coupling patterns, following abbreviations were used: s (singlet), d (doublet), dd (duplicated doublet), t (triplet), q (quartet), m (multiplet), bs (broad signal).

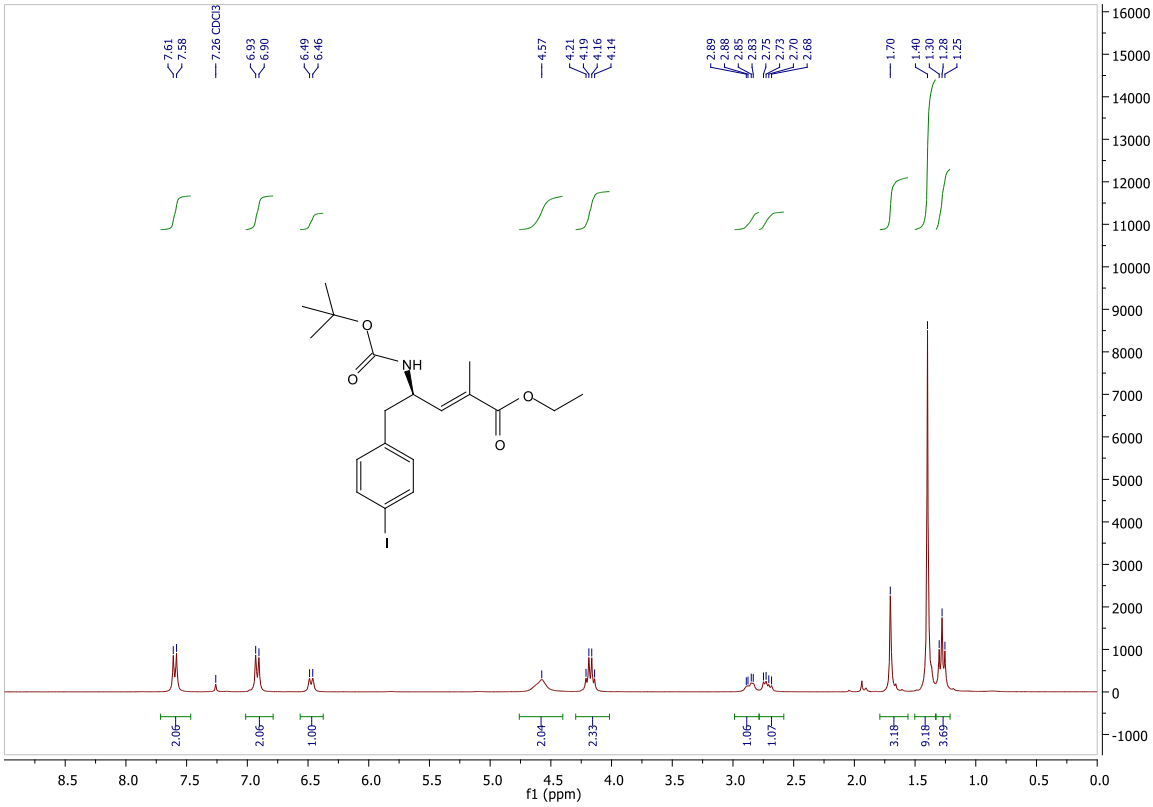

Figure D-S1: ^{1}H-NMR of **13** in $CDCl_3$.

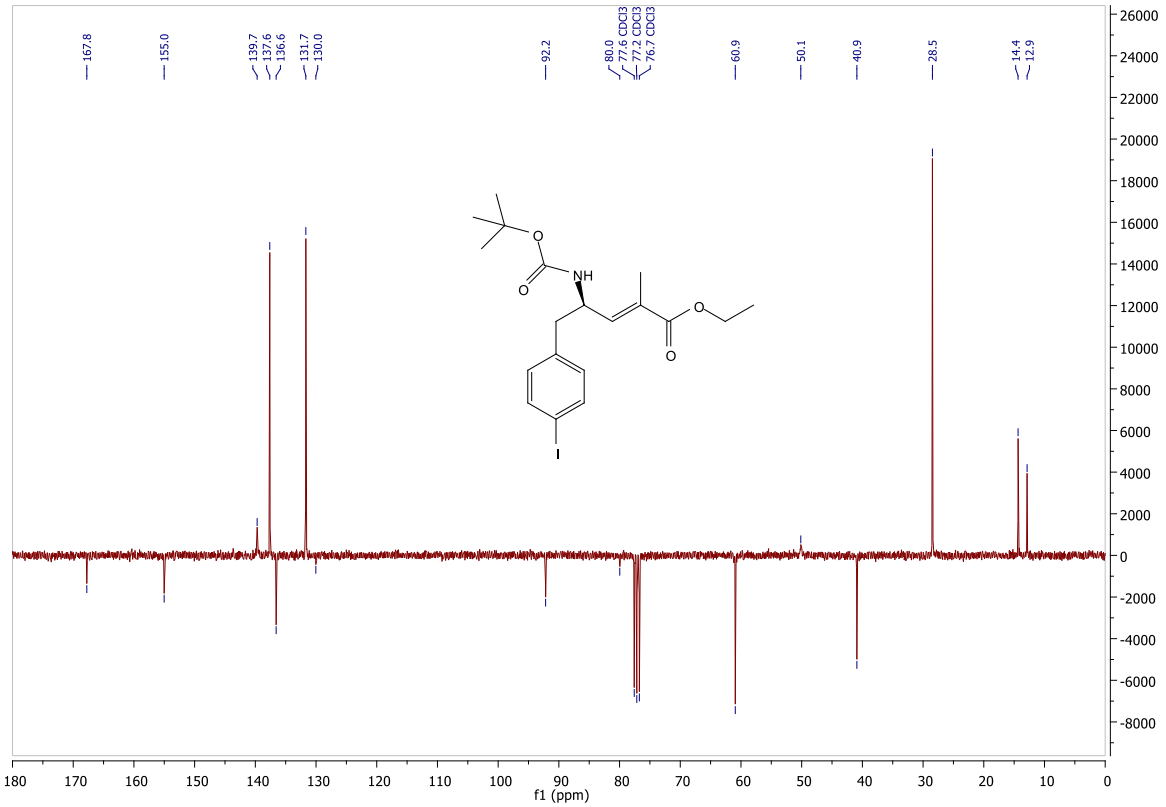

Figure D-S2: ^{13}C-NMR (APT) of **13** in $CDCl_3$.

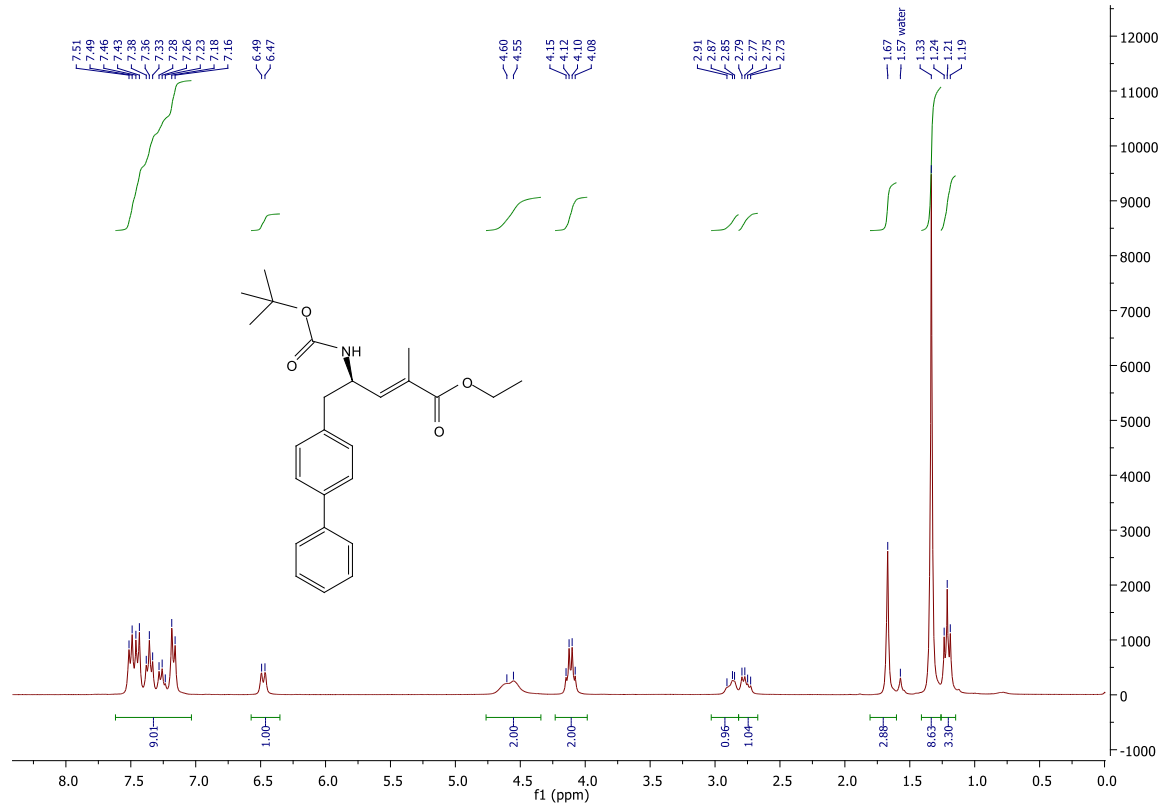

Figure D-S3: ^{1}H-NMR of **14** in $CDCl_3$.

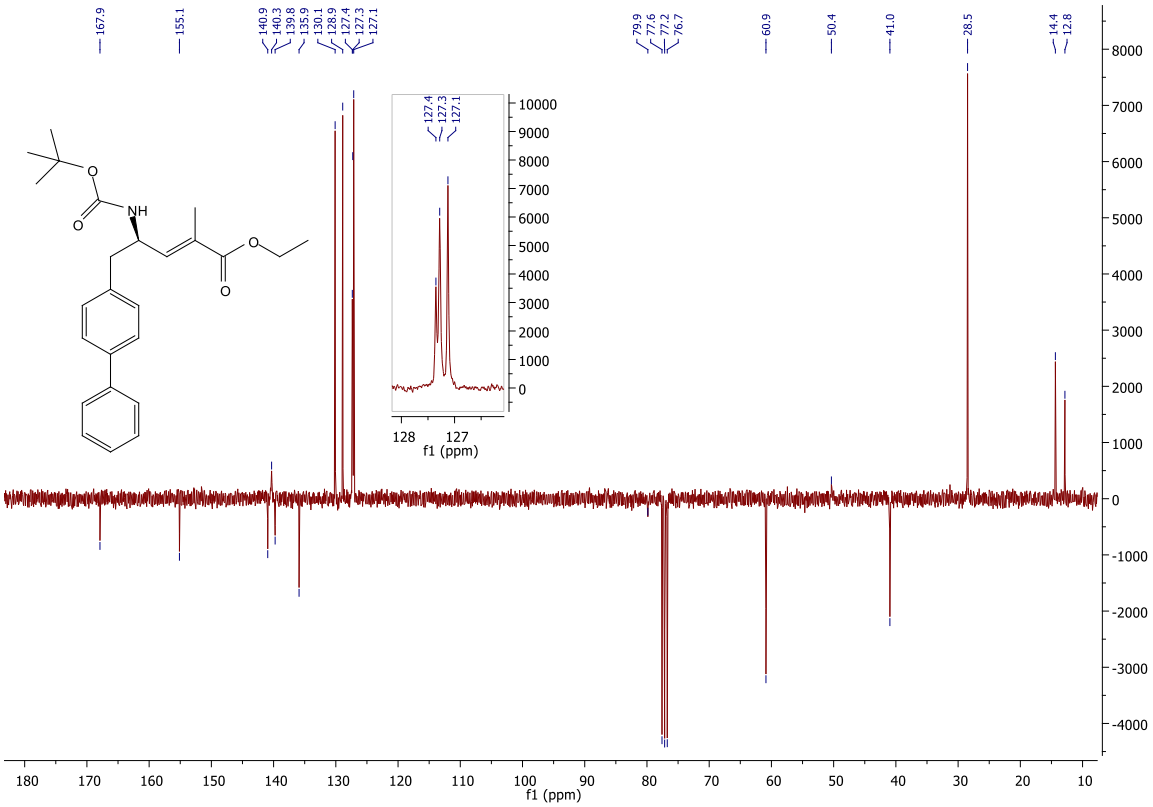

Figure D-S4: ^{13}C-NMR (APT) of **14** in $CDCl_3$.

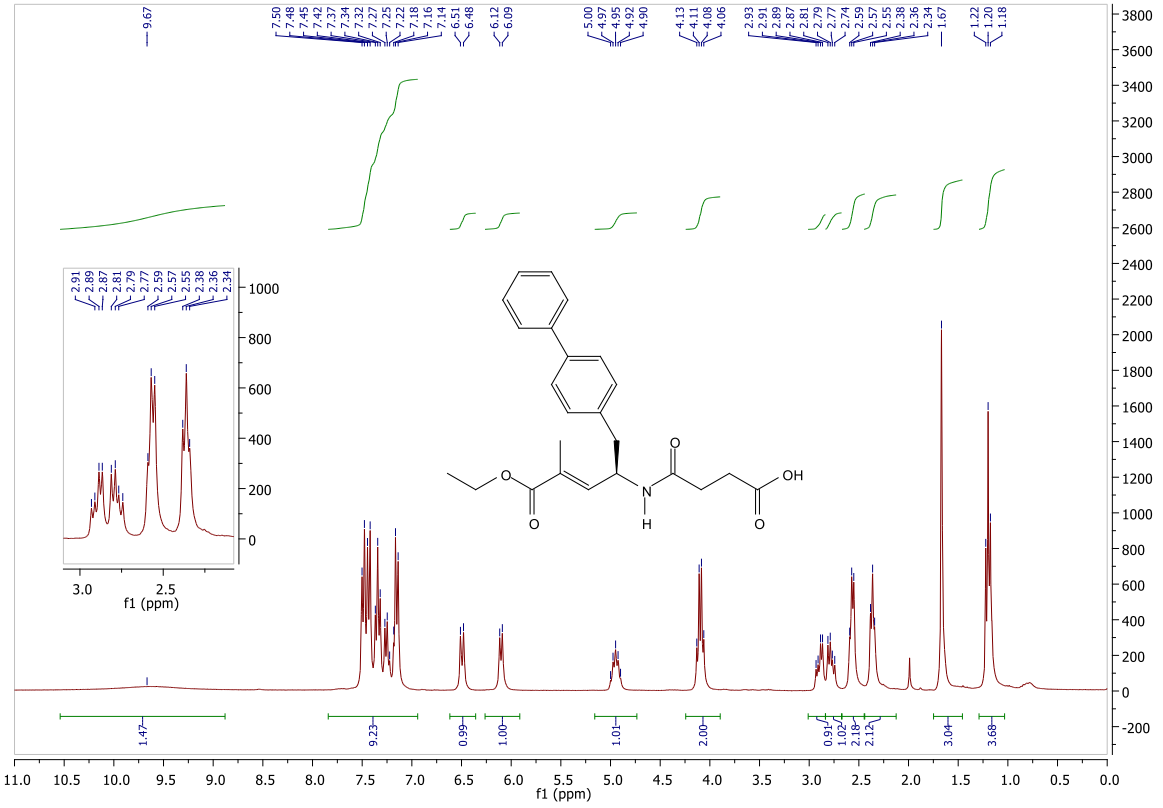

Figure D-S5: ^{1}H-NMR of **16** in $CDCl_3$.

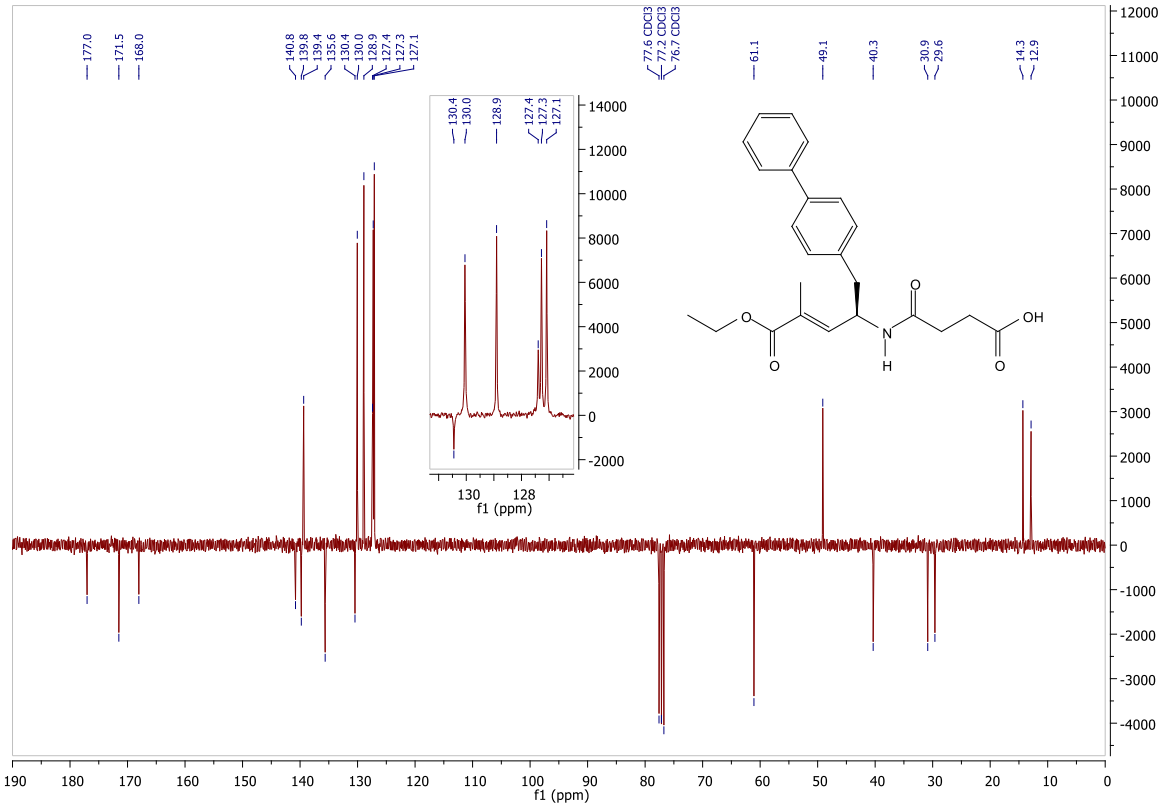

Figure D-S6: ^{13}C-NMR (APT) of **16** in $CDCl_3$.

6.2 High performance liquid chromatography (HPLC)

6.2.1 Reaction monitoring

The reaction progress of the flow reactions was monitored by High Performance Liquid Chromatography. Aliquots drawn from the flow reaction outlet were quenched with the respective sample diluent and analyzed using an Agilent 1100 series HPLC system equipped with an online degasser, quaternary pump, autosampler, thermostated column compartment and UV-visible diode array detector. As mobile phases, MeOH (solvent A) and aq. phosphoric acid (H_2O:H_3PO_4=300:1 v/v; solvent B) were used. Compounds were separated using a ThermoFischer Scientific Accucore™ C18 reversed phase column (50 x 4.6 mm; 2.6 µm) at 25 °C with a flow rate of 1 mL/min and detected by UV-absorption over the run time of 5 min. Used isocratic elution methods are summarized in Table D-S1.

Table D-S1: HPLC methods (% A = % MeOH, % B = % H_2O:H_3PO_4=300:1 v/v) for monitoring of the reaction progress.

Method	% A (v/v)	% B (v/v)	Sample diluent	Flow [mL/min]
A	55	45	MeOH:H_2O=55:45	1
B	75	25	MeOH:H_2O=75:25	1

The retention times (t_R) of the analyzed compounds are apparent from Table D-S2.

Table D-S2: Retention times of compounds separated by HPLC.

Compound	Method	λ [nm]	t_R [min]
Anisole	A	270	1.6
	B	270	0.8
13	B	237	2.2
14	B	237	3.2
16	B	237	1.1
17	A	210	3.6
18	A	210	0.5
19	A	210	0.8

6.2.2 Determination of enantiomeric purity

Enantiomeric excess of compounds **13**, **14** and **16** was determined using an Agilent 1100 Series HPLC system equipped with a temperature-controlled oven and a UV detector. As mobile phase, n-hexane:ethanol (+ trifluoroacetic acid as mobile phase modifier if necessary) was used and samples were prepared in ethanol. A Daicel Chiralpak® OJ-H column (250 x 4.6 mm, 5 µm) was employed for separation of the chiral compounds over the run time of 20 min. Utilized isocratic elution methods are summarized in Table D-S3. The chromatographic elution order of the stereoisomers was determined by comparison with synthesized (*S*)- and (*R*)-reference compounds.

Table D-S3: HPLC methods (% A= % n-heptane, % B= % ethanol, % C= % trifluoroacetic acid) for determination of the enantiomeric excess.

Method	% A (v/v)	% B (v/v)	% C (v/v)	T [°C]	Flow [mL/min]	Time [min]
A	80	20	0	40	1.5	20
B	80	20	0.01	40	1.5	20

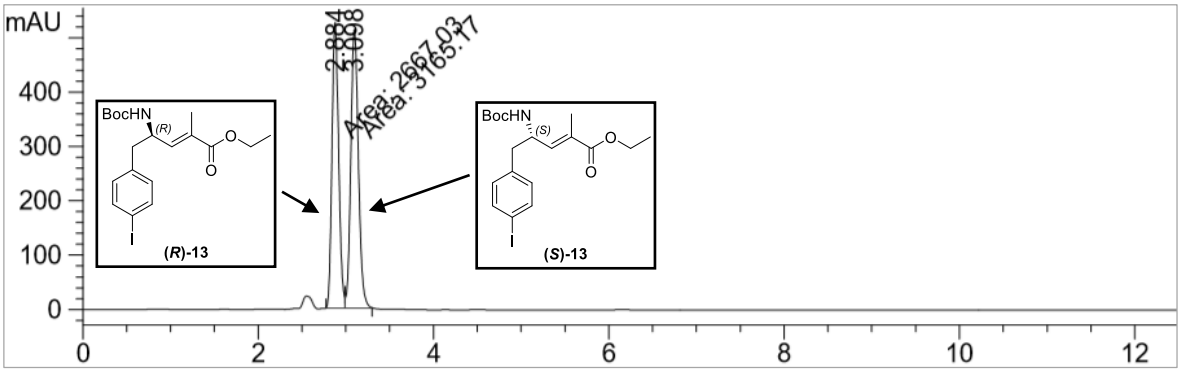

Figure D-S7: Chiral separation of **(*R*)-** and **(*S*)-13** by HPLC (λ= 237 nm).

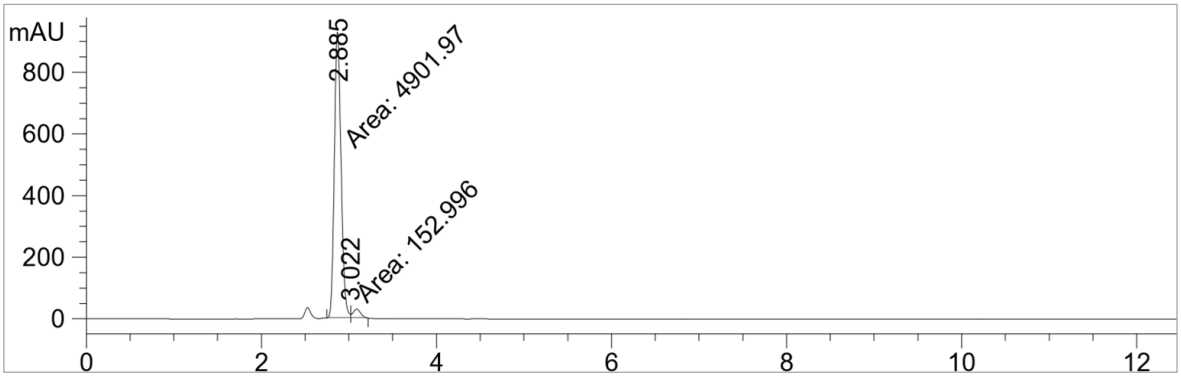

Figure D-S8: Determination of enantiomeric excess of compound **13** synthesized in batch (λ= 237 nm).

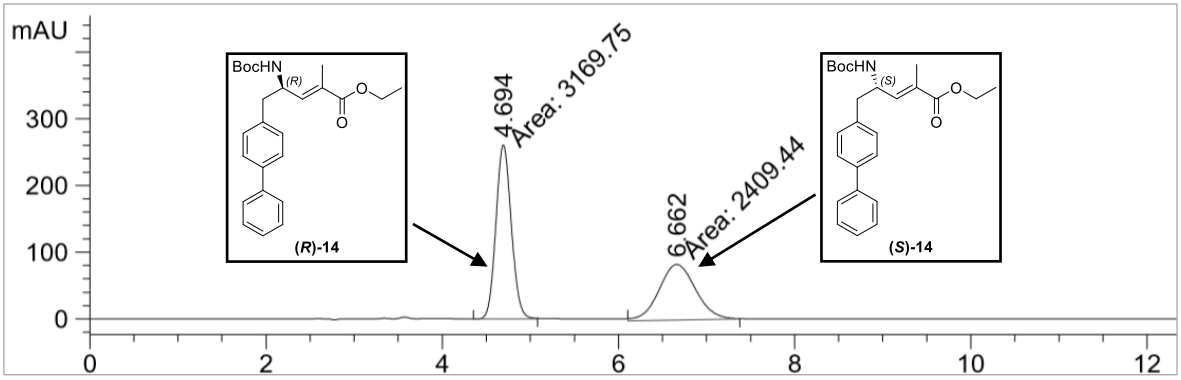

Figure D-S9: Chiral separation of **(*R*)-** and **(*S*)-14** by HPLC (λ= 270 nm).

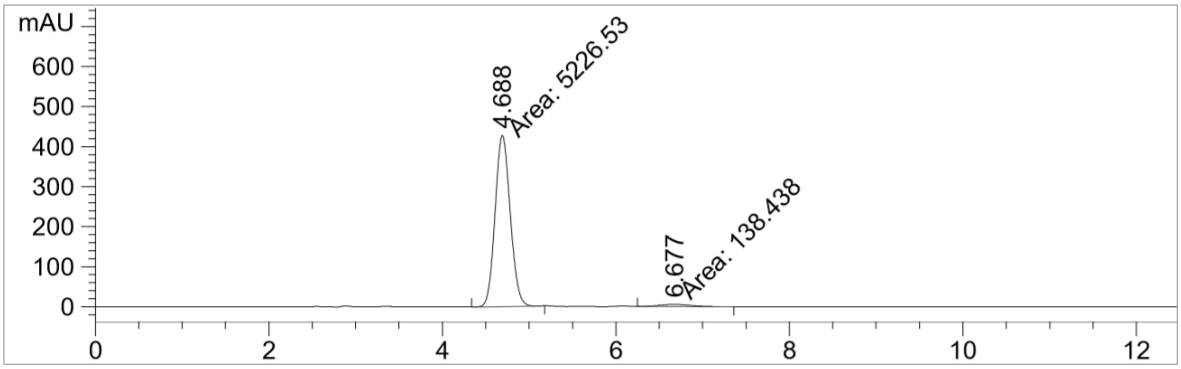

Figure D-S10: Determination of enantiomeric excess of compound **14** synthesized in flow (λ= 270 nm).

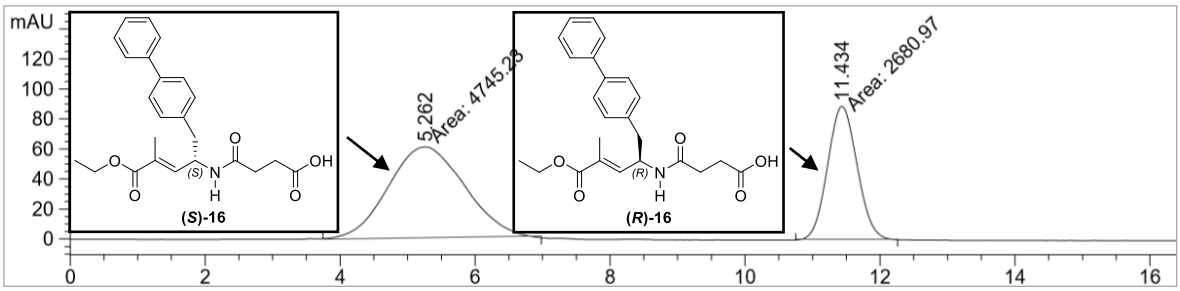

Figure D-S11: Chiral separation of **(*R*)-** and **(*S*)-16** by HPLC (λ= 270 nm).

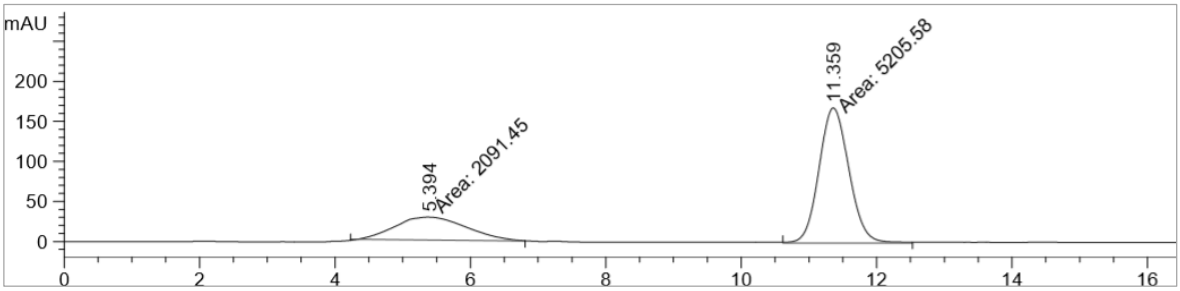

Figure D-S12: Determination of enantiomeric excess of compound **16** synthesized in flow (λ= 270 nm).

Table D-S4: Retention times of compounds separated by chiral HPLC.

Compound	Method	λ [nm]	t_R [min]
(*R*)-13	A	237	2.9
(*S*)-13	A	237	3.1
(*R*)-14	A	270	4.7
(*S*)-14	A	270	6.7
(*R*)-16	B	270	11.4
(*S*)-16	B	270	5.3

6.3 Chemical syntheses of 13, 14, 16 and $Ce_{0.20}Sn_{0.79}Pd_{0.01}O_{2-\delta}$

*6.3.1 Synthesis of ethyl-(R,E)-4-((tert-butoxycarbonyl)amino)-5-(4-iodophenyl)-2-methylpent-2-enoate **13***

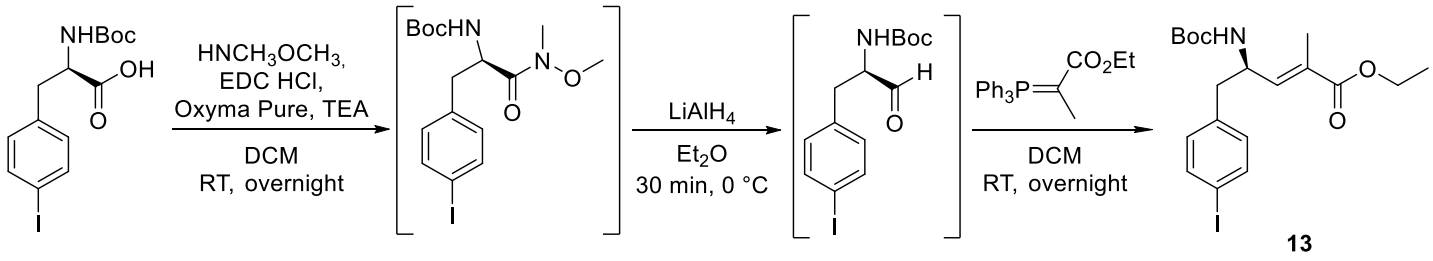

The reaction was performed based on a similar synthesis procedure described by Ksander et al. [S1] under argon atmosphere using Schlenk technique. Boc-4-iodo-D-phenylalanine (2.92 g, 7.48 mmol, 1.15 mol eq.), *O*,*N*-dimethylhydroxylamine hydrochloride (0.63 g, 6.50 mmol), 1-ethyl-3-(3-dimethylaminopropyl)carbodiimide hydrochloride (2.85 g, 14.9 mmol, 2.29 mol eq.), ethyl(hydroxyimino)cyanoacetate (1.60 g, 11.3 mmol, 1.73 mol eq.) and triethylamine (1.24 mL, 8.91 mmol, 1.37 mol eq.) were dissolved in dichloromethane (25 mL) and the orange reaction solution was stirred overnight at room temperature. The solvent was carefully evaporated from the dark brown reaction mixture and the residue was diluted with ethyl acetate (50 mL). The organic phase was washed with sat. aq. $NaHCO_3$ (2 x 30 mL), 1 M HCl (2 x 30 mL) and brine (1 x 30 mL) successively and dried over Na_2SO_4. The solvent was removed under reduced pressure to yield crude *tert*-butyl-(*R*)-(3-(4-iodophenyl)-1-(methoxy(methyl)amino)-1-oxopropan-2-yl)carbamate as a brownish viscous oil, which was directly used in the next step without further purification.

Crude *tert*-butyl-(*R*)-(3-(4-iodophenyl)-1-(methoxy(methyl)amino)-1-oxopropan-2-yl)carbamate (6.50 mmol) was dissolved in dry diethyl ether (110 mL) and cooled to 0 °C. $LiAlH_4$ (1.0 M in diethyl ether, 13.0 mL, 13.0 mmol, 2.00 mol eq.) was added dropwise and the reaction mixture was kept stirring for 30 min at 0 °C. After quenching the reaction with cold 5% aq. $KHSO_4$ (44.3 mL, 16.3 mmol, 2.50 mol eq.), the reaction mixture was warmed to room temperature and washed with cold 1 M HCl (2 x 40 mL) and brine (2 x 40 mL, 1 x 20 mL) successively. The organic phase was dried over Na_2SO_4. The solvent was removed under reduced pressure to yield crude *tert*-butyl-(*R*)-(1-(4-iodophenyl)-3-oxopropan-2-yl)carbamate as a yellow solid, which was used in the next step without further purification.

Crude *tert*-butyl-(*R*)-(1-(4-iodophenyl)-3-oxopropan-2-yl)carbamate (6.50 mmol) and (carbethoxyethylidene)triphenylphosphorane (4.71 g, 13.0 mmol, 2.00 mol eq.) were dissolved in dichloromethane (110 mL) and the reaction mixture was stirred at room temperature overnight. Then, the solvent was removed under reduced pressure and crude **13** was purified by column chromatography (silica gel, toluene:ethyl acetate = 95:5) giving **13** (1.64 g, 3.58 mmol) as a white solid in 55% overall yield.

Thin layer chromatography (SiO_2): toluene:ethyl acetate = 95:5, R_f = 0.3

^{1}H-NMR (300 MHz, $CDCl_3$): δ_H [ppm]= 7.60 (d, *J*= 8.1 Hz, 2H, -C*H*Cl-), 6.92 (d, *J*= 8.1 Hz, 2H, -C*H*CHCl-), 6.47 (d, *J*= 7.8 Hz, 1H, -C*H*=C-), 4.76 – 4.40 (m, 2H, -C*H*N*H*-), 4.18 (q, *J*= 7.1 Hz, 2H, -CH_2CH$_3$-), 2.86 (dd, J_1= 12.6 Hz, J_2= 4.5 Hz, 1H, -C_{ar}CH_2-), 2.72 (dd, J_1= 13.4 Hz, J_2=6.7 Hz, 1H, -C_{ar}CH_2-), 1.70 (s, 3H, -CH=C(CH_3)-), 1.40 (s, 9H, -C(CH_3)$_3$), 1.28 (t, *J*= 7.1 Hz, 3H, -CH$_2$CH_3).

^{13}C-NMR (75 MHz, $CDCl_3$): δ_C [ppm]= 167.8 (-C*C*OO-), 155.0 (-N*C*OO-), 139.7 (-*C*H=C-), 137.6 (2C, -*C*HCl-), 136.6 (-*C*$_{ar}$CH$_2$-), 131.7 (2C, -*C*HCHI-), 130.0 (-CH=*C*-), 92.2 (-*C*I-), 80.0 (-*C*(CH$_3$)$_3$-), 60.9 (-*C*H$_2$CH$_3$), 50.1 (-*C*HNH-), 40.9 (-C_{ar}*C*H$_2$-), 28.5 (3C, -C(*C*H$_3$)$_3$), 14.4 (-CH$_2$*C*H$_3$), 12.9 (-CH=C(*C*H$_3$)).

No NMR data of **13** were available in literature. However, ^{1}H- and ^{13}C-NMR data are in accordance with the corresponding literature data of a similar compound, where the iodo-substituent on the aromatic ring is replaced by a hydrogen atom [S2].

HPLC/MS-ES (*m/z*) found 460.33, calcd for $[M+H]^+$ 460.32

*6.3.2 Synthesis of ethyl-(R,E)-5-([1,1'-biphenyl]-4-yl)-4-((tert-butoxycarbonyl)amino)-2-methyl-pent-2-enoate **14***

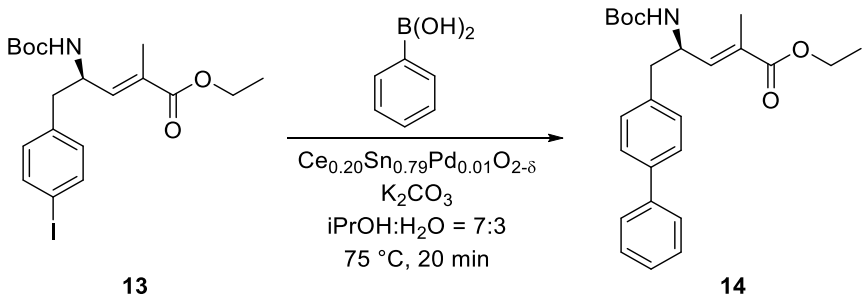

13 **14**

Compound **13** (300 mg, 0.65 mmol), phenylboronic acid (120 mg, 0.98 mmol, 1.50 mol eq.) and potassium carbonate (135 mg, 0.98 mmol, 1.50 mol eq.) were dissolved in 2-propanol:H_2O = 7:3 (v/v, 25 mL). The reaction mixture was stirred at 75 °C until all reactants were dissolved and Pd catalyst $Ce_{0.20}Sn_{0.79}Pd_{0.01}O_{2-\delta}$ (94 mg, 1 mol%) was added. After 20 min, HPLC analysis showed completion of the reaction. The solvent was evaporated under reduced pressure, the residue was diluted with ethyl acetate (25 mL) and washed with H_2O (2 x 15 mL) as well as brine (1 x 15 mL). The organic phase was dried over Na_2SO_4 and the solvent was removed under reduced pressure. The crude product was purified by column chromatography (silica gel, PE:EtOAc = 85:15) to give **14** (165 mg, 0.40 mmol) as a white solid in 62% yield.

Thin layer chromatography (SiO_2): Petrol ether:ethyl acetate = 85:15, R_f = 0.7

^{1}H-NMR (300 MHz, $CDCl_3$): δ_H [ppm]= 7.62 – 6.99 (m, 9H, all -C*H*$_{ar}$-), 6.48 (d, *J*= 7.9 Hz, 1H, -C*H*=C-), 4.82 – 4.40 (m, 2H, -C*H*N*H*-), 4.11 (q, *J*= 7.0 Hz, 2H, -C*H*$_2$CH$_3$), 2.88 (dd, J_1= 12.8 Hz, J_2=5.0 Hz, 1H, -C*H*$_2$C$_{ar}$-), 2.76 (dd, J_1= 13.3 Hz, J_2= 6.7 Hz, 1H, -C*H*$_2$C$_{ar}$-), 1.67 (s, 3H, -CH=C(C*H*$_3$)-), 1.33 (s, 9H, -C(C*H*$_3$)$_3$), 1.21 (t, *J*= 7.1 Hz, 3H, -CH$_2$C*H*$_3$).

^{13}C-NMR (75 MHz, $CDCl_3$): δ_C [ppm]= 167.9 (-*C*OOCH$_2$CH$_3$), 155.1 (-*C*OOC(CH$_3$)$_3$), 140.9 (-CH$_2$Ph*C*$_{ar}$-), 140.3 (-*C*H=C-), 139.8 (-CH$_2$(CCHCH*C*)$_{ar}$-), 135.9 (-CH$_2$*C*$_{ar}$-), 130.1 (2C, -CH$_2$(C*C*H)$_{ar}$-), 128.9 (2C, -CH$_2$Ph(CCH*C*H)$_{ar}$-), 127.4 (-CH$_2$Ph(CCHCH*C*H)$_{ar}$-), 127.3 (2C, -CH$_2$Ph(C*C*H)$_{ar}$-), 127.1 (2C, -CH$_2$(CCH*C*H)$_{ar}$-), 79.9 (-*C*(CH$_3$)$_3$), 60.9 (-*C*H$_2$CH$_3$), 50.4 (-*C*HNH-), 41.0 (-*C*H$_2$C$_{ar}$-), 28.5 (3C, -C(*C*H$_3$)$_3$), 14.4 (-CH$_2$*C*H$_3$), 12.8 (-CH=C(*C*H$_3$)-).

^{1}H-data were in accordance with the literature values [S1]. No ^{13}C-NMR data of **14** were available in literature. However, the ^{13}C-NMR were in accordance with the corresponding literature values (C_q=CH signal too weak to be visible) of a similar compound bearing a phenyl instead of a biphenyl substituent [S2].

HPLC/MS-ES (*m/z*) found 410.45, calcd for $[M+H]^+$ 410.53

*6.3.3 Synthesis of (R,E)-4-((1-([1,1'-biphenyl]-4-yl)-5-ethoxy-4-methyl-5-oxopent-3-en-2-yl)amino)-4-oxobutanoic acid **16***

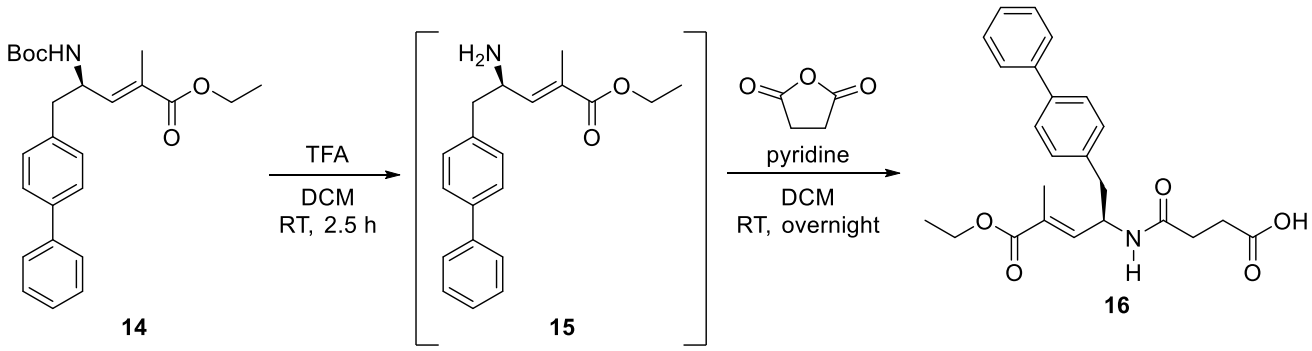

Compound **14** (100 mg, 0.25 mmol) was dissolved in dichloromethane (1.5 mL) and trifluoroacetic acid (1.50 mL, 19.6 mmol, 80.0 mol eq.) was added slowly to the reaction mixture, which was kept stirring at room temperature for 2.5 h. The solvent was removed under reduced pressure and the residual oil was diluted with ethyl acetate (20 mL) and washed with sat. aq. Na_2CO_3 (2 x 10 mL) as well as brine (1 x 10 mL) successively. The organic phase was dried over Na_2SO_4 and the solvent was removed under reduced pressure to yield **15** (75.8 mg) as a yellow oil. The crude product was used in the next step without further purification.

Based on a similar synthesis procedure performed by Ksander et al. [S1], crude **15** (0.25 mmol) was dissolved in dichloromethane (1.5 mL) and pyridine (1.5 mL). Succinic anhydride (37.2 mg, 0.37 mmol, 1.52 mol eq.) was added. After stirring the reaction mixture overnight at room temperature, the solvent was removed by rotary evaporation. The residue was diluted with ethyl acetate (20 mL), washed with 1 M HCl (3 x 10 mL) and brine (1 x 10 mL) successively and the organic phase was dried over Na_2SO_4. The solvent was removed under reduced pressure and crude **16** was purified by column chromatography (silica gel, ethyl acetate + 0.5% acetic acid) giving **16** (70.2 mg, 0.17 mmol) as a yellowish oil in 70% overall yield.

Thin layer chromatography (SiO_2): ethyl acetate + 0.5% acetic acid, R_f = 0.6

^{1}H-NMR (300 MHz, $CDCl_3$): δ_H [ppm]= 9.67 (bs, 1H, -O*H*), 7.85 – 6.91 (m, 9H, -C_{ar}*H*-), 6.50 (d, *J*= 9.2 Hz, 1H, -C*H*=C-), 6.10 (d, *J*= 7.9 Hz, 1H, -N*H*), 4.95 (dt, J_1= 14.9 Hz, J_2= 7.4 Hz, 1H, -C*H*NH-), 4.10 (q, *J*= 7.0 Hz, 2H, -C$H_2$$CH_3$-), 2.90 (dd, J_1= 13.5 Hz, J_2= 6.1 Hz, 1H, -C_{ar}CH_2-), 2.78

(dd, J_1= 13.5 Hz, J_2= 7.2 Hz, 1H, -$C_{ar}CH_2$-), 2.57 (t, J= 6.0 Hz, 2H, -CH_2COOH), 2.36 (t, J= 6.2 Hz, 2H, -CH_2CH_2COOH), 1.67 (s, 3H, -CH=C(CH_3)-), 1.20 (t, J= 7.1 Hz, 3H, -CH_2CH_3).

^{13}C-NMR (75 MHz, $CDCl_3$): δ_C [ppm]= 177.0 (-*C*OOH), 171.5 (-*C*ONH-), 168.0 (-*C*OOCH$_2$-), 140.8 (-CH$_2$Ph*C*$_{ar}$-), 139.8 (-CH$_2$(CCHCH*C*)$_{ar}$-), 139.4 (-*C*H=C-), 135.6 (-CH$_2$*C*$_{ar}$-), 130.4 (-CH=*C*-), 130.0 (2C, -CH$_2$(C*C*H)$_{ar}$-), 128.9 (2C, -CH$_2$Ph(CCH*C*H)$_{ar}$-), 127.4 (-CH$_2$Ph(CCHCH*C*H)$_{ar}$-), 127.3 (2C, -CH$_2$Ph(C*C*H)$_{ar}$-), 127.1 (2C, -CH$_2$(CCH*C*H)$_{ar}$-), 61.1 (-*C*H$_2$CH$_3$), 49.1 (-*C*HNH-), 40.3 (-C$_{ar}$*C*H$_2$-), 30.9 (-*C*H$_2$COOH), 29.6 (-*C*H$_2$CH$_2$COOH), 14.3 (-CH$_2$*C*H$_3$), 12.9 (-CH=C(*C*H$_3$)-).

No NMR data of compound **16** were available in literature. However, the ^{1}H- and ^{13}C-NMR values were comparable with the corresponding literature data of sacubitril [S3] except from the signals corresponding to the C-C double bond.

HPLC/MS-ES (*m/z*) found 410.46, calcd for $[M+H]^+$ 410.48

6.3.4 Synthesis of the heterogeneous Pd catalyst $Ce_{0.20}Sn_{0.79}Pd_{0.01}O_{2-\delta}$

The used heterogeneous Pd catalysts of formula $Ce_{0.20}Sn_{0.79}Pd_{0.01}O_{2-\delta}$ was synthesized using a modified solution combustion method, which was already reported by Baidya et al. [S4]. For the synthesis of 3 g catalyst, ammonium cerium(IV) nitrate (2.12 g), tin(II) oxalate (3.16 g), palladium(II) chloride (34 mg) and glycine (3.35 g) were pestled in a mortar until a fine powder was achieved. HPLC-grade water (2 mL) was added and the mixture was sonicated for 30 min. After combustion in the oven for 1 h at 350 °C, the catalyst was pestled again and the resulting yellow powder was dried in the oven over night at 350 °C. The catalyst was obtained in quantitative yield and used as such for Suzuki-Miyaura cross-coupling reactions.

6.4 Design of Experiments

For the DoE analysis of Boc-deprotection and *N*-amidation in continuous flow, the software MODDE Pro (Version 12.1.0.5491, Copyright © Sartorius Stedim Data Analytics AB) was utilized. In both cases, we chose a full-factorial design with 2 quantitative multilevel factors (Boc-deprotection: *T* and *mol eq. HCl*, *N*-amidation: *Mol eq. succinic anhydride* and *mol eq. DIPEA*) and two replicates of the center point. As response factor, we set the conversion of compounds **17** and **18**, respectively. The corresponding experimental raw data used for DoE analysis is given in Table D-S5 (Boc-deprotection) and Table D-S6 (*N*-amidation).

Table D-S5: Experimental raw data for DoE analysis of Boc-deprotection in continuous flow.

Entry	T [°C]	Mol eq. HCl	Conversion[a] [%]
1	80	5	81.4
2	75	5	61.7
3	70	5	46.4
4	80	10	96.9
5	75	10	87.4
6	75	10	87.6
7	75	10	86.6
8	70	10	69.5
9	80	15	>99.9
10	75	15	97.6
11	70	15	87.8

[a] Conversion of **17** determined as mean value of measured conversion at τ= 3, 3.5, 4 (determined by HPLC)

Table D-S6: Experimental raw data for DoE analysis of *N*-amidation in continuous flow.

Entry	Mol eq. $Succ_2O$	Mol eq. DIPEA	Conversion[a] [%]
1	2.0	1.5	97.5
2	2.0	1.0	97.7
3	2.0	0.5	97.0
4	1.5	1.5	89.4
5	1.5	1.0	93.7
6	1.5	1.0	93.4
7	1.5	1.0	93.6
8	1.5	0.5	93.4
9	1.0	1.5	60.5
10	1.0	1.0	73.1
11	1.0	0.5	78.6

[a] Conversion of **18** determined as mean value of measured conversion at τ= 3, 3.5, 4 (determined by HPLC)

Regarding the DoE analysis of Boc-deprotection, first the replicate plot of the experimental data (A, Figure D-S13) showed low variability of the replicates. The corresponding histogram plot revealed approximate normal distribution of the experimental data and therefore, no data transformation was necessary. Furthermore, "*temperature*", "*mol eq. HCl*", "*mol eq. HCl*mol eq. HCl*" as well as "*temperature*mol eq. HCl*" were identified to be significant model terms (C, Figure D-S13). The statistical parameters of obtained model are given in Table D-S7 as well as visualized in the Fit plot (B, Figure D-S13). The performance indicators R^2 (0= no model, 1= perfect model) and Q^2 (>0.5) indicate a very useful model. Furthermore, the low variation of the replicates compared to the overall variability is reflected in the high value for the model reproducibility (>0.5). The validity of the model exhibits a relatively low value. However, very good models (Q^2>0.9) or models with extremely good replicates are prone to show low model validity due to the high sensitivity in the test. Furthermore, the normal probability plot (D, Figure D-S13) displays the absence of outliers and as the points approximately resemble a straight line, the residuals are likely to be normally distributed noise.

Concerning the DoE analysis of *N*-amidation, the replicate plot again revealed low variability of the replicates (A, Figure D-S14). Owing to the fact that the histogram plot indicated negative skewness, a negative logarithmic transformation of the data was performed. In the following, the model terms "*mol eq. succinic anhydride*", "*mol eq. DIPEA*", "*mol eq. DIPEA*mol eq. DIPEA*" and "*mol eq. succinic anhydride*mol eq. DIPEA*" were identified to have a significant influence on the response and were therefore included in the model (C, Figure D-S14). The statistical parameters describing the model quality are given in Table D-S7 and depicted in the Fit plot (B, Figure D-S14). Again, the relatively low model validity can be probably ascribed to the low replicate variability. Once more, the normal probability plot (D, Figure D-S14) suggests the residuals to be normally distributed noise.

Table D-S7: Statistical parameters of the DoE-models for Boc-deprotection and *N*-amidation.

Statistical parameter	Model Boc-deprotection	Model *N*-amidation
R^2	0.986526	0.991149
Q^2	0.941737	0.965226
Model validity	0.122941	0.10089
Reproducibility	0.998978	0.999386

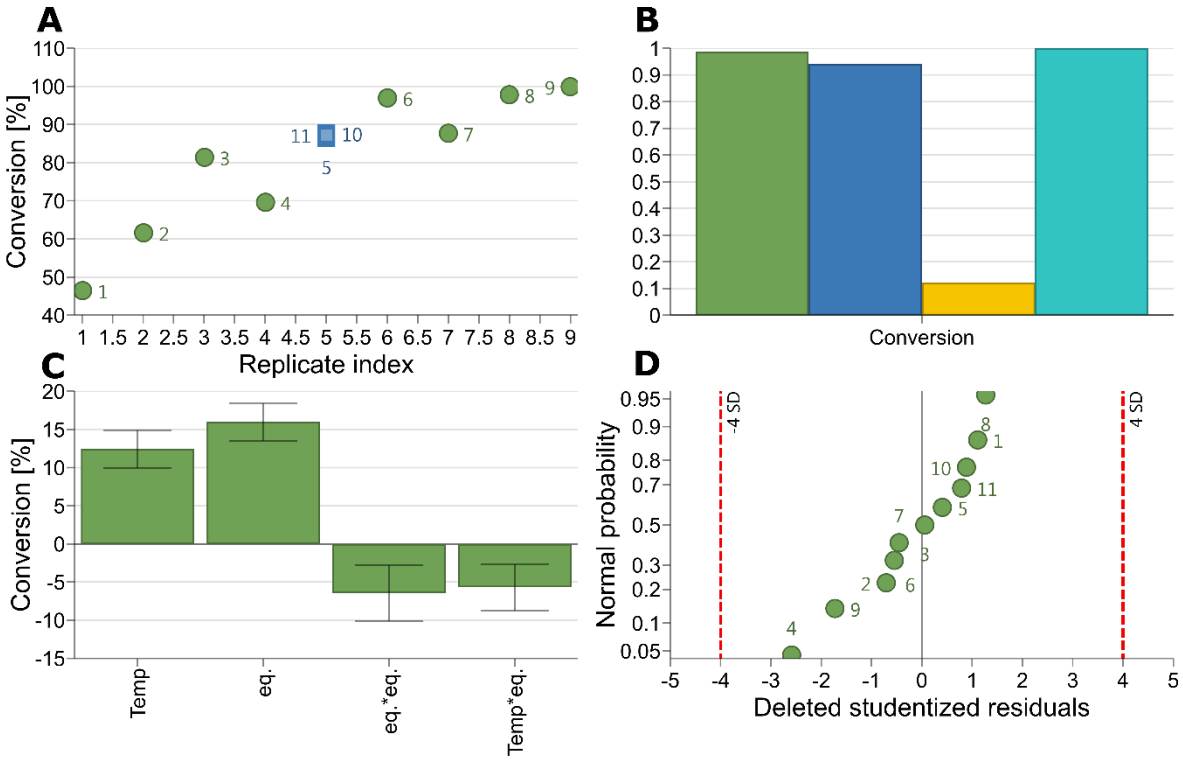

Figure D-S13: Overview plot of the Boc-deprotection model created with MODDE Pro
(A: Replicate Plot, B: Summary of Fit Plot, C: Coefficient Plot, D: Residuals Normal Probability Plot).

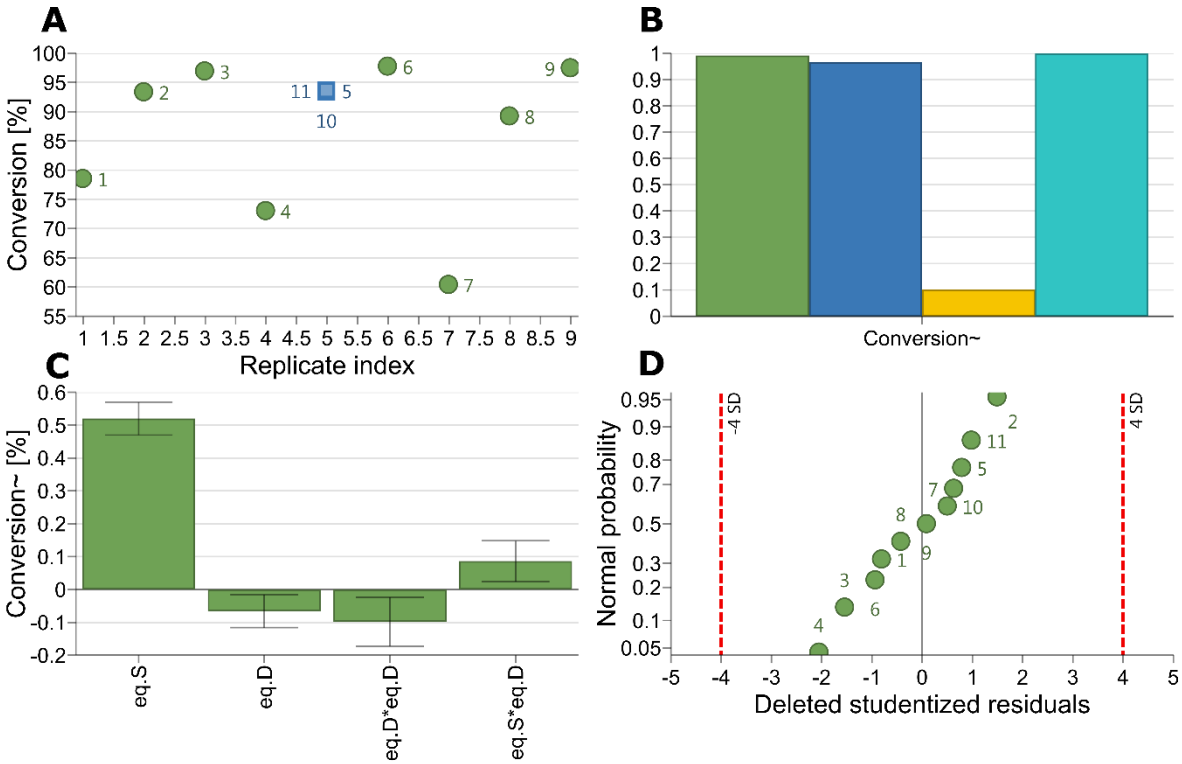

Figure D-S14: Overview plot of the *N*-amidation model created with MODDE Pro (A: Replicate Plot, B: Summary of Fit Plot, C: Coefficient Plot, D: Residuals Normal Probability Plot).

6.5 Multistep continuous setup for the synthesis of 16

The course of conversion of starting compound **13** as well as the yield of target molecule **16** over time using the three-step continuous setup is apparent from Figure D-S15.

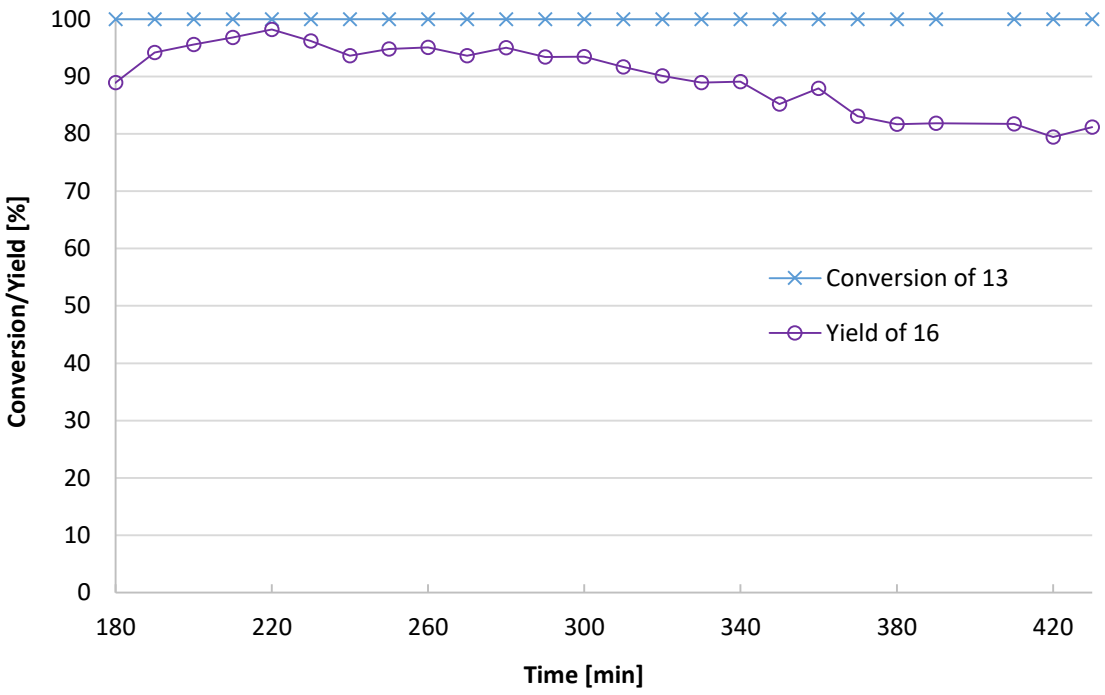

Figure D-S15: Conversion of **13** and yield of **16** utilizing the multistep setup for the synthesis of sacubitril precursor **16** in continuous flow (at t= 400 min: refill of syringe in syringe pump, no sample was taken).

6.6 References

S1. Ksander GM, Ghai RD, deJesus R, Diefenbacher CG, Yuan A, Berry C, Sakane Y, Trapani A (1995) J Med Chem 38:1689-1700

S2. Chai Y, Ullrich A, Kazmaier U, Muller R (2010) Bioactive pre-tubulysins and use thereof. PCT Int. Appl. WO 2010/034724 A1, Apr 1, 2010; (2010) Chem Abstr 166:485194

S3. Wang Y, Chen F-E, Shi Y, Tian W-S (2016) Tetrahedron Lett 57:5928-5930

S4. Baidya T, Gupta A, Deshpandey PA, Madras G, Hegde MS (2009) J Phys Chem C 113:4059-4068

E Outlook

Continuous flow technology, especially coupled with heterogeneous transition metal catalysis, offers great potential for pharmaceutical companies to design greener and more sustainable manufacturing processes. Within the framework of this thesis and based on the principles of the ONE-FLOW project, recent efforts regarding the development of novel approaches and multistep routes for the formation of active pharmaceutical ingredients in continuous flow have been outlined. Besides the implementation of heterogeneous palladium catalysts into Pickering emulsions, aimed to be applicable for the performance of reaction cascades in a "single step" according to the ONE-FLOW approach, new concepts for the continuous synthesis of advanced precursors of valsartan as well as sacubitril in three steps have been presented. Moreover, the potential of 3D printed microreactors, as utilized for the synthesis of the valsartan intermediate, for the formation of APIs in continuous flow has been highlighted and on this subject, a research article has been published very recently by our group (Maier et al., doi.org/10.1021/acs.oprd.0c00228).

Regarding the use of Ce-Sn-Pd oxides as stabilizers for Pickering emulsions, succeeding studies focused on the utilization of this compartmentalization technique for catalytic cascade reaction. Unfortunately, the concept proved to be unsuccessful for targeted Suzuki-Miyaura cross-coupling reactions. However, the use of silica particles as emulsifiers instead along with homogeneous Pd species shows first promising results and is currently under investigation for the realization of the ONE-FLOW concept for C-C bond formation.

As far as the continuous setup for synthesis of a late-stage valsartan precursor in three steps is concerned, future work should focus on improving the enantiomeric excess of the target molecule. High concentrations of NaOH as well as elevated temperatures applied for methyl ester hydrolysis most probably caused partial racemization of the API precursor. Alternative milder hydrolysis procedures, such as the use of only a slight excess of base in combination with a longer residence time or enzymatic cleavage, are conceivable and would be strongly favored in terms of the synthesis of enantiopure products valuable for the pharmaceutical industry. Furthermore, subsequent triazole formation via hazardous azide chemistry, giving the final API, seems to be predestined to be performed using microreaction technology. In this way, the developed process could be further extended and become more attractive for large-

scale applications. Concerning the implementation of the fundamental ONE-FLOW idea into the process, a novel membrane/fixed-bed reactor achieving the simultaneous performance of the cross-coupling as well as ester hydrolysis step is currently under development in cooperation with an industrial project partner.

Referring to the multistep approach for formation of a sacubitril precursor in continuous flow, enhancing the enantiomeric purity of the obtained compound is once more of high importance in order to render the process industrially appealing. Consequently, tuning of the Boc-deprotection step, responsible for the decrease in optical purity, should be a future target. Furthermore, studying the formation of sacubitril via stereoselective hydrogenation of the double bond would be another reasonable task to increase the scientific impact.

Summarizing, presented novel approaches for continuous API manufacturing are in the early stages of development but promising. In view of their potential application for the actual production of biologically active compounds, the concepts need to be further developed and improved, especially in terms of enantioselectivity. Nevertheless, with our research we hope to contribute a bit to establishing continuous flow technology as a key element in the toolbox of pharmaceutical chemists and promote research in this rapidly developing field.